

SYNTHESIS, THERMO-PHYSICAL PROPERTIES AND
CONVECTION HEAT TRANSFER OF CARBON BASED HYBRID
NANOFLUIDS

HOUMAN YARMAND

THESIS SUBMITTED IN FULFILMENT OF THE
REQUIREMENTS FOR THE DEGREE OF DOCTOR
OF PHILOSOPHY

FACULTY OF ENGINEERING
UNIVERSITY OF MALAYA
KUALA LUMPUR

2016

UNIVERSITY OF MALAYA
ORIGINAL LITERARY WORK DECLARATION

Name of Candidate: Houman Yarmand [REDACTED]

Registration/Matric No: KHA 130098

Name of Degree: **DOCTOR OF PHILOSOPHY**

Title of Project Paper/Research Report/Dissertation/Thesis ("this Work"):

Study of synthesis, thermo-physical properties and convection heat transfer to carbon based hybrid nanofluids

Field of Study: **HEAT TRANSFER**

I do solemnly and sincerely declare that:

- (1) I am the sole author/writer of this Work;
- (2) This Work is original;
- (3) Any use of any work in which copyright exists was done by way of fair dealing and for permitted purposes and any excerpt or extract from, or reference to or reproduction of any copyright work has been disclosed expressly and sufficiently and the title of the Work and its authorship have been acknowledged in this Work;
- (4) I do not have any actual knowledge nor do I ought reasonably to know that the making of this work constitutes an infringement of any copyright work;
- (5) I hereby assign all and every rights in the copyright to this Work to the University of Malaya ("UM"), who henceforth shall be owner of the copyright in this Work and that any reproduction or use in any form or by any means whatsoever is prohibited without the written consent of UM having been first had and obtained;
- (6) I am fully aware that if in the course of making this Work I have infringed any copyright whether intentionally or otherwise, I may be subject to legal action or any other action as may be determined by UM.

Candidate's Signature

Date:

Subscribed and solemnly declared before,

Witness's Signature

Date:

Name:

Designation:

ABSTRACT

Water, engine oil and ethylene glycol are commonly used as working fluids for transfer of heat in many industrial equipment such as heat exchangers, cooling devices and solar collectors. Little improvement in efficiency of heat exchanging equipment could lead to huge savings in initial and operational costs. One way to achieve this aim is to enhance the effective thermal conductivity of fluids that transfer the heat. Since the thermal conductivity of most of the heat exchanging liquids is low, there has been interest to use suspended solid particles to enhance the thermal conductivity of the base-fluid. Dispersion of micrometer or even millimeter particles in base-fluid was attempted earlier by researchers. However, these earlier attempts had faced obstacles such as, increase in pressure drop, sedimentation of particles and erosion of equipment. Choi and his co-worker in 1995 had found a new class of fluids with suspension of nanoparticles that is called “nanofluid”. Investigation supports that the nanoparticles have the ability to improve the effective thermal conductivity of base fluid and are useful for different industrial applications.

In the present study, a facile method is used for synthesis of functionalized graphene nanoplatelets (f-GNP) nanofluids and hybrid carbon based nanofluids. The effective thermal conductivity, density, viscosity, specific heat capacity, heat transfer coefficient and friction factor for fully developed turbulent flow of functionalized GNP/water and hybrid nanofluids flowing through a square pipe at a constant heat flux were studied. The surface characterization was performed by various techniques such as XRD, FESEM, FTIR and Raman. All the nanofluids were prepared by dispersing the functionalized nanoparticles in base fluid (water) without adding the surfactants. The synthesized nanofluids were stable for a long time and no sedimentation was observed. The experimental data for all the prepared nanofluids have shown significant enhancement in thermal conductivity and heat transfer coefficient in comparison to the corresponding

base fluid the water data. In this investigation, some improved empirical correlations were proposed based on the experimental data for evaluation of the Nusselt number and friction factor.

University of Malaya

ABSTRAK

Air, minyak enjin dan glikol etilina biasanya digunakan sebagai cecair kerja untuk pemindahan haba dalam banyak peralatan industri seperti penukar haba, peranti penyejukan dan pengumpul solar. Peningkatan kecil dalam kecekapan penukaran peralatan haba boleh membawa kepada penjimatan yang besar dalam kos permulaan dan operasi. Salah satu cara untuk mencapai matlamat ini adalah untuk meningkatkan keberkesanan kekonduksian haba cecair yang memindahkan haba. Disebabkan kekonduksian haba kebanyakan cecair adalah rendah, terdapat faedah untuk menggunakan zarah pepejal terampai untuk meningkatkan kekonduksian haba dalam bentuk asas cecair. Penyebaran zarah mikrometer mahupun milimeter dalam bentuk asas-cecair telah digunakan sebelum ini oleh penyelidik. Walaubagaimanapun, percubaan awal ini telah menghadapi pelbagai halangan seperti, peningkatan penurunan tekanan, pemendapan zarah dan hakisan peralatan. Choi dan rakan sekerja pada tahun 1995 mendapati kelas baru cecair dengan penggantungan nanopartikel yang dipanggil "nanofluid". Siasatan menunjukkan bahawa nanopartikel mempunyai keupayaan untuk meningkatkan keberkesanan kekonduksian haba untuk bentuk cecair asas adalah berguna untuk aplikasi dalam industri yang berbeza.

Dalam kajian ini, kaedah 'facile' digunakan untuk penyediaan nanoplatelets berfungsi-graphene (f-GNP) 'nanofluid' dan juga karbon hibrid berasaskan 'nanofluid'. Keberkesanan kekonduksian haba, ketumpatan, kelikatan, muatan haba tentu, pekali pemindahan haba dan faktor geseran untuk pembangunan lengkap aliran gelora f-GNP / air dan hibrid nanofluids mengalir melalui paip bersegi di fluks haba tetap telah dikaji. Pencirian permukaan telah dilakukan oleh pelbagai teknik seperti XRD, FESEM, FTIR dan Raman. Semua 'nanofluid' telah disediakan dengan pensuraian nanopartikel berfungsi dalam bentuk cecair asas (air) tanpa bantuan dari surfaktan. Sintesis 'nanofluid' adalah stabil untuk masa yang lama dan tiada pemendapan dapat diperhatikan. Data

eksperimen untuk semua 'nanofluid' yang disediakan telah menunjukkan peningkatan yang ketara dalam kekonduksian haba dan pekali haba pemindahan berbanding dengan cecair asas oleh data air. Di dalam penyiasatan ini, korelasi empirik bertambah baik telah dicadangkan berdasarkan data eksperimen untuk penilaian nombor Nusselt dan faktor geseran.

University of Malaya

Acknowledgement

I would like to express my deep gratitude to my advisor Dr. Salim Newaz Kazi, for all the help and supervision he has extended to me throughout my years at the University of Malaya at Malaysia. He was like a kind father to me during my study in Malaysia. Dr. Kazi is not only a great teacher of heat transfer, but of life also.

Also, I would like to express my special thanks to my co-Advisor Dr. Mahidzal Dahari for his advice and guidance of this research project and thesis. Working with him has been a useful research experience.

My sincerest thanks to my friends and colleagues Farid Shirazi, Samira Gharekhani and Mohammad Reza Safaie for their friendship, help and valuable suggestions.

Finally, I will express my deepest gratitude to my parents Hamid and Mitra, my sister Hanie and my brother Homam because of their support and encouragement.

TABLE OF CONTENTS

ABSTRACT	III
ABSTRAK	V
TABLE OF CONTENTS	VIII
LIST OF FIGURES	XIV
LIST OF TABLES	XIX
LIST OF SYMBOLS AND ABBREVIATIONS	XX
List of Appendices	XXII
CHAPTER 1: INTRODUCTION.....	1
1.1 Background	1
1.2. Significance of study	2
1.3. Application of the nanofluids	3
1.4. Objective of the study.....	4
1.5. Thesis outlines	4
CHAPTER 2: LITERATURE REVIEW.....	5
2.1. Background	5
2.2. Nanofluid preparation.....	6
2.3. Stability of Nanofluid	7
2.3.1. Surface chemical treatment (pH control).....	8
2.3.2. Ultrasonic vibration	8
2.3.3. Addition of surfactant	9
2.4. Stability Examined Tools	9
2.4.1. Zeta potential	10
2.4.2. UV–Vis spectrophotometer	10

2.4.3. TEM (Transmission Electron Microscopy) and SEM (Scanning Electron Microscopy).....	11
2.4.4. Three omega method	11
2.4.5. Sedimentation balance method	12
2.4.6. Sediment photograph capturing method	12
2.5. Thermos-physical properties of nanofluid.....	12
2.5.1. Thermal conductivity of nanofluids.....	12
2.5.1.1. Thermal conductivity measurement methods for nanofluids.....	13
2.5.1.2. Enhancement in thermal conductivity of nanofluid.....	22
2.5.2. Viscosity of nanofluids	25
2.5.2.1. Newtonian and Non-Newtonian Behavior.....	25
2.5.2.2. Effects of temperature.....	26
2.5.2.3. Effects of volume concentration	26
2.5.2.4. Effects of particle shape and size.....	27
2.5.2.5. Effects of base fluid	27
2.5.3. Density of nanofluids.....	28
2.5.4. Specific heat capacity of nanofluids	30
2.6. Electrical conductivity of nanofluids.....	32
2.7. Convective heat transfer performance of nanofluids	32
2.8. Hybrid nanofluids.....	43
2.8.1. Preparation of hybrid nanofluid.....	44
2.8.2. Thermos-physical properties.....	46
2.8.3. Heat transfer and pressure drop	47

2.9. Summary	49
CHAPTER 3: METHODOLOGY	51
3.1. Characterization methods	51
3.1.1. XRD	51
3.1.2. FESEM	51
3.1.3. TEM	52
3.1.4. FTIR	52
3.1.5. Raman	53
3.2. Thermos-physical measurement equipment	53
3.2.1. Rheometer	53
3.2.2. DSC	54
3.2.3. Density meter	54
3.2.4. Thermal and Electrical conductivity	54
3.3. Experimental setup	56
3.3.1. Test section	59
3.3.2. Heater	59
3.3.3. Thermocouple	60
3.3.4. Tank	60
3.3.5. Chiller	60
3.3.6. Power supplier	61
3.3.7. Pump	61
3.3.8. Data logger, clamp meter and multi-meter	61
3.3.9. Others	62

3.4. Lab equipment	62
3.5. Data reduction	63
3.6. Optimization method	66
CHAPTER 4: PREPARATION, CHARACTERIZATION AND THERMOS- PHYSICAL PROPERTIES OF NANOFLUIDS	67
4.1. Introduction	67
4.2. Functionalized GNP water based nanofluid	67
4.2.1. Preparation	67
4.2.2. Characterization of f-GNP nanoparticles	68
4.2.3. Stability and particle size distribution	71
4.2.4. Thermo-physical properties of f-GNP nanofluids	73
4.3. Functionalized GNP- Ag water based hybrid nanofluid	77
4.3.1. Synthesis of GNP-Ag nanocomposite	77
4.3.2. Characterization of GNP-Ag nanocomposite	79
4.3.3. Thermo-physical properties of GNP-Ag hybrid nanofluids	82
4.4. Activated Hybrid of Biomass Carbon/Graphene Oxide Ethylene Glycol based nanofluid.....	85
4.4.1. Synthesis of hybrid nanocomposite and nanofluid preparation.....	85
4.4.2. Characterization of ACG nanocomposite	87
4.4.3. Thermo-physical properties of ACG hybrid nanofluids	89
4.5. Functionalized GNP-Pt water based hybrid nanofluid	95
4.5.1. Synthesis of GNP-Pt nanocomposite	95
4.5.2. Characterization of GNP-Pt nanocomposite.....	96

4.5.3. Thermo-physical properties of GNP-Pt hybrid nanofluids.....	100
4.6. Summary	105
CHAPTER 5: HEAT TRANSFER AND FRICTION FACTOR OF NANOFLUIDS	
.....	107
5.1. Introduction	107
5.2. Validation of experimental heat transfer set up.....	107
5.3. f-GNP/ Water nanofluids.....	109
5.3.1. Nusselt number and heat transfer coefficient of f-GNP nanofluids.....	109
5.3.2. Friction factor of f-GNP nanofluids.....	111
5.3.3. Pumping power and performance index	112
5.4. GNP-Pt/ Water nanofluids.....	114
5.4.1. Nusselt number of GNP-Pt hybrid nanofluids	114
5.4.2. Friction factor of GNP-Pt hybrid nanofluids	115
5.5. GNP-Ag/ Water nanofluids	116
5.5.1. Nusselt number of GNP-Ag hybrid nanofluids	116
5.5.2. Friction factor of GNP-Ag hybrid nanofluids.....	119
5.6. Summary	122
CHAPTER 6: CONCLUSIONS AND RECOMMENDATIONS	124
6.1. Conclusions	124
6.2. Recommendations for further works	125
References	127
List of publications and papers presented	145
Appendix A	147

Appendix B	150
Appendix C	153

University of Malaya

LIST OF FIGURES

Figure 2.1: Various thermal conductivity measurement methods for nanofluids(Paul et al., 2010).	14
Figure 2.2: Comparison of the thermal conductivity measurement techniques for nanofluids (Paul et al., 2010).	15
Figure 2.3: Schematic diagram of transient hot-wire (THW) experimental set up (Paul et al., 2010).	16
Figure 2.4: (a) Experimental setup for transient plate source method and (b) Schematic diagram of TPS sensor (Paul et al., 2010).....	18
Figure 2.5: Schematic diagram of the experimental set up for steady-state parallel-plate method (Paul et al., 2010).	19
Figure 2.6: Schematic diagram of the cylindrical cell equipment (Paul et al., 2010)....	20
Figure 2.7: Experimental set up for temperature oscillation technique (Paul et al., 2010).	21
Figure 2.8: Comparison of experimental density values (Vajjha et al) with theoretical correlation (Pak and Cho) for different particle volumetric concentrations as a function of temperature(R. S. Vajjha & Das, 2012).....	29
Figure 2.9: Schematic of experimental setup for convective heat transfer and viscous pressure drop measurement (Rea et al., 2009)	35
Figure 2.10: Schematic of experimental setup to measure heat transfer and pressure drop of Nanofluid, (Duangthongsuk & Wongwises, 2009a).....	38
Figure 2.11: Comparison of Nusselt number of Al ₂ O ₃ -Cu/water hybrid nanofluid with the Nusselt number of Al ₂ O ₃ /water nanofluid (Suresh, Venkitaraj, et al., 2012)	48
Figure 3.1: Photograph of the thermal properties analyzer (KD2 pro).	55
Figure 3.2: Schematic and photograph of the experimental setup.....	58
Figure 3.3: Schematic of the test section.	59

Figure 4.1: Schematic of functionalization process and making of nanofluid.....	68
Figure 4.2: (a and b) FTIR and Raman spectra of GNP and f-GNP and (c) XRD pattern of f-GNP.....	70
Figure 4.3: (a and b) TEM images and (c and d) FESEM images of pristine GNP and f-GNP.....	71
Figure 4.4: Particle size distribution of (a) pristine GNP-based water nanofluid and (b) functionalized GNP-based water nanofluid.	72
Figure 4.5: (a) UV-vis spectrum of functionalized GNP-based water nanofluid and (b) the colloidal stability of functionalized GNP-based water nanofluid as a function of time.	73
Figure 4.6: Thermal conductivity of f-GNP nanofluids as a function of temperature for different weight fractions.	74
Figure 4.7: Viscosity of f-GNP nanofluids as a function of temperature at different weight fractions.	75
Figure 4.8: Density of f-GNP nanofluids as a function of temperature for different weight fractions.....	76
Figure 4.9: Schematic of molecular structure of GNP-Ag nanocomposite	78
Figure 4.10: XRD pattern of GNP-Ag nanocomposite.....	79
Figure 4.11: Raman spectra of GNP-Ag nanocomposite.....	80
Figure 4.12: FESEM image of GNP-Ag nanocomposite.....	81
Figure 4.13: TEM images of GNP-Ag nanocomposite.....	82
Figure 4.14: Variation of experimental data for thermal conductivity of GNP-Ag hybrid nanofluids with the effect of temperatures and particle concentrations.....	83
Figure 4.15: Variation of experimental data for viscosity of GNP-Ag hybrid nanofluids with temperatures and particle concentrations.	84

Figure 4.16: Variation of the experimental data for density of GNP-Ag hybrid nanofluids with temperatures and particle concentrations.....	85
Figure 4.17: FESEM images of (a) pure AC, (b) ACG and (c) TEM image of ACG ...	87
Figure 4.18: (a) X-ray diffraction analysis of samples and (b) Raman spectra of AC and ACG.....	89
Figure 4.19: (a) Thermal conductivity and (b) electrical conductivity of EG and ACG hybrid nanofluids.....	90
Figure 4.20: Optical images of ACG/EG hybrid nanofluids at (a) 0.02 wt%, (b) 0.04 wt% and (c) 0.06 wt%.....	91
Figure 4.21: (a) Viscosity versus shear rate and (b) dynamic viscosity versus temperature of ACG/EG hybrid nanofluids at different weight concentrations and shear rate of 500/s.....	92
Figure 4.22: Density of EG and ACG hybrid nanofluids at different temperatures.....	93
Figure 4.23: Specific heat capacity of ACG/EG nanofluids at different temperature...	94
Figure 4.24: Schematic of the synthesis of GNP-Pt nanocomposite and then making of nanofluid.....	96
Figure 4.25: XRD pattern of GNP–Pt nanocomposite.....	97
Figure 4.26: FESEM images of GNP–Pt nanocomposite; (a) low and (b) high magnifications.....	98
Figure 4.27: TEM image of GNP-Pt nanocomposite.....	98
Figure 4.28: (a) UV-vis spectrum of functionalized GNP-Pt based water nanofluid and (b) the colloidal stability of functionalized GNP-Pt based water nanofluid as a function of time.....	100
Figure 4.29: Thermal conductivity of functionalized GNP-Pt hybrid nanofluids as a function of temperature at different weight concentrations.....	102

Figure 4.30: Viscosity of functionalized GNP-Pt hybrid nanofluids as a function of temperature at different weight concentrations.....	103
Figure 4.31: Density of functionalized GNP-Pt hybrid nanofluids as a function of temperature for different weight concentrations.....	104
Figure 5.1: Comparison of measured Nusselt number of water with the correlations of Dittus- Boelter and Petukhov.....	108
Figure 5.2: Comparison of measured friction factor of water with the correlations of Petukhov and Blasius.....	108
Figure 5.3: effect of test section cross section on the Nusselt number.....	109
Figure 5.4: Nusselt number of f-GNP nanofluids as a function of Reynolds number for different weight concentrations.....	110
Figure 5.5: Convective heat transfer coefficient of f-GNP nanofluids as a function of Reynolds number at different weight concentrations.....	111
Figure 5.6: Friction factors of f-GNP nanofluids as a function of Reynolds number at different weight concentrations.....	112
Figure 5.7: (a) Performance index and (b) pumping power ratio of functionalized GNP-based water nanofluids for different weight concentrations.....	113
Figure 5.8: Nusselt number of functionalized GNP-Pt hybrid nanofluids as a function of Reynolds number for different weight concentrations.....	114
Figure 5.9: Friction factors of functionalized GNP-Pt hybrid nanofluids as a function of Reynolds number at different weight concentrations.....	115
Figure 5.10: Variation of the experimental data for Nusselt number of GNP-Ag hybrid nanofluids with temperatures and particle concentrations.....	117
Figure 5.11: Comparison of measured Nusselt numbers of GNP-Ag nanofluids with the correlations of Suander, Pak&Cho and Maiga.....	118

Figure 5.12: Nusselt number of GNP-Ag nanofluid estimated from experimental data is in comparison with the developed Nusselt number correlation of Eq. (5.1).....	119
Figure 5.13: Variation of the experimental data for friction factor of GNP-Ag hybrid nanofluids with temperatures and particle concentrations.	120
Figure 5.14: Comparison of measured friction factor of GNP-Ag nanofluids with the correlations of Sundar and Blasius.....	121
Figure 5.15: Friction factor of GNP-Ag nanofluid estimated from experimental data is in comparison with the developed Nusselt number correlation of Eq. (5.2).....	122
Figure C.1: Comparison of the experimental data of thermal conductivity using KD2 Pro thermal properties analyzer for distilled water with the standard data.	153
Figure C.2: Comparison of the experimental data of viscosity using TA rheometer for distilled water with the standard data.....	154

LIST OF TABLES

Table 2.1: Zeta potential value and stability	10
Table 2.2: Synthesis methods for hybrid nanofluids (Sarkar et al., 2015).....	46
Table 4.1: Specific heat capacity of water and f-GNP water based nanofluids at different weight fraction and temperature.	77
Table 4.2: Thermo-physical properties of water and f-GNP water based nanofluis at mean bulk temperature.....	77
Table 4.3: Specific heat capacity of water and functionalized GNP-Pt hybrid water based nanofluids at different weight concentration and temperature.....	105
Table 4.4: Comparison study for thermal conductivity enhancement of the various samples at 0.1% weight concentration.	105
Table 5.1: Comparison study for thermal conductivity enhancement of the various samples at 0.1% weight concentration.	122
Table A.1: λ/t value for each thermocouple installed on the test section.....	149
Table B.1: Range of uncertainty for instruments used within the present study	150

LIST OF SYMBOLS AND ABBREVIATIONS

A	Area, m ²
AC	Activated carbon
ACG	Activated carbon/Graphene oxide
C _p	Specific heat, J/kg K
D	Inner diameter of the tube, m
f	Friction factor
GNP	Graphene nanoplatelet
h	Heat transfer coefficient, W/m ² K
I	Current, Amp
k	Thermal conductivity, W/m K
l	Length of the tube, m
ṁ	Mass flow rate, kg/s
Nu	Nusselt number,
P	Power, Watts
Pr	Prandtl number, μC/k
Q	Heat flow, Watts
q	Heat flux, W/m ²
Re	Reynolds number,
T	Temperature, °C
V	Voltage, Volts
v	Velocity, m/s
Greek symbols	
Δp	Pressure drop
φ	Weight concentration of nanoparticles, %

μ Viscosity, kg/m² s

ρ Density, kg/m

ε Performance index

Subscripts

b Bulk

Exp Experimental

i Inlet

o Outlet

Reg Regression

w Wall

University of Malaya

List of Appendices

Appendix A: Appendix A: Calculation of Inner wall	147
Appendix B: Uncertainty analysis	150
Appendix C: Comparison of measured thermal conductivity and viscosity with standard data.....	153

University of Malaya

CHAPTER 1: INTRODUCTION

1.1 Background

Enhancing heat transfer has been an interesting topic for many research studies. Newly, enhanced forced convection heat transfer to nanofluids has been attracted the interest of many researchers (Chol, 1995). In the engineering applications size, weight and initial cost of heat exchanger is reduced with the improvement of the convective heat transfer in thermal system. Using of turbulent forced convection fluid flow is a way to enhance the heat transfer in heat exchangers. Wide range of geometric shape of pipe have been examined in recent years. The most common geometry is circular, another's usual shapes are square, rectangular and triangle. All mentioned types of pipe were applicable in various field of engineering such as heat exchanger, gas cooled reactors, solar collector and air conditioning systems(Maïga et al., 2006; Pak & Cho, 1998).

Recently, the interest of research on ability of nanofluids for enhancing applications in heat transfer is increased. Nanofluid is a well dispersion of nanoparticles in a base fluid. The common base fluids are water, ethylene glycol, polymer solution, oil and other lubricant etc. Many kinds of particles could be used as additive like metal oxides and carbon based materials. Thermos-physical properties of nanoparticles and base fluid both have affected the convective heat transfer performance of nanofluids. Also, method of particle suspension synthesis, particles size, shape of particles and weight fraction of nanoparticles have been influenced. Thermal conductivity of nanofluids have been significantly enhanced with the addition of small amount of nanoparticle to the pure base fluids(L. F. Chen et al., 2014). Effect of nanofluids on convective heat transfer have been investigated in a suitable test rig. As it is an interesting topic, many researches have been done on it. As suspected, nanofluids made a dramatical heat transfer enhancement when applied as working fluid. Different types of nanofluids have been shown various changes

on thermal conductivity and convective heat transfer. It is obvious that the cost, sustainability and safety of different nanofluids are not the same.

In the past decade, a large number of experimental works have been conducted on synthesis of nanofluids. Further investigations on thermo-physical properties, stability and heat transfer performance of nanofluids are interesting challenges for the researchers. To validate the experimental results, the numerical study or comparison with the existing developed correlation derived from the previous experimental data have been employed by researchers(Sundar et al., 2014b). In addition, establishment of a new correlation based on experimental data is an important part of the nanofluids investigation.

1.2. Significance of study

One of the most important parameters of efficiency in many industrial applications such as cooling and heating process, power generation and transportation is working fluid (heat transfer fluid) such as water, oil and ethylene glycol. An enhancement in thermal conductivity of the mentioned conventional working fluids could make an improvement in heat transfer capability of the systems. Therefore, it had come in mind of researchers to find suitable solid particles (especially nano sized particles) which could hold thermal conductivity several thousand times higher than that of the conventional working fluid. Addition of those nanoparticles to the conventional base fluid can make a huge improvement on heat transfer characteristics of the base fluid. Many researches were conducted on dispersion, stability and thermos-physical properties of metal oxide nanofluids such as Al_2O_3 , SiO_2 and ZnO but only a few research have been reported about the non-metallic nanofluids. Current research has focused on investigation of synthesis, dispersion, thermo-physical properties and heat transfer performance of hybrid carbon based nanofluids. Functionalized graphene nanoplatelet (GNP), hybrid nanocomposite of

GNP-Silver, GNP-Platinum and activated carbon-graphene oxide have been studied in this research.

1.3. Application of the nanofluids

Wide range of applications can be found for nanofluids. The most important application of nanofluids have been listed as below.

1. Cooling of electronic elements: as there is space limitation, high level of heat generation in CPU of PC, nanofluids can be used in mini fin channel heat sink for cooling the CPU(Naphon et al., 2009).
2. Nuclear reactor: nanofluids can be used in nuclear reactor to improve critical heat flux (CHF).The development of nanofluids could be applied in water-cooled sector of nuclear reactor which can provide a huge enhancement on their efficiency and economic performance (Buongiorno & Hu, 2009).
3. Fuel cell: nanofluids can be employed to enhance efficiency of fuel cell whenever the heat exchanger phenomenon happens within a fuel cell or its auxiliary heat recovery systems.
4. Heat exchanger : when nanoparticles are added to the convectonal base fluid, the convective heat transfer has been enhanced significantly which make use of the nanofluids as a promising developed approach in heat exchanger application (Mapa & Mazhar, 2005).
5. Grinding application: the grinding procedure needs a huge energy for removal of materials which is converted to heat at the outlet. Due to that high temperature the work piece is damaged and the phase transformations are occurred. The advanced heat transfer and tribological properties of nanofluids can provide better cooling and lubrication in the MQL grinding process (Shen, 2008).
6. Solar water heating: nanofluids can be used as an absorbing medium, it enhances the efficiency of the conventional solar water heater (Tyagi et al., 2009).

7. Other applications: nanofluids have possibility for many other applications such as chillers, domestic refrigerators, oscillating heat pipes and transformers.

1.4. Objective of the study

The main objectives of this research are highlighted as follows:

1. To synthesize new types of carbon based hybrid nanofluids and find out the characterization of the new synthesized nanocomposites.
2. To investigate thermo-physical and electrical properties of the prepared nanofluids and compare with those of base fluids.
3. To investigate experimentally the heat transfer performance and friction losses of nanofluids in closed conduit flow test rig to figure out the alterations in comparison to the conventional base fluids.
4. To developed a new cluster of empirical correlations for the evaluation of Nusselt numbers and Friction factors.

1.5. Thesis outlines

This thesis includes 6 chapters. First chapter starts with an introduction of the current research and contains research background, importance of the study, application of the nanofluids and objectives of this research. Chapter 2 involves literature review of previous research on synthesis, preparation and stability, thermo-physical property, friction loss and convective heat transfer of nanofluids. Instrument, characterization devices and methods, equipment which is needed for research, the experimental test rig and test section, methods of data reduction and governing equations, calibration of devices and numerical method are introduced in chapter 3. The validation of the experimental test rig, thermo-physical property, heat transfer performance and friction loss of nanofluids are discussed in chapter 4 and 5. Summary of the work and recommendations for future work are stated in the last chapter (chapter 6).

CHAPTER 2: LITERATURE REVIEW

2.1. Background

Water, engine oil and ethylene glycol are commonly used as working fluids for transfer of heat in many industrial equipment such as heat exchangers, cooling devices and solar collectors. Small improvement in efficiency of heat exchanger equipment could lead to huge saving in initial and operational costs. One way to achieve this aim is to enhance the effective thermal conductivity of fluids that transfer the heat. Since the thermal conductivity of most liquids is low, there has been interest to use suspended solid particles to enhance the thermal conductivity of the base-fluid. Dispersion of micrometer or even millimeter particles in base-fluid was used earlier by researchers. However these earlier attempts have faced obstacles such as, increasing in pressure drop, sedimentation of particles and erosion of equipment. Choi and his co-worker in 1995 have found a new class of fluids with suspension of nanoparticles that is called “nanofluid”. Investigation showed that nanoparticles have the ability to improve the effective thermal conductivity of base fluid and are useful for different industrial applications (Aly, 2014; Chol, 1995; Kasaeian et al., 2015).

In the past decade, researchers examined many kinds of nanomaterials for preparing nanofluids. Al_2O_3 , CuO, TiO_2 and ZnO were typically used in many nanofluids compared to other kinds of metal oxide nanomaterials (Khoshvaght-Aliabadi, 2014; Yarmand et al., 2014). Carbon based materials such as, CNT, GO (Parambath Sudeep et al., 2014) and Graphene were also examined experimentally by a number of researcher (Amiri, Sadri, Shanbedi, Ahmadi, Chew, et al., 2015; Aravind & Ramaprabhu, 2013; Choi et al., 2001; Das et al., 2003; Karthikeyan et al., 2008; Turgut et al., 2009). Nanofluids have attracted researchers since the material in the nanometer size have shown unique physical and chemical properties. In particular, many nanofluids have shown enhanced thermal conductivity, which makes them suitable for use as working fluids. Experimental studies

also revealed that adding nanoparticles to base fluids not only enhances thermal conductivity but also augments convective heat transfer compared to the pure base fluids.

In the recent years, significant investigations on the use of carbon-based nanomaterials such as, single-wall carbon nanotube, multi-wall carbon nanotube, graphene oxide and graphene platelet to make nanofluids were reported in the literature (Ding et al., 2006; Yu et al., 2010; Yu, Xie, Wang, et al., 2011; Zheng et al., 2011). New research indicates that carbon based nanofluids could provide higher thermal conductivity enhancement in comparison to other tested nanofluids. Carbon based materials have better thermal conductivity, higher mechanical strength and also electrical conductivity. The excellent thermo-physical properties of those particles has made them an excellent candidate for synthesis of nanofluids (Novoselov et al., 2004).

In the current chapter earlier reported various methods for preparation, stability, thermos-physical property and convective heat transfer of nanofluids have been reviewed.

2.2. Nanofluid preparation

One of the important steps for any kind of nanofluid applications is the preparation of nanofluids. The production of nanofluid usually is a complicated process which has significant effect on thermal performance of final production. Two techniques have been reported: Single step method and two-step method.

Combination of preparation process of nanoparticles with synthesis of nanofluids is called “single –step” method, the nanoparticles are directly made by liquid chemical technique or physical vapour deposition (PVD) method. The storage, drying, transportation and dispersion processes are no need in this method. In addition, the nanofluids are highly dispersed/stable and sedimentation is minimized. But the applications of this method is limited because only low vapour pressure fluids are compatible to withstand this process (Y. Li et al., 2009).

Dispersion of nanoparticles in the base fluids is named “two-step” method. Firstly, dry nanoparticles are made with various methods such as mechanical alloying, chemical vapour deposition, inert gas condensation or another appropriate methods and then as-prepared nano-powder dispersed into a liquid in a next processing step. Agglomeration is a big problem for this method, the agglomeration cause clogging and settlement of channels and also decrease the effective thermal conductivity of fluids. Some methods are used for decrease of the aggregation and enhance dispersion capability such as adding surfactant, ultrasonication (bath or probe) or functionalization of the nano-powder. Industrial scale of nanopowder synthesis are already have been done by many companies, there are promising cost effective advantages to use these powder particles for two-step synthesis methods. Only a highlighted obstacle that must be considered/solved is stability of nanofluids (Hong et al., 2005).

2.3. Stability of Nanofluid

Stability of homogeneous suspension is a key point for nanofluid application. Since van der Waals interface between nanoparticles is very strong, they naturally prefer agglomeration form. Homogeneous suspension of nanoparticles have direct effect on thermal conductivity and conductive heat transfer of nanofluids. Therefore, to find stable nanofluids, some parameters are investigated and various techniques are suggested. Since there is a theory that confirmed aggregation and clustering are main key point in significant enhancement in thermal conductivity of nanofluids but it is important to find an optimized link between thermal conductivity and stability (Evans et al., 2008; Timofeeva et al., 2007). There are some common methods for improving the stability of nanofluids such as surface chemical treatment (pH control), addition of surfactant and ultrasonic vibration (Ghadimi et al., 2011). Some researchers used one method (Chandrasekar, Suresh, & Bose, 2010) but the others prefer to apply two or three

techniques together to make a stable nanofluid (Pantzali, Kanaris, et al., 2009). The important parameters on stability of nanofluids are listed below:

2.3.1. Surface chemical treatment (pH control)

Electro-kinetic properties have direct influence on stability of aqueous nanofluids. Due to an enhanced surface charge density, powerful repulsive forces can stabilize a well homogenous dispersed suspension (X.-j. Wang & Zhu, 2009). Sometimes a simple acid treatment process of nanoparticles make a well-stable suspension (Xie et al., 2003), this is owing to the changes of surface nature from hydrophobic to hydrophilic because of introducing of functional hydroxy group.

This behaviour can be described by introducing of the isoelectric point (IEP). As the pH of the nanofluid goes far away from the IEP, the surface charge rises due to more frequent attacks to the surface phenyl sulfonic group and hydroxyl groups by potential-determining ions (phenyl sulfonic group, H^+ and OH^-), and the colloidal particles become more stable and finally vary the thermal conductivity of the fluid (Yousefi et al., 2012).

2.3.2. Ultrasonic vibration

Ultrasonication method was introduced for procurement of stable homogeneous nanofluid. Purpose of all the methods is to change the surface behaviour of nanoparticles and to overcome aggregation of particles with the final goal of making stable nanofluids. Bath and probe ultrasonication are powerful instruments to break down the particles and avoid the agglomeration of nanoparticles. But sometimes after exceeding the optimized time of ultrasonication or applying high energy sonication, it can make a serious defect on the agglomerating particles and provide rapid sedimentation (X. F. Li et al., 2008).

2.3.3. Addition of surfactant

Adding of activator surfactant is one of the common methods to prevent settlement of nanoparticles. Adding of surfactant can enhance the dispersion and stability of the nanoparticles. It is due to the fact that the surfactant can change the hydrophobic surface feature of nanoparticle to hydrophilic. Enough amount of surfactant must be added to the liquid, if inadequate surfactant is applied then it cannot provide an appropriate coating to overcome the electrostatic repulsion (Jiang et al., 2003). It is noticeable that adding of surfactants usually increase the viscosity of nanofluid significantly which is not admirable. Another disadvantage of surfactant is temperature limitation, it means for application with the temperature of higher than 60 °C the bonding between nanoparticles and surfactant could be loosened along with the strength of stability (Assael et al., 2005; X.-Q. Wang & Mujumdar, 2008).

There are some popular surfactants such as cetyltrimethylammoniumbromide (CTAB) (Assael et al., 2005; Pantzali, Mouza, et al., 2009) , sodium dodecylsulfate (SDS) (Y Hwang et al., 2007), Sodium dodecylbenzenesulfonate (SDBS) (X.-j. Wang & Zhu, 2009), Polyvinylpyrrolidone (PVP) (H. Zhu et al., 2007), salt and oleic acid (Yujin Hwang et al., 2008) and Gum Arabic(GA).

Selecting the appropriate surfactant with adequate amount is very important and there is no standard procedure for choosing a surfactant.

2.4. Stability Examined Tools

Despite the importance of stability of nanofluids in the applications, there is a lack of investigation on this issue. There are common tools and techniques which can evaluate the stability of nanofluid such as zeta potential, UV-Vis spectrophotometer, light scattering, TEM (Transmission Electron Microscopy) and SEM (Scanning Electron Microscopy), three omega, sedimentation balance and sediment photograph capturing

method. Then, sedimentation percentage of nanoparticles can be evaluated by exploring the data.

2.4.1. Zeta potential

Zeta potential test is the most common method for stability evaluation of nanofluid. It is work based on electrophoretic rule, the electrostatic expulsion within the nanoparticles rise when zeta potential shows high value (absolute) then it makes at the well-stable nanofluids (D. Lee et al., 2006). Particles with a low surface charge have a tendency to agglomerate. Normally, the suspension with absolute measured zeta potential value higher 30 mV (positive or negative) is accepted as a well-stable nanofluid (see table 1) (Vandsberger, 2009). Most important parameter in zeta potential value of suspension is pH with the change of pH the zeta potential value is altered. X. Li et al. (2007) has investigated the effect of pH on zeta potential and the stability of nanofluids.

Table 2.1: Zeta potential value and stability

Z potential (absolute value [mv])	Stability
0-15	No stable
15-30	Low stable with settling lightly
30-45	Stable
45-60	Well stable, possible settle down
< 60	Very well stable, low sedimentation

2.4.2. UV–Vis spectrophotometer

One of the most common and reliable instrument for stability evaluation of suspension is Ultra Violet–Visible spectrophotometer (UV–Vis). It is noticeable that this tool is applicable for stability measurement of all kinds of base fluids, but zeta potential has limitation for the viscosity of the fluids. This method employed the law that the light intensity of each material is different by scattering and absorbing of light passing through

a liquid. Stability of suspension is found by measuring the sediment weight percentage versus the time with UV–Vis spectrophotometer (K. Lee et al., 2009).

The procedure of stability measurement is briefly explained as follows. Firstly, scan very dilute suspension to figure out the peak absorbance of nanoparticles. After that, prepare the wanted volume concentration of suspensions and keep it aside for a period of time. Every times it is desired to check the stability, the relative concentration can be graded by UV–Vis spectrophotometer and also concentration could be plotted versus time (Y Hwang et al., 2007).

2.4.3. TEM (Transmission Electron Microscopy) and SEM (Scanning Electron Microscopy)

SEM and TEM are very suitable instruments to determine the size, shape and dissemination of nanoparticles. But they cannot show the real position of nanoparticles in base liquid. For solving this difficulty the Cryogenic electron microscopy (Cryo-SEM and Cryo-TEM) method has been employed, this method is useful if the nanofluids microstructure is not altered throughout cryoation. Also Aggregation of nanoparticles can be investigated by these tools. The brief standard procedure for TEM and SEM photographs of nanofluid is as follows. Stable solution of nanaofluid is prepared and then allow one drop of it on carbon grid of TEM (sticky tape of top surface of the SEM specimen holder in the case of SEM). After that the carbon grid is dried with the liquid in natural air or in the vacuum oven, then coated with Pd and Au. The obtain nanopowder is then put into the TEM or SEM vacuum chamber for taking pictures.

2.4.4. Three omega method

Three omega method can be shown for the stability of nanofluid but only a few research have been done with this technique. It can be assessed by identifying the thermal

conductivity growth caused by the nanoparticle sedimentation in a wide nanoparticle volume fraction range.

2.4.5. Sedimentation balance method

Sedimentation method is another way to identify the stability of nanofluid. The weight of residue nanoparticles throughout a define period of time is calculated. The weight suspension fraction of nanofluid at a certain time is measured by the equation $F_s = (W_0 - W)/W_0$. The weight of the sediment nanoparticles at a certain time is named W and the total weight of nanoparticles in this period of time is W_0 (H. Zhu et al., 2007).

2.4.6. Sediment photograph capturing method

Photo capturing is an elementary method to figure out the stability of suspension. Whenever the nanofluid is prepared, specific amount of sample will keep aside to take photos after some times. With comparison of these photos of nanofluids samples the stability of suspension will be found. But as it is obvious this is not an accurate and trustable method.

2.5. Thermos-physical properties of nanofluid

One of the important step for finding the heat transfer ability of nanofluids is investigation of the thermos-physical properties. There are several methods and equipment for measurement. The main parameters which are measured in this project are thermal conductivity, density, specific heat capacity and viscosity. This section will discuss about measurement method of above mentioned parameters and available literature for thermos-physical properties of nanofluids.

2.5.1. Thermal conductivity of nanofluids

Since thermal conductivity is the most important thermal transport parameter and shows the heat transfer ability of materials, many researchers worked on this topic and found adding small amount of nanoparticles have strange effect on thermal conductivity

of basefluid. Various mechanism for this significant improvement of thermal conductivity have been introduced such as interfacial layer, aggregation of particles and Brownian motion and also some theory like Maxwell or Hamilton theories. In this part, available literature regarding to different method for measuring the thermal conductivity, important parameter, theoretical models and existing experimental measurement has been reviewed.

2.5.1.1. Thermal conductivity measurement methods for nanofluids

Many method has been employed for thermal conductivity measurement of liquid, some of them have also been adopted for nanofluids (Figure 2.1). Among all of the methods, the transient hot-wire technique is the most common way to find the thermal conductivity of nanofluids.

University of Malaysia

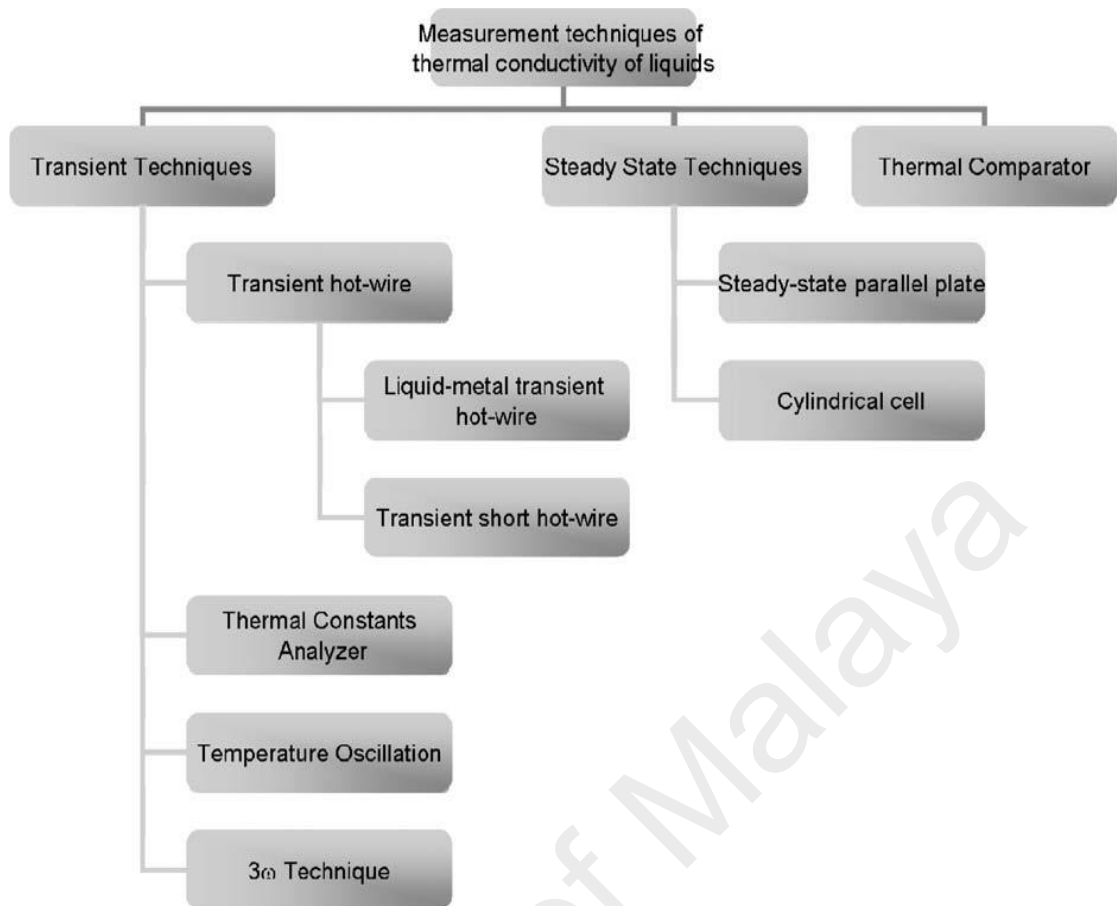


Figure 2.1: Various thermal conductivity measurement methods for nanofluids(Paul et al., 2010).

According to the available literature survey a relative frequency and popularity of use of each of the techniques for the thermal conductivity of nanofluids has been shown in Figure 2.2 .Brief explanation of the methods mentioned in Figure 2.1 are given in the below sections.

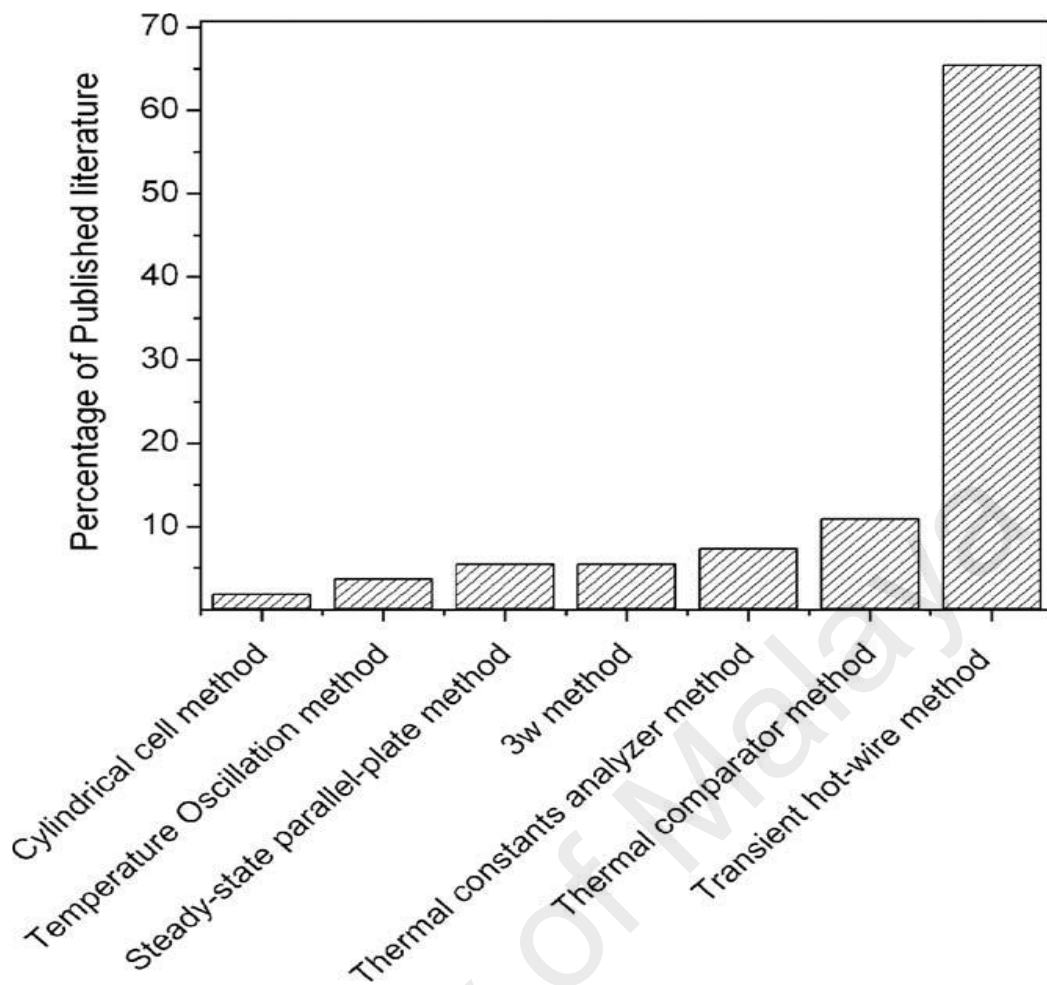


Figure 2.2: Comparison of the thermal conductivity measurement techniques for nanofluids (Paul et al., 2010).

(a) Transient hot-wire method

Stalhane and Pyk are the first researchers who introduced Transient hot-wire (THW) method for measure the thermal conductivity of powders(Horrocks & McLaughlin, 1963). After that some researchers have improved the procedure to make it more suitable. THW method has some advantage in comparison with other techniques. THW has capacity for experimentally eliminating the error due to natural convection for fluid application which is most advantage of this method. Moreover, the conceptual design of the THW device is easy compared to the arrangements required for other techniques and also this method is very fast in comparison to other methods.

In this technique, a wire of platinum has been employed both as a thermometer and as a heater. Measurement of temperature versus time response of the wire subjected to a rapid electrical pulse is the concept of the THW method. Typical apparatuses using this THW technique has been modified during past decade. Generally, the probe which is inserted into the fluids for the measurement has two function as thermometer and also heat source. To increase the temperature of wire and fluid a constant current has been supplied to the probe. There is a relation between increase of the temperature and thermal conductivity of liquid which is probe is inserted. Many researchers in the world have preferred THW method for the investigation of thermal conductivity of nanofluids (Xing Zhang et al., 2007), (J.-H. Lee et al., 2008), (Y. He et al., 2007). Figure 2.3 shows the schematic diagram of the transient hot-wire experimental set up.

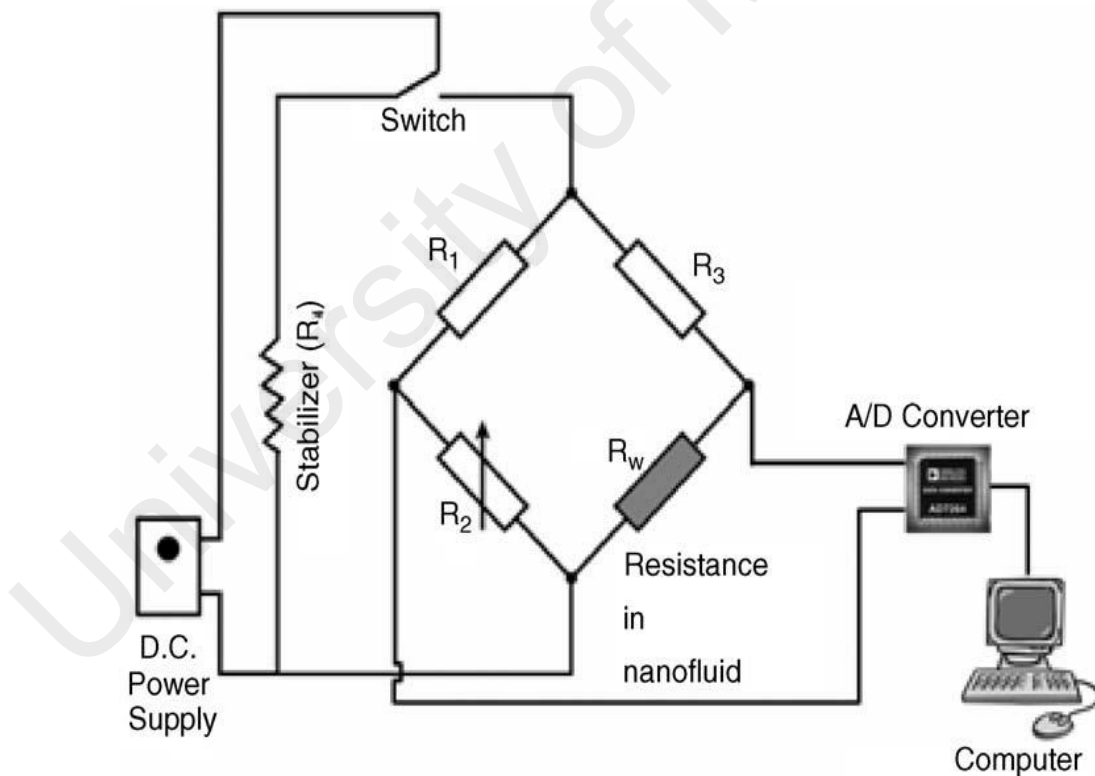


Figure 2.3: Schematic diagram of transient hot-wire (THW) experimental set up (Paul et al., 2010).

Two variations of THW method have been employed to find the thermal conductivity of nanofluids, transient short hot-wire technique and liquid metal transient hot-wire. Thermal conductivity of highly corrosive fluids like molten carbonate short hot-wire (SHW) method has been used, since it is very challenging to keep initial homogeneous constant temperature for such an extended sector which is very important to get a reliable results. This problem solved by using a smaller wire probe (10 mm height) for measuring the thermal conductivity abovementioned nanofluids in a smaller container cell (Xie et al., 2006). The liquid metal transient hot-wire is employed for electrically conducting nanofluids. A mercury-filled glass capillary is kept in the dispersion or fluid, with the glass capillary serving to insulate the mercury “hot-wire” from the electrically conducting fluid or dispersion. The mercury wire forms one resistor in a Wheatstone bridge circuit and is heated when a constant voltage is applied to the bridge. The temperature increase of the wire is calculated from the change in the resistance of the mercury with time, obtained by measuring the voltage offset of the initially balanced Wheatstone bridge.

(b) Thermal constants analyzer method

Transient plane source (TPS) theory has been employed for thermal conductivity measurement of nanofluid with thermal constants analyzer technique. TPS works as a heat source and thermometer. Fourier law is used as fundamental principle for calculating the thermal conductivity of fluid. The experimental set up contains of thermometer, thermal constants analyzer, constant temperature bath and a vessel (Figure 2.4a). The probe of the thermal constants analyzer is suspended vertically in the vessel having the nanofluid. The vessel kept in a constant temperature bath and the thermometer hold in the vessel to monitor the temperature of fluid. The thermal conductivity of the nanofluid is found by measuring the resistance of the probe. The probe comprises of an electrically conducting thin foil of a usual form which is sandwiched inside an insulating layer, as

shown in Figure 2.4b when a constant power is applied to the probe, the temperature increase of the probe, can be calculated by the probe resistance versus time.

The thermal conductivity of the fluid can be obtained from the slope of the line $(W/\pi^{1.5}r_p) k$.

Where W is the electric power supplied to the probe, k is the thermal conductivity of fluid and r_p is the radius of the probe (D. Zhu et al., 2009).

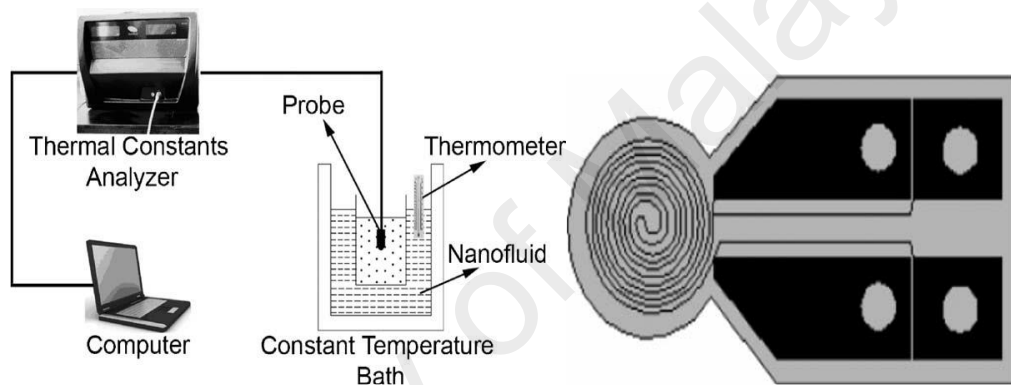


Figure 2.4: (a) Experimental setup for transient plate source method and (b) Schematic diagram of TPS sensor (Paul et al., 2010).

(c) Steady-state parallel-plate method

Steady-state parallel-plate technique is another method for thermal conductivity measurement of nanofluid, different design of cells can be used. To simplify the heat transfer mainly in one direction either concentric cylindrical cell type or parallel-plate type is preferred. A schematic experimental set up is shown in Figure 2.5. Small amount of liquid is placed between gaps of two parallel round plates. Two important parameters must be carefully considered in this method: (1) need to precisely monitor the temperature in every thermocouple. The change in temperature measuring must to be minimized when the thermocouples are at similar temperature. (2) need to be carefully controlled that no

heat loss from the liquid to the surrounding is happened. A guard heater is installed to keep the temperature constant. The guard heater must heated with a same temperature of fluid to prevent heat losses from fluid.

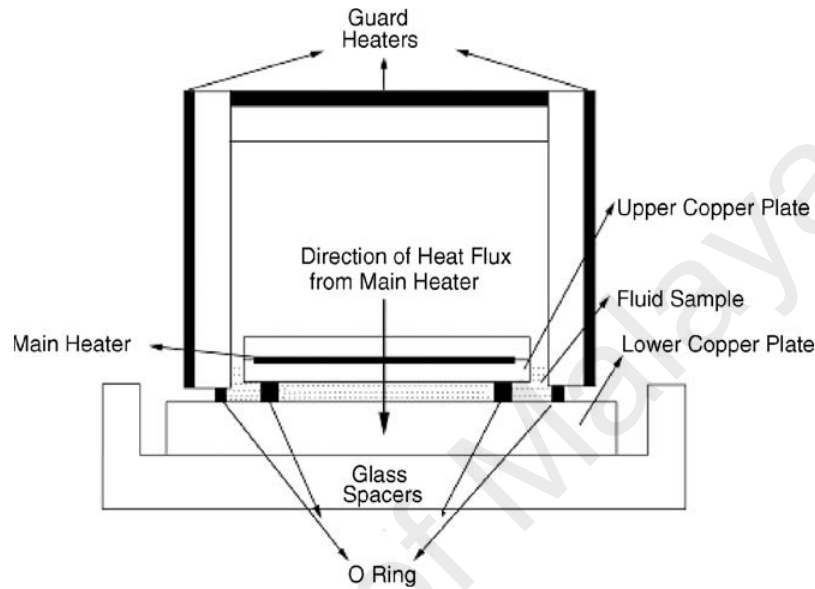


Figure 2.5: Schematic diagram of the experimental set up for steady-state parallel-plate method (Paul et al., 2010).

Thermal conductivity of the liquid can be found as following equation:

$$k = \frac{k_s - k_g S_g}{s - s_g} \quad (2.1)$$

Where, k_g , S , and S_g are the thermal conductivity, cross-sectional area of the top copper plate, and the total cross-sectional area of the glass spacers, respectively.

(d) Cylindrical cell method

One of the common steady-state techniques for measuring the thermal conductivity of nanofluid is cylindrical cell method. The nanofluid filled in an annular gap between two horizontal concentric cylinders. The equipment includes a bunch of coaxial inner copper cylinder and outer galvanized cylinder. A heater is installed inside the inward pipe and the back and front sides of the apparatus are insulated to avoid the heat loss during the

test. Two thermocouples are placed in the middle of test section and linked to a digital data logger. Heat flows in the radial direction outwards through the test liquid (Kurt & Kayfeci, 2009). The thermal conductivity of nanofluid in the gap can be found as follow,

$$k = \frac{\ln(r_2/r_1)}{2\pi L \left[\left(\frac{\Delta T}{\dot{Q}} \right) - \left(\frac{\ln r_3/r_2}{2\pi L k_c} \right) \right]} \quad (2.2)$$

Where, \dot{Q} is the input heat, ΔT is the temperature difference $T_o - T_i$, k_c is the thermal conductivity of cooper and L is the length of the tube, r_1 , r_2 and r_3 are the outward radius of the glass tube, inner and outer radius of the inner pipe respectively (Figure 2.6).

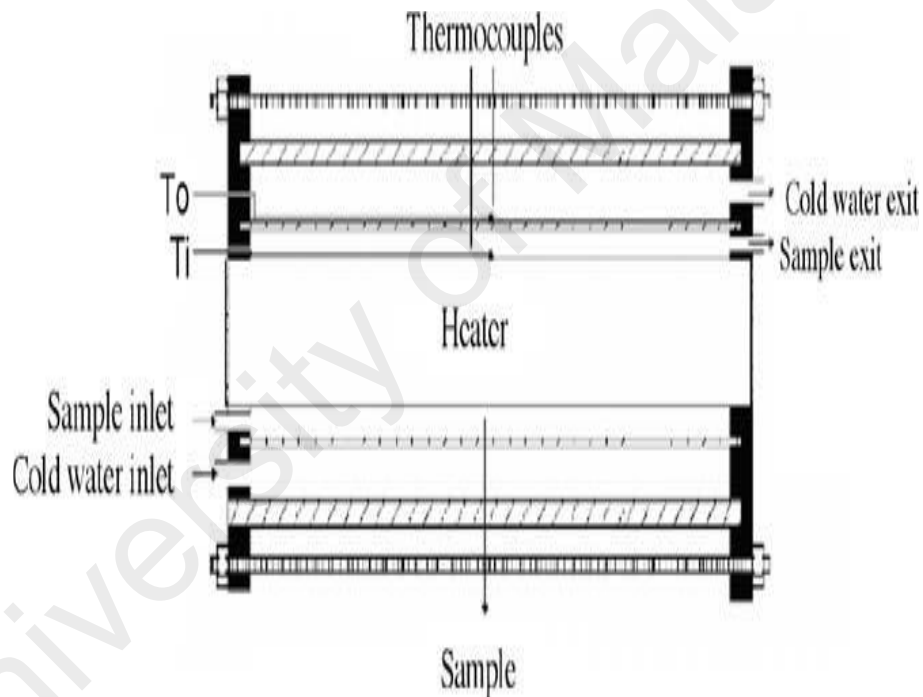


Figure 2.6: Schematic diagram of the cylindrical cell equipment (Paul et al., 2010).

(e) Temperature oscillation method

The technique which measures the temperature response of fluid when heat flux or temperature oscillation applied is called temperature oscillation method. The monitored temperature response of the fluid is the outcome of localized or averaged thermal conductivity of nanofluid in the direction of chamber height. The experimental method work based on oscillation theory. Experimental set up shown in Figure 2.7.

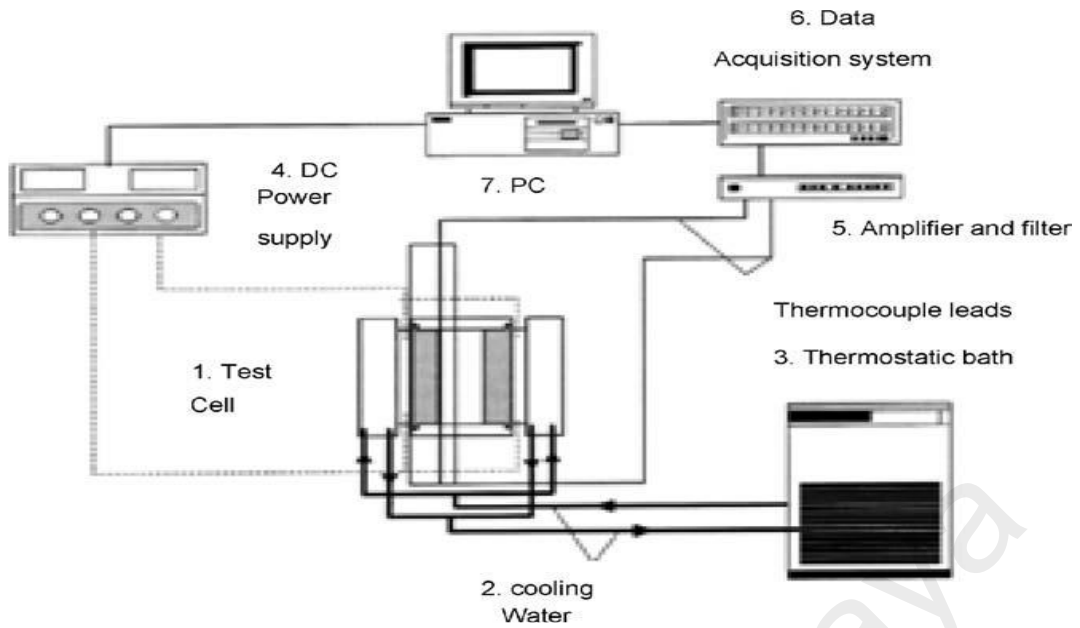


Figure 2.7: Experimental set up for temperature oscillation technique (Paul et al., 2010).

The thermal conductivity can be found as,

$$k_{nf} = \alpha_{nf} \rho_{nf} C_{p,nf} \quad (2.3)$$

Where ρ_{nf} is density of nanofluid, $C_{p,nf}$ is the specific heat of nanofluid and α_{nf} is the thermal diffusivity of nanofluid, thermal diffusivity of the fluid can be measured very accurately by considering amplitude attenuating of thermal oscillation from the boundary to the axis of the fluid. Hence, thermal diffusivity of nanofluid can be measured from experiment.

(f) 3ω method

3ω method employed similar methodology for thermal conductivity measurement with hot-wire technique. An element used both as thermometer and heat source, use of the temperature oscillation as an alternative of the time dependent response is the key change. A periodic sinusoidal current passes across the metal element and creates a heat wave at 2ω and it can be deduced by the voltage synthesizer at frequency 3ω .

The 3ω equipment is manufactured by patterning and metal deposition, the device is coupled to a metal heater with wire. A well is made around the heater which is containing

the nanofluids. The micro-device is sited inside of a temperature controlled cryostat. This technique is generally applied for the measurement of temperature dependent thermal conductivity of nanofluids (Oh et al., 2008).

2.5.1.2. Enhancement in thermal conductivity of nanofluid

Since the most important parameter on heat transfer ability of the nanofluid is thermal conductivity many research has been done on this area. All the experimental works have confirmed the improvement of the thermal conductivity by adding of nanoparticles. Copper oxide and alumina are the most common and low-cost nanoparticles used by numerous researchers in their experimental studies.

Eastman et al. (1996) investigated the thermal conductivity of nanofluids having CuO, Cu and Al₂O₃ nanoparticles with two different base fluids: oil and water. A 60% enhancement of the thermal conductivity was observed as compared to the base fluids for 5 vol % of nanoparticles. They also confirmed that the use of one –step method make higher enhancement than use of two-step method. Patel et al.(Patel et al., 2003) worked on silver and gold nanoparticles in water basefluid. They found 5%–21% enrichment of the thermal conductivity of water based nanofluids at a very low concentration of 0.00026 vol% of silver particles and also reported enhancement of 7%–14% for gold-water nanofluid at volume concentration of 0.011%. Hong and Yang (Hong et al., 2005) prepared Fe-ethylene glycol with a chemical vapor process. They observed higher enhancement of thermal conductivity in comparison with cu-ethylene glycol nanofluid, their investigation confirmed that the thermal conductivity of particle is not an only parameter on enhancement of thermal conductivity of nanofluid it means sometimes a particle with a lower thermal conductivity can make higher enhancement. Also, they established that the thermal conductivity of nanofluids improved non-linearly with the particles volume fraction.

Recently, many researchers found that the largest rises in thermal conductivity have been detected in suspensions of carbon based nanoparticles, which have very high thermal conductivity and very high aspect ratio. Choi et al.(Choi et al., 2001) investigated effective thermal conductivity of MWCNT (multi wall carbon nano-tube), they found that the measured thermal conductivity was extraordinary greater than other nanoparticle materials examined previously, the carbon nanotubes reached the highest conductivity enhancement and provided wide opportunities for many applications. Biercuk et al.(2002) reported the thermal conductivity of single wall carbon nanotubes (SWNT). Their result showed 125% enhancement for 1.0 wt% SWNT. They pointed out that the bundling of nanotubes could be an important factor for thermal transport characteristics and they pointed out that the bundling of nanotube can be most important reason of this enormous improvement. New research indicates that graphene based nanofluids could provide higher thermal conductivity enhancement in comparison to other tested carbon based nanofluid (Shirazi et al., 2015).

Previous studies confirm that thermal conductivity of nanofluids depends on various factors such as particle material, volume fraction, particle size, particle shape, base fluid material, temperature and Acidity of the nanofluid. In this section, a specific parameter that is effective on thermal conductivity is briefly explained.

- 1) Effect of particle material: The researches confirm that particle material is a most important parameter that have effect on the thermal conductivity of nanofluids.

At first view, it may seem that the variance in the thermal conductivities of particle materials is the key cause of this effect. However, new experiment show that particle type might be affected the thermal conductivity of nanofluids in other ways. Effect of particle material is much more significant when carbon based nanoparticles are used for the nanofluids preparation.

- 2) Effect of volume fraction: Particle volume fraction is a parameter that is examined in most of the experimental researches and the results are generally in compromise qualitatively. Most of them confirm that enhancing thermal conductivity with increasing particle volume fraction and usually there is a linear relation. Nevertheless, there are also few researches, which report nonlinear behavior.
- 3) Effect of particle size: Another important parameter on thermal conductivity of nanofluid is size of particle. Generally nanoparticles are in range of 5 to 100 nm. The overall trend of available experiment confirm that thermal conductivity of nanofluid decrease with increasing particle size. This phenomena is due to two physical insight mechanism; liquid layering around nanoparticles and Brownian motion of nanoparticles. . However, there are also some inconsistent result in the literature that show increasing thermal conductivity with increasing particle size.
- 4) Effect of particle shape: spherical particles and cylindrical particles are two common shape of nanoparticle which is used in nanofluid applications. Recently, graphene nanoparticle which has plate shape attract the interest of researcher because of larger surface area. Generally, cylindrical nanoparticle make more improvement in thermal conductivity of nanofluid rather than spherical particles. In addition, graphene nano platelets (multi-layer plate surface area) has the highest enhancement in thermal conductivity of nanofluid.
- 5) Effect of base fluid: Different base fluid has various viscosity and viscosity of base fluid has direct effect on Brownian motion of nano particle that in turn affect the thermal conductivity of the nanofluid (Xuan et al., 2003). Additionally, Lee (D. Lee, 2007) studied the effect of electric double layer forming around nanoparticles on the thermal conductivity of nanofluids and indicated that the thermal conductivity and thickness of the layer has direct relation to the base fluid.

- 6) Effect of temperature: change of temperature have effect on the clustering of nanoparticles and Brownian motion of nanoparticles, which has direct influence on significant change of thermal conductivity of nanofluids. Most of available literature confirm that thermal conductivity of nanofluid enhances with increase of temperature (C. H. Li & Peterson, 2006). However , there are some contradictory results which is reported with Turgut et al (Turgut et al., 2009) and Masuda et al (Masuda et al., 1993).
- 7) Effect of acidity: The number of researches reports regarding the acidity value of nanofluids is very limited when compared to research on effect of other parameters. The exact optimum PH values are not found yet. But the fact that at the optimum acidity value, nanoparticle have higher surface charge which makes more repulsive forces between nanoparticles. As a result of this phenomena, severe clustering of nanoparticles is avoided which has negative effect on thermal conductivity of nanofluid (X.-j. Wang & Zhu, 2009).

2.5.2. Viscosity of nanofluids

However, nanofluid can enhance the efficiency and thermal performance of energetic processes, but some limitations which include abnormal viscous behavior must be considered as well. In this section, effects of the parametric variables and theoretical models which are employed to forecast the viscosity of nanofluids have been reviewed.

2.5.2.1. Newtonian and Non-Newtonian Behavior

The phenomenon of Newtonian behavior of nanoparticles suspension has been extensively investigated by many researchers. Yu et al. (Yu, Xie, Li, et al., 2011) reported an experimental research into the viscosity of aluminum nitride nanofluids. Aluminum nitride nanoparticles (AINs) were dispersed in propylene glycol (PG) and ethylene glycol (EG) base fluids. For a volume concentration less than 5.0%, both fluids showed Newtonian behavior, but for higher volume concentrations, the shear-thinning behavior

of nanofluids have been indicated. Prasher et al. (2006) studied that the rheological behavior of $\text{Al}_2\text{O}_3/\text{PG}$ nanofluids, they found that viscosity of sample independent of shear rate, and increased with volume fractions. Most of experimental results showed that some nanofluids have Newtonian behavior but another's nanofluid exhibited shear-thinning behavior. And also, for some nanofluid for lower volume concentration the behavior of nanofluids was Newtonian but with increasing of volume fraction the behavior was changed (Garg et al., 2008).

2.5.2.2. Effects of temperature

Since in industry most of the time different temperature of working fluids is required, this is very important for researchers to find the effect of temperature on the viscosity of nanofluid. Godson et al. (2010) investigated the viscosity of Ag/water nanofluids in the temperature range of 50 °C to 90 °C and reported 45% improvement at 0.9% volume concentration. Duangthongsuk and Wongwises (2009b) found 4–15% enhancement for viscosity of $\text{TiO}_2/\text{water}$ nanofluid for the volume concentrations of 0.2–2.0% and at the temperature range of 15–35 °C. All the above mentioned researchers conclude that same trend for nanofluid and confirmed that viscosity of various type of nanofluids decrease with increase of temperature. Also most of the other researches showed same result data (Kole & Dey, 2010),(Ferrouillat et al., 2011) and (Aladag et al., 2012).

2.5.2.3. Effects of volume concentration

Viscosity of nanofluid enhances with the increase of nanoparticle volume concentration in the base fluid. Pak and Cho (1998) studied the viscosity of TiO_2 and Al_2O_3 nanofluids in the volume concentration from 1.0% to 10% and found viscosity improvement. Bobbo et al. (2012) obtained viscosity improvement of 12.9% for SWCNT nanofluid and 6.8% viscosity enhancement for $\text{TiO}_2/\text{water}$ nanofluid at 1.0% volume concentration. All of others researches showed the same trend regarding the effect of

volume concentration of nanoparticles on viscosity of nanofluid (X. Wang et al., 1999) , (Phuoc & Massoudi, 2009).

2.5.2.4. Effects of particle shape and size

Nguyen, Desgranges, Roy, Galanis, Mare, Boucher, and Angue Mintsa (2007) studied the viscosity of Al_2O_3 aqueous nanofluid for the different size of particles. They used two particle sizes of 36 and 47nm of Al_2O_3 and found that the viscosity of 47 nm size particle is higher than 36 nm size particle at same volume concentration of nanoparticle. Chevalier et al. (2007) investigated the viscosity of Silicon dioxide/ethanol nanofluid with the particle sizes of 35, 94 and 190 nm in the volume concentration range of 1.4–7% and found that viscosity rises with the decrease of particle size. Timofeeva et al. (2009) clarified that the viscosity of nanofluid is toughly dependent on the particle shape and they established higher results with elongated particles such as cylinders and platelets compared to spherical nanoparticles.

2.5.2.5. Effects of base fluid

Viscosity of nanofluids are strongly dependent to the viscosity of base fluids. Water, propylene glycol, ethylene glycol and mixture of water/ethylene glycol are commonly used base fluid for preparation of nanofluids. L. Chen et al. (2008) made MWCNTs nanofluids by using various base fluids (water, glycerol, silicon oil and ethylene glycol) and found that glycerol and ethylene glycol based nanofluids reduce the viscosity enhancement when the temperature is more than 55 °C. They also prepared TiO_2 /Water and TiO_2 /EG nanofluids and reported maximum viscosity improvement of 23% with 1.86% volume concentration of TiO_2 /EG nanofluid and highest viscosity enrichment of 11% with 1.2% volume concentration of TiO_2 /water nanofluid (H. Chen et al., 2007). Sundar et al. (2012) examined three different kind of base fluids such as 20:80%, 40:60% and 60:40% Water/EG mixtures for making Fe_3O_4 nanofluids. They observed 296%

viscosity enhancement with 60:40% Water/EG mixture based nanofluid compared to other nanofluids.

2.5.3. Density of nanofluids

The correlation for the density measurement of two-phase mixtures flow of micrometer size is introduced by Cheremisinoff (1986). Pak and Cho (1998) approved the same equation for nanopowder size particles, which is remarked by the following formula:

$$\rho_{nf} = (1 - \phi)\rho_{bf} + \phi\rho_{np} \quad (2.4)$$

Where ρ_f and ρ_{np} are the mass densities of the based fluid and the solid nanoparticles, respectively.

Pak and Cho measured the density at only one temperature (25 °C) for TiO₂ and Al₂O₃ nanofluids up to 4.5% volume concentration to verify above mentioned equation. R. Vajjha et al. (2009) studied the density of three types of nanofluids including zinc oxide, antimony-tin oxide, aluminum oxide nanoparticles in a base fluid of 60:40 EG/W, they used Anton Paar digital density meter. Those measurements were compared with the theoretical equation introduced by Pak and Cho.

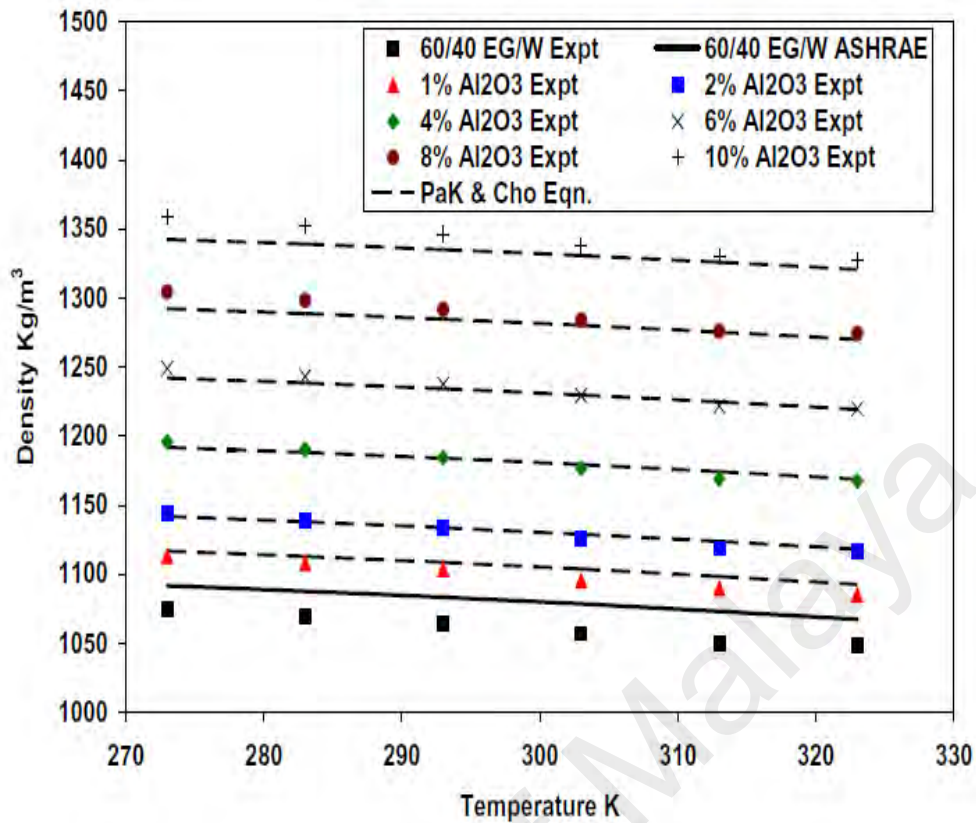


Figure 2.8: Comparison of experimental density values (Vajjha et al) with theoretical correlation (Pak and Cho) for different particle volumetric concentrations as a function of temperature (R. S. Vajjha & Das, 2012).

The assessments between theoretical equation values (Pak and Cho) and experimental values for the Al_2O_3 nanofluid have been shown in Figure 2.8. A good agreement between the predicted and experimental measured values is observed. They also investigated the densities of the SiO_2 and CuO nanofluids and found similar close agreement. Therefore, the Pak and Cho equation can be accepted for all kind of nanofluids. The density of nanofluids increases with an increase in the volumetric concentration of the particles as their densities are higher than that of the base fluid. The density of nanofluid decreases very modestly with temperature mostly due to the effect on the fluid. Not enough density measurements have been reported for different nanofluids at different temperatures in the available literature. It is important to highlight that there is lack of research for density measurement of cylindrical (CNT) and plate (GNP) nanoparticles.

2.5.4. Specific heat capacity of nanofluids

Many different models of differential scanning calorimeter (DSC) has been used by research groups to investigate the specific heat capacity of nanofluids. Some of them made own setup to measure heat capacity of the nanofluids samples. Using the few existing correlations and mixing theory equation are other ways to measure the specific heat capacity of nanofluids. Pak and Cho (1998) introduced the first correlation for the specific heat capacity of nanofluids as follow;

$$C_{nf} = (1 - \phi_v)C_w + \phi_v + C_{np} \quad (2.5)$$

Where, C is the specific heat capacity, ϕ is volume fraction of nanoparticles, w is the water and np means nanoparticles.

Later Xuan and Roetzel (Xuan & Roetzel, 2000) modified the Eq. (2.5) and introduced an improved fit equation ;

$$(\rho C_p)_{nf} = (1 - \phi)(\rho C_p)_f + \phi (\rho C_p)_{np} \quad (2.6)$$

Where ρ_{nf} is the density of the nanofluid and C_p is the specific heat of the nanofluid. In addition, f, np and nf refer to fluid, and nanoparticle and nanofluid, respectively.

Hanley et al. (O'Hanley et al., 2012) measured experimentally the specific heat of three different nanofluid at various volume fraction by using DSC (TA Instruments Q2000). They found very good agreement between experimental result and theoretical data (Eq.6) but they mentioned that Eq.5 has significant deviation from experimental data and not very accurate for measuring the specific heat capacity of nanofluid. Murshed (2011) also confirmed that Eq.6 has excellent agreement with experimental data. Later , Kulkarni et al. (2008), Vajjha & Das (2009), Zou et al (2010) and some other researchers have been derived developed correlation for different type of nanofluids (Pakdaman et al., 2012; Shin & Banerjee, 2011).

Some available literature investigated the effect of volume fraction on the specific heat capacity of nanofluids. Some research confirmed that specific heat of nanofluid is increased with the decrease of volume fraction. S. Zhou and Ni (2008) reported that with increase the volume fraction of Al_2O_3 in water the specific heat of nanofluid is decreased up to 25%. P. Namburu et al. (2007) observed that specific heat of SiO_2 -EG/Water (60:40) nanofluid decreased 12% by increase of nanoparticle up to 10%. Murshed (Murshed, 2011, 2012) have examined simultaneously the specific heat of four different nanofluid at various volume concentration, he dispersed Al_2O_3 , TiO_2 and AL in ethylene glycol and found for all of samples with increase of volume fraction the specific heat of nanofluids fall down. Ghosati et al. (2014) also found the specific heat of graphene nanofluid decreased with increase of nanoparticle weight fraction. On the other hand, some researcher observed opposite result for the effect of volume concentration on the specific heat of nanofluids. Mohebbi (2012) reported that specific heat of nanofluids decrease with decreasing of nanoparticles volume concentration. S. Sonawane et al. (2011) found very interesting result, they examined Al_2O_3 -ATF (aviation turbine fuel) and observed at low volume concentration the specific heat is less than base fluid but for high volume concentration the specific heat is more than basefluid. Also some other researchers found some challenging results about relation between volume concentration of nanoparticles and specific heat of nanofluids (Ho & Pan, 2014; Kumaresan & Velraj, 2012; Shin & Banerjee, 2014).

Majority of available researches confirmed the significant effect of temperature on specific heat of suspension. Gangacharyulu (2010) reported that the specific heat of Al_2O_3 -water increased with the decrease of temperature. Saedinia et al. (2012) also found same trend for CuO -PEO (pure engine oil) nanofluid. But De Robertis et al. (2012) prepared a suspension of Cu -EG and found that the specific heat of nanofluids increasing with increase of temperature Kumaresan and Velraj (2012) found the specific heat of

MWCNT-EG/water (30:70) first has been increased by temperature but dropped down for higher than 30 °C. Liu et al.(2014), Ghazvini et al.(2012) and some others also observed that, the specific heat of the nanofluids increased with the increase of the temperature(Pakdaman et al., 2012; Xuan & Roetzel, 2000). But also few opposite result has been reported by researchers (Q. He et al., 2012). As a conclusion of this section, this is difficult to conclude above mentioned literature in an one sentences about the effect of adding nanoparticles to basfluid , volume fraction and temperature on specific heat of nanofluid. It seems this field of research still need more investigation in the future.

2.6. Electrical conductivity of nanofluids

In the past decade there has been extensive amount of study on thermos-physical properties of nanofluid, but few researcher worked on electrical conductivity of nanoparticle suspension.Ganguly et al. (2009) studied the electrical conductivity of alumina nanofluids, they reported that significant improvement of electrical conductivity with both increase in temperature and volume fraction but they found that effect of volume fraction is more important.Minea and Luciu (2012) also experimentally investigated the electrical conductivity of Al₂O₃ and they indicated that about 391% enhancement at 60 °C for a volume fraction of 4%. Baby and Ramaprabhu (2010) also found the huge electrical conductivity enhancement for exfoliated graphene based nanofluid, An augmentation of 1400% was measured for a volume fraction of 0.03% at 25 °C. Another research group found the enormous enhancement for graphene based ethylene glycol nanofluid (Kole & Dey, 2013). It can be concluded that, suspension of nanoparticles enhanced the electrical conductivity of that base fluid.

2.7. Convective heat transfer performance of nanofluids

Many experimental researches have been done on the heat transfer characteristics and thermal efficiency of nanofluids in a heat pipe. The result of all available experimental

investigations confirmed that with good dispersion of small amount of nanoparticle in base fluid, the thermal performance of working fluid increased.

Naphon et al. (2008) experimentally studied the enhancement of thermal efficiency for a heat pipe with using TiO_2 -alcohol nanofluid. The test section made from a conventional copper pipe with length of 600 mm and outer diameter is 15 mm. they tested alcohol, distilled water and TiO_2 -alcohol nanofluids as a working fluids. They prepared stable nanofluids by using an ultrasonication device. They observed with the dispersion of nanoparticles in base fluids the efficiency of heat pipe has been enhanced significantly. The main considered parameters are the effects of nanoparticle volume concentrations, charge amount of working fluid and heat pipe tilt angle on the thermal efficiency of heat pipe. The thermal efficiency of heat pipe has been enhanced up to 10.60% with adding of 0.10% volume concentration nanoparticles.

Saleh et al. (2013) also experimentally investigated the effect of using nanofluid in a copper heat pipe with an inner diameter of 7.44 mm , an outer diameter of 8 mm and length of 200 mm. They prepared ZnO-ethylene glycol nanofluids with two step method. They carefully observed the thermal resistance and temperature distribution of the heat pipe when it filled with conventional base fluid and nanofluid at different volume fraction from 0.025-0.5 %. The experimental result indicated that a small volume fraction of nanoparticles can enhanced the heat pipe resistance and temperature distribution. In addition, they noticed effect of particles size on temperature distribution.

S. S. Sonawane et al. (2013) experimentally investigated the heat transfer characteristics of Al_2O_3 water nanofluids as working fluid used in concentric tube heat exchanger. The experimental data revealed in a varied range of Reynolds numbers and nanoparticle volume concentrations the nanofluids made significant enhancement in heat transfer performance in comparison with conventional base fluids.

Rea et al. (2009) measured the convective heat transfer and pressure drop for alumina water and zirconia-water nanofluid in a vertical heated tube. Their experimental setup consisted of a flow loop made up of stainless steel tubing. The loop consisted of a gear pump to pump the fluid, a turbine meter for volumetric flow measurement; control valve, pressure transducer, and a heat exchanger to cool the fluid coming out from the test section (see Figure 2.9). The test section was kept vertical made up of stainless tube with an inner diameter of 4.5 mm and outer diameter of 6.4 mm and a length of 1.01 m. T-type thermocouples were cemented along the length of the test section and two T-type thermocouples were inserted into the flow channel before and after the test section for bulk fluid temperature measurement. The test section was heated with a DC power supply. They used alumina/water and zirconia/water nanofluids with 6% and 3% volume concentration of nanoparticles with particle size of 50 nm. They measured the thermal conductivity of these nanofluids with transient hot wire method with measurement accuracy of $\pm 2\%$. The viscosity of the nanofluid was measured with a capillary viscometer submerged in a temperature controlled bath with measurement accuracy of 0.5%. They found out that the thermal conductivity dependence on temperature of the nanofluid is same that of the base fluid or water.

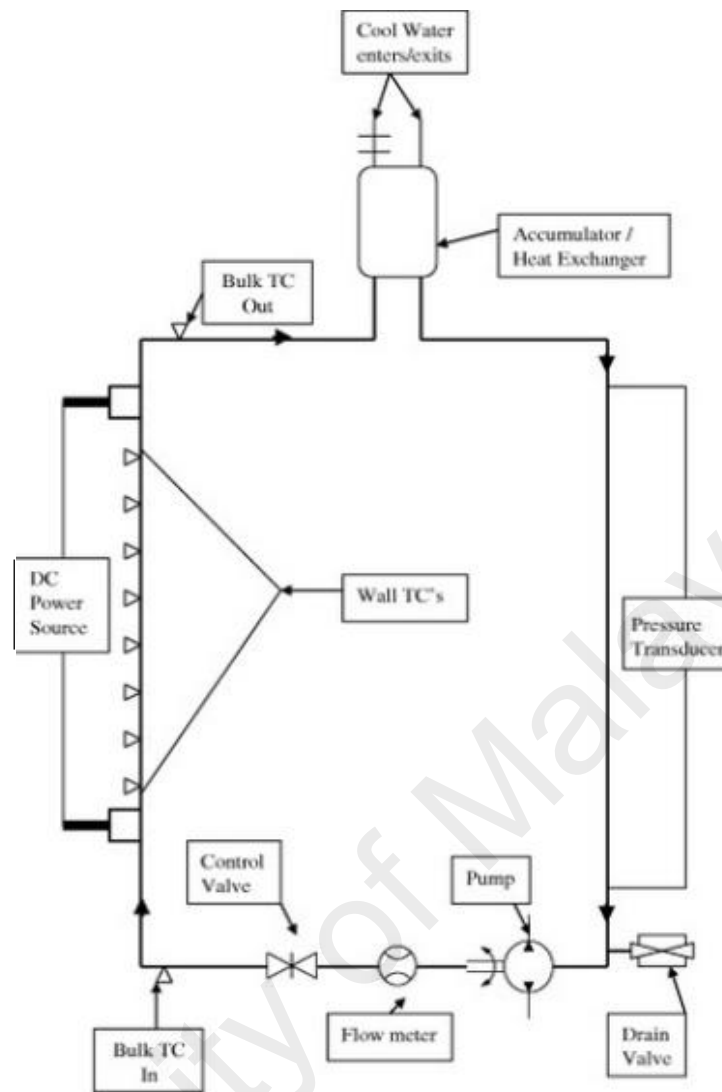


Figure 2.9: Schematic of experimental setup for convective heat transfer and viscous pressure drop measurement (Rea et al., 2009)

Haghshenas Fard et al. (2010) studied heat transfer efficiency numerically in case of laminar convective heat transfer of nanofluids in a uniformly heated-wall pipe. They employed both the single-phase and two-phase models for estimation of temperature, velocity, and heat transfer coefficient. The two-phase model was reported to be more accurate than the single-phase model. Furthermore, it is found that the heat transfer coefficient of nanofluids increases with the volume fraction of nanofluids and Peclet number raise. On the other hand, it was observed that at the fixed Peclet number of 6500, the heat transfer coefficient for 3% CuO-Water nanofluid increases by 1.54 times relative

to the base conventional fluid. Finally increasing the nanofluid volume fraction from 0.2% to 3%, leads to 27.8% increase in the heat transfer coefficient. At a particular volume fraction, CuO-Water nanofluid is of higher heat transfer coefficient as well. Similarly laminar mixed convection of Al₂O₃-water nanofluid in a horizontal tube with heating at the top half surface of a copper tube was investigated numerically by Allahyari et al.(2011). Two-phase mixture model have been employed to assess hydrodynamic and thermal performance of the nanofluid over a wide range of nanoparticle volume fraction. They have shown that increasing the nanoparticle concentration remarkably enhances the heat transfer coefficient whereas the skin friction coefficient was not considerably influenced. The natural convection in an isosceles triangular enclosure where a heat source locating at the bottom wall and filling with a Cu- Ethylene Glycol nanofluid was simulated by Aminossadati and Ghasemi (2011). A heat transfer enhancement was observed by them when the solid volume fraction and Rayleigh number were used. Mahmoudi et al. (2010) simulated a cooling system working with natural convection as a heat sink horizontally installed to the left vertical wall of a cavity filled with Cu-water nanofluid while the left vertical wall was kept at the constant temperature, and the rest ones were kept adiabatic. According to the conclusions of this study the average Nusselt number increases linearly with the increase of solid volume fraction of nanoparticles. M. Mansour et al. (2010) numerically studied a mixed convection flow in a square lid-driven cavity partially heated from below and filled with different water-based nanofluids such as Cu, Ag, Al₂O₃ and TiO₂ to find the effect of particles type and concentration on heat transfer. Finite difference method was adopted to solve the dimensionless governing equations of the problem. They reported that increase in solid volume fraction raises the corresponding average Nusselt number. Moreover, the results depicted Nusselt numbers of base fluid where it was enhanced by the addition of alumina (Al₂O₃) nanoparticles more than that of enhancement done by adding titanium oxide (TiO₂) nanoparticles to the

same base fluid. Shahi et al. (2011) analyzed the heat transfer enhancement of a nanofluid by simulation of an annular tube driven by inner heat generating solid cylinder. The finite volume method was employed with using SIMPLE algorithm on the collocated arrangement. It has been shown that the averages Nusselt numbers were increasingly depend on the solid concentration. The investigation of the effect of the inclination angle indicated that the maximum average Nusselt number and the minimum level of fluid temperature are obtained at $\gamma=0^\circ$. In addition, Izadi et al. (2009) worked on forced convection Al_2O_3 -water nanofluid flow in an annular tube by simulation. They reported that the nanoparticle concentration impact on the nanofluid is significant. In general the higher nanoparticle volume fraction is added to base fluid, the more convective heat transfer coefficient is resulted. On the other hand, at the higher Reynolds number in which the momentum and energy increases this dependency on the nanoparticle volume fraction declines.

Duangthongsuk and Wongwises (2009a) measured the heat transfer and pressure drop characteristics of 0.2 % by volume of TiO_2 /water nanofluid. The TiO_2 nanoparticles had a mean diameter of 21 nm. They used surface activators and ultrasonication to achieve better suspension characteristics of the nanofluids. The experimental setup (see Figure 2.10) they used consist of a test section, two receiver tanks, a magnetic gear pump, a hot water pump, a cooler tank, a hot water tank and a collection tank. Their test section was a 1.5 m long counter flow horizontal double-tube heat exchanger with nanofluid flowing inside the inner tube with inner diameter of 8.13 mm and outer diameter of diameter 9.53 mm. Hot water flowed through the annular PVC tube with inside diameter of 27.8 mm and outside diameter of 33.9 mm. Differential pressure transmitter and T-type thermocouples were mounted at both ends of the test section to measure the pressure drop and bulk temperatures. Thermocouples were mounted at different locations along the test section on the inner tube surface for measuring the heat transfer. They found that the heat

transfer coefficient of nanofluid increases with an increasing Reynolds number. They show that the 0.2% vol. TiO₂/water Nanofluid has a higher heat transfer coefficient than that of water by around approximately 6–11%. For 0.2% vol. TiO₂/water nanofluid, they found out that the friction factor does not change compared to that of water. This is attributed to the fact that the small addition of nanoparticles in the liquid does not change the flow behavior in the fluid and can be treated as a single phase flow.

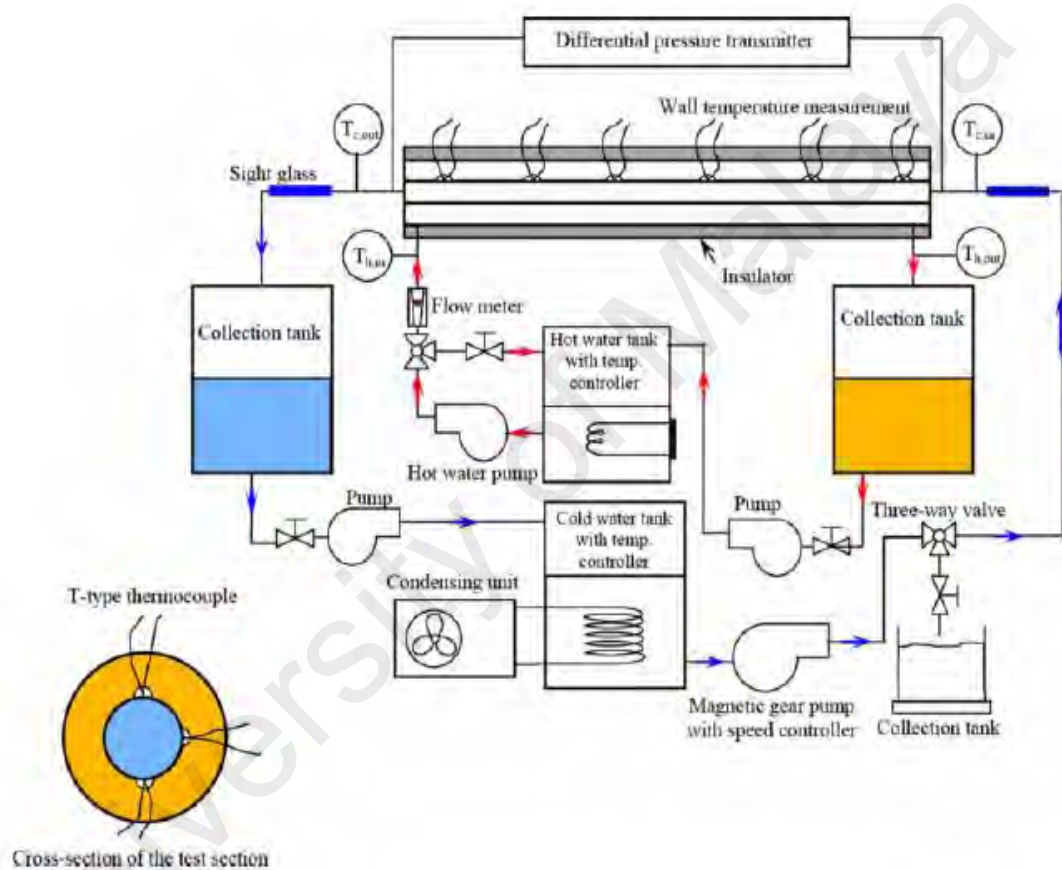


Figure 2.10: Schematic of experimental setup to measure heat transfer and pressure drop of Nanofluid, (Duangthongsuk & Wongwises, 2009a)

Chandrasekar, Suresh, and Chandra Bose (2010) investigated the friction factor and heat transfer of Al₂O₃/water nanofluid flowing through a uniformly heated horizontal tube. The 43 nm Al₂O₃ nanoparticles were prepared from an aqueous solution of aluminum chloride by microwave assisted chemical precipitation method. Nanofluid with specified volume concentration was prepared by ultra-sonication of the solution to get a

stable Al_2O_3 /water nanofluid. For the heat transfer measurement, they built a test loop consisting of a reservoir, a peristaltic pump, cooling section, test section and a collecting station. A straight copper tube of 1200 mm in length and 4.85 mm in diameter was used as the test section. RTDs are placed along the test section for heat transfer measurements. Pressure ports are connected at the inlet and outlet to the test section to measure the pressure drop. For 0.1% volume fraction, they found out that the Nusselt number increased by 12.24% at $Re = 2275$ compared to distilled water. This increase in Nusselt number is attributed to mixing effects near the wall, Brownian motion of the particles, increased thermal conductivity, particle migration and rearrangement, reduction in boundary layer thickness and delay in boundary layer development. For 0.1% volume concentration, for laminar flow they found no significant increase in the friction factor compared to distilled water. The reason for this may be attributed to the fact that the nanofluid has a low volume concentration (around 0.1%) of nanoparticles.

Suresh, Chandrasekar, et al. (2012) carried out experiments on the convective heat transfer and frictional factor characteristics of CuO/water nanofluid under laminar flow and constant heat flux. The CuO particles were prepared by sol-gel method with average particle size of 15.7 nm. The sol-gel method involves a reaction of copper chloride and sodium hydroxide. The particles formed from the reaction is filtered, washed, dried, scraped off and then ground to obtain the nanoparticles. They prepared nanofluid with concentration of 0.1%, 0.2% and 0.3% by dispersing required amount of nanoparticles in water by using ultrasonic agitation. The thermal conductivity of the CuO/water nanofluid is measured with a KD2 thermal property analyzer from Decagon Devices. The thermal conductivities of 0.1%, 0.2% and 0.3% volume concentrations of CuO/water nanofluids was reported to be 0.671, 0.682 and 0.727 W/m.K, respectively. The viscosity was measured with a Brookfield DV-I+Pro viscometer. The viscosities of 0.1%, 0.2%, and 0.3% volume concentrations of CuO/water nanofluids were reported to be 0.83, 0.86, and

0.88 cP, respectively, at 27°C. Their experimental loop setup consists of a test section pipe of 4.85 mm in diameter and 800 mm in length, heat exchanger, flow measurement device and a reservoir. Pressure transducer ports are connected to the inlet and outlet of the test section and thermocouples are attached at different locations along the test section for measuring the friction factor and heat transfer. For a Reynolds number of 2200, the experimental Nusselt for 0.1, 0.2 and 0.3% volume concentrations of CuO nanoparticles were reported to be 6, 9.9 and 12.6 %, respectively, higher than that obtained with distilled water. The friction factor for 0.1, 0.2 and 0.3% volume concentrations of CuO nanoparticles were reported to be 8, 13 and 20.7 %, respectively, higher compared to that of distilled water.

P. K. Namburu et al. (2009) simulated turbulent flow and heat transfer enhancement for three kinds of nanoparticles (CuO, Al₂O₃ and SiO₂) added to both ethylene glycol and water mixture flowing through a circular pipe under constant wall-heat flux condition. They considered the impacts of different nanoparticles and also particles concentration. In this study κ - ϵ turbulent model proposed by Launder and Spalding (Launder & Spalding, 1974) was adopted. The κ - ϵ turbulent model offers two extra equations namely turbulent kinetic energy (κ) and rate of dissipation (ϵ). The conclusions illustrated that an increase in concentration of nanofluid is led to rise of the average Nusselt number. Furthermore, the result depicted that at a specific Reynolds number of 20000, Nusselt number for 6% CuO concentration increases by 1.35 times more than the base fluid. Finally for the same concentration of CuO, Al₂O₃ and SiO₂, at a specific Reynolds number, the research results reported CuO nanofluid is of the highest heat transfer rate. Lotfi et al. (2010) reported the effect of different models of nanoparticle simulation on forced convection turbulent flow in a circular tube. They made comparisons among three different single-phase, two-phase mixture and Eulerian models. Comparison of the experimental values showed that the mixture model is the most accurate one. Finally they

concluded that the rate of thermal enhancement decreases with the increase of nanoparticles volume concentration. Ghaffari et al. (2010) studied numerically the turbulent mixed convection heat transfer of an Al_2O_3 -water nanofluid with particles size of about 28 nm throughout a horizontal curved pipe. They have applied two-phase mixture model for the simulation. The effect of the buoyancy force, centrifugal force, and nanoparticles concentration are assessed in this study. The result illustrated that increases of the nanoparticle volume fraction enhanced the Nusselt number even though its impact on the skin friction coefficient was not remarkable. Nanoparticle concentration increase also strengthened the secondary flow and indirectly influenced the skin friction coefficient. Additionally although at the low Gr turbulent intensity was insignificant, as the Gr increased the effect became more remarkable. The turbulent flow of nanofluids with different volume fractions of nanoparticles flowing through a two-dimensional duct under constant heat flux condition was simulated by Rostamani et al. (2010). The mixtures of copper oxide (CuO), alumina (Al_2O_3) and oxide titanium (TiO_2) nanoparticles and water were selected to be bended as a kind of nanofluid. The results show that both the Nusselt number and the heat transfer coefficient of nanofluid are strongly dependent on nanoparticles and increase by increasing of the volume concentration of nanoparticles. In addition the results presented that by increasing the volume fraction, the shear stress increases. The result depicted for a constant volume concentration and Reynolds number, CuO nanoparticles show the most influence to augment the Nusselt number.

L. Yu et al. (2012) investigated the thermo-physical properties and convective heat transfer phenomenon of Al_2O_3 -polyalphaolefin (PAO) nanofluids containing both spherical (NF1) and rod (NF2) like particles. The nanofluids were prepared by dispersing alumina nanoparticles in PAO under ultrasonication. Special dispersants were added to the PAO to lessen the aggregation of the nanoparticles and stabilize the nanofluid. The diameter of the spherical nanoparticles was found to be 60 nm with the aid of a dynamic

light scattering (DLS) instrument. The diameter and length of the rod like nanoparticles was found to be 7 nm and 85 nm, respectively. The experimental setup of convective heat transfer and pressure drop measurements established by Yu et al. (2012) consists of a gear pump, turbine flow meter, heat exchanger, pressure transducer and thermocouples. All the data were collected by a data acquisition unit. The test section is a circular tube made up of stainless steel with 1.09 mm inner diameter, 0.25 mm wall thickness and 306 mm length. The test section was heated using a DC power supply. Pressure transducers and thermocouples were placed in the inlet and outlet of the test section for measuring the pressure drop and bulk fluid inlet and outlet temperature. Thermocouples were also placed along the test section for measuring the heat transfer. The pressure drop experiment was conducted for a maximum Reynolds number of 460 which was limited due to the high viscosity of PAO as well as the nanofluid. They conducted the experiment for 0.65% vol. and 1.3% vol. of spherical and rod shaped particles, respectively. They found out that the nanofluids incur higher pressure drop than the base fluid and the difference get higher with increasing volume concentration of nanoparticles. Also the pressure drop of the nanofluid containing non-spherical nanoparticles was found to be always greater than the spherical particles for the same volume fraction. For medium to high Reynolds number (200–400), the friction factor for the nanofluids containing non spherical particles was seen to drop below than that given by Hagen-Poiseuille equation ($f Re = 64$). This is attributed to the strong alignment of the nano rods under the shear stress causing the effective viscosity of nanofluids to decrease in a manner similar to shear thinning. The convective heat transfer experiments were conducted for 0.65% vol. and 1.3% vol. of spherical and non-spherical nanoparticles, respectively. The local heat transfer coefficients were measured at 5 axial locations for Reynolds numbers of 350 and 490. They found out that the heat transfer of nanofluids is enhanced than that of the base fluid

and the increment increases proportionally to Reynolds number and the loading of nanoparticles.

Manca et al. (2012) numerically studied the turbulent flow of an Al_2O_3 -water Nanofluid in ribbed channels, for which the Reynolds numbers are in the range of 20,000 to 60,000. The solid particle diameter was 38 nm and the volume fraction was varied from 0% to 4%. All the fluid properties were considered to be temperature-independent. A uniform heat flux was applied along the walls. The heat transfer performance improved with an increase in volume fraction of the solid particles and was found to be maximum for high Reynolds numbers, however, this also increased the required pumping power.

2.8. Hybrid nanofluids

Many researches have been done in the last two decades about preparation, modelling, characterization, application, boiling and convective heat transfer of nanofluids. But hybrid nanofluids are a very novel class of nanofluids which is recently attracting the interest of the research groups. Hybrid nanofluids can be synthesized by adding nanocomposite (hybrid) nanoparticles or two/more than two of nanoparticles in the base fluid. A hybrid substance is a homogenous phase composite material which combines chemical and physical properties of the two or more than two materials simultaneously. Nanocomposite materials have remarkable thermos-physical properties that are superior and higher than the single components. Large number of researchers have been worked on the superior property of the composites and investigated possible usage of them in industry but the application of hybrid nanocomposite in nanofluids has not been investigated enough. The available researches on hybrid nanofluid is very limited and this is an interesting open area for further researches. The most important goal of synthesizing hybrid nanofluids is to gain the advantages of the properties of its constituent nanomaterials. A single nanoparticle does not have all the favorable properties needed for a particular application; it may have acceptable in rheological properties or thermal

properties but in many industrial applications the trade-off between some characters are required and that is where the hybrid nanofluids have been employed. Moreover, the hybrid nanofluids have better thermal conductivity compared to single nanofluids because of synergistic effect. Carbon based nanoparticles have plenty of unique characteristics such as mechanical resistance, chemical stability, high thermal conductivity and superior electrical conductivity. These interesting properties have attracted many research groups towards carbon based nanofluids as well as in expansion of a recent class of hybrid nanofluids containing one or two kinds of carbon nanoparticles with metallic, non-conductive or semi-conductive nanoparticles (Guo et al., 2008; H. Li et al., 2009).

2.8.1. Preparation of hybrid nanofluid

Munkhbayar et al. (2013) prepared Ag/MWNT water based hybrid nanofluid. MWNT single nanofluids were filled into an exploding glass, which was afterward fitted in the main section of the pulsed-wire evaporation apparatus. After that, silver nanoparticles were synthesized by the pulsed-wire evaporation technique and made direct contact with the base fluid inside the chamber wall. A water-based Ag/MWCNT nanofluid without any surface stain was finally achieved.

Abbasi et al. (2013) synthesized Al_2O_3 /MWNT hybrid nanofluid. Alumina nano powders were dissolved in ethanol after that the functionalized MWNT was added to the suspension and kept in an ultrasonic bath. Ammonia was added to the suspension drop wisely and then, the suspension was placed in a Teflon-lined stainless steel autoclave chamber, after which solvothermal synthesis was completed. Finally, Gum Arabic was added to the deionized water and the solution was put in bath ultrasonic, with the hybrid nanocomposite added to the solution and dispersed with bath ultrasonication.

Baby and Ramaprabhu (Baby & Ramaprabhu, 2011; Baby & Sundara, 2013) prepared MWNT-HEG (hydrogen exfoliated graphene) nanocomposite by catalytic chemical

vapor deposition (CCVD). Most of functional groups of graphene removed during the exfoliation process and the nanocomposite became hydrophobic. Therefore, the hybrid nanocomposite were functionalized with H_2SO_4 and HNO_3 acid medium. A specified amount of silver nitrate solution was added to the above mentioned solution with stirring. After some times, nanofluids were synthesized by dispersing a specific quantity of hybrid nanoparticles in deionized water with the assistance of ultrasonication.

Suresh et al. (Suresh, Venkitaraj, & Selvakumar, 2011; Suresh, Venkitaraj, Selvakumar, et al., 2011) prepared alumina-copper hybrid nanoparticles by a thermos-physical synthesis technique. They prepared water suspension of soluble nitrates of aluminum and copper. Then spray dried these solution to achieve the precursor powder and after that the sample was heated in air atmosphere to get the powder mixture form of stable Al_2O_3 and copper oxide. The mixture powder was then put in an alumina boat and placed in a horizontal alumina tube of the furnace. Alumina was kept in its original forms without any change but CuO was reduced in hydrogen and changed to metallic copper. Then the Al_2O_3 -Cu hybrid nanocomposite was ball milled to get a homogeneous powder. Finally, the prepared sample was dispersed in water by assistance of sodium lauryl sulfate (SLS) as a surfactant and by ultrasonication.

Han et al. (2007) made a CNT/Sphere hybrid nanofluid by using two-step method. They prepared the spherical nanoparticles with spray pyrolysis, then growth CNT through catalytic procedure. Finally, hybrid nanocomposite has been dispersed in oil. Botha et al. (2011) also prepared a hybrid oil based nanofluid, they prepared a silver-silica nanocomposite with one-step method.

Most of the hybrid nanofluids have been prepared by two-step method which is listed in table 2.2.

Table 2.2: Synthesis methods for hybrid nanofluids (Sarkar et al., 2015).

Methods, process type	Base fluids	Materials
One-step method, chemical	Transformer oil	Silver/silica
One-step method, thermal	Water	Silver/CNT
two-step method, mechanical	Water	CNT, AuNP, CuNP
Two-step method, mechanical	Water	Al ₂ O ₃ /PCM
Two-step method, mechanical	Water	Cu/Cu ₂ O
Two-step method, mechanical	EG	Al ₉₅ Zn ₀₅
Two-step method, mechanical	Water	CNT/Fe ₂ O ₃
Two-step method, mechanical	Water	Silver/TiO ₂
Two-step method, chemical	poly-alpha-olefin	Sphere/CNT
Two-step method, chemical	Water	Al ₂ O ₃ /Cu
Two-step method, chemical	Water	Silica/CNT
Two-step method, chemical	Water	Al ₂ O ₃ /CNT
Two-step method, chemical	Water, EG	Silver, CNT, CuO, HEG
Two-step method, chemical	Water	Cu/TiO ₂
Two-step method, chemical	Water	CNT/Fe ₃ O ₄
Two-step method, chemical	Water	Diamond/nickel

2.8.2. Thermos-physical properties

Han et al (2007) investigated the thermal conductivity of CNT/Sphere hybrid nanofluid by 3 ω -wire technique. They reported that hybrid nanofluid can enhance thermal conductivity of base fluid higher than simple metallic and oxides of metals nanofluids and a slight higher than simple CNT nanofluid. They found that the thermal conductivity of the basefluid has been improved 21% for volume fractions of 0.2% at room temperature.

Chen et al. (2014) also measured the thermal conductivity of Fe₂O₃–MWNT nanofluid and found that the synergistic effect on thermal conductivity of this hybrid nanofluids. They confirmed that thermal conductivity of this hybrid nanofluid is more than mono nanofluid. Same synergistic effect has been reported for Ag/TiO₂-water and Graphene–MWNT/water hybrid nanofluids (Aravind & Ramaprabhu, 2012; Batmunkh et al., 2014).

Munkhbayar et al. (2013) studied the thermal conductivity of MWCNT/Ag hybrid nanofluid by using one-step method. They found that the thermal conductivity of hybrid

nanofluid is about 15% higher than the thermal conductivity of mono nanofluid. Nine et al. (Nine et al., 2012) reported the thermal conductivity of alumina-water and hybrid nanofluid of alumina with two different types of MWNT (ground and non-ground) at different volume fractions. They found a slightly enhancement in thermal conductivity of hybrid nanofluid in comparison with simple nanofluid. Their results also indicated that the thermal conductivity of non-ground MWNT hybrid nanofluid is better than the ground MWNT. This might be due to the larger aspect ratio of non-ground nanoparticles.

On the other hand, Jana et al. (2007) found a contrariwise result. They measured the thermal conductivity of CNT-Cu and CNT-Au water based nanofluids. They indicated that the synergistic effect was not occurred for the examined hybrid nanofluids which was expected to happen. Accordingly, the CNT nanoparticles did not enhance the thermal conductivity of both mono nanofluid (Cu-Water and Au-Water) and also the thermal conductivity of hybrid nanofluids are lower than the thermal conductivity of respective single nanofluid.

2.8.3. Heat transfer and pressure drop

Heat transfer and pressure drop performance of hybrid nanofluids have been investigated by some researchers, but it seems more research needed to be done before their practical applications in the industries.

Suresh et al.(Suresh et al., 2014; Suresh, Venkitaraj, et al., 2012) investigated convective heat transfer and pressure drop of both developed laminar and turbulent $\text{Al}_2\text{O}_3\text{-Cu}$ /water hybrid nanofluids. The experimental set up consists of a test section, tank, pump, chiller and heater. They found that for both the fluid regimes (laminar and turbulent), Nusselt number of $\text{Al}_2\text{O}_3\text{-Cu}$ hybrid nanofluids is higher than Nusselt number of simple nanofluid significantly. Experimental data also revealed that hybrid nanofluids

make more penalty in pumping power in comparison with Al_2O_3 dispersed water nanofluids (Figure 2.11).

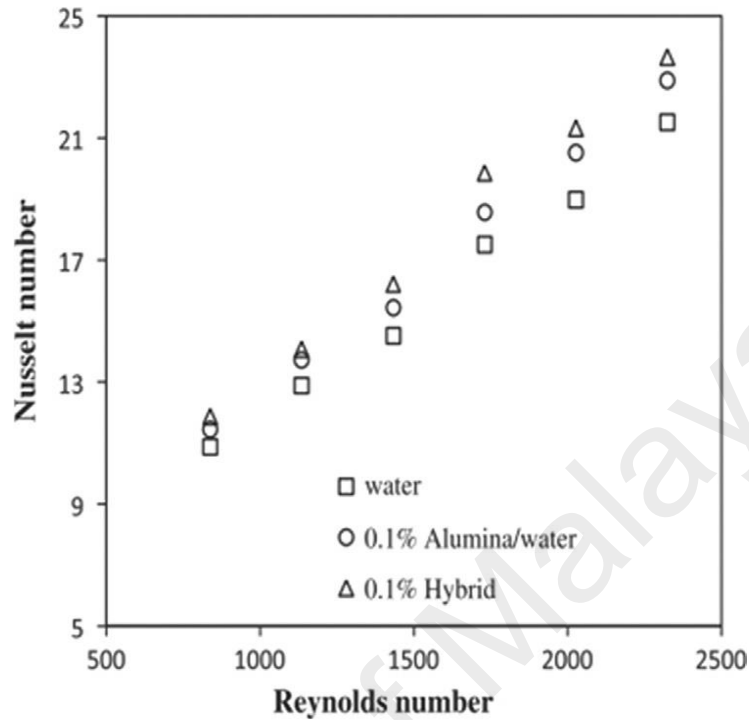


Figure 2.11: Comparison of Nusselt number of Al_2O_3 -Cu/water hybrid nanofluid with the Nusselt number of Al_2O_3 /water nanofluid (Suresh, Venkataraj, et al., 2012)

Sundar et al. (2014a) investigated Nusselt number and friction factor of turbulent flow of MWCNT- Fe_3O_4 /water hybrid nanofluids under a constant heat flux in round pipe. They stated about 31 % improvement in Nusselt number with a penalty of 18% increase of pumping power for the Reynolds number of 22,000 at volume concentration of 0.3% as compared to basefluid data. They believed that the thermal performance of hybrid nanofluids is superior compared to mono-particle base nanofluids.

Furthermore, Baby and Sundara (2011) studied heat transfer coefficient of CuO/HEG nanocomposite dispersed in EG and distilled water. They found that heat transfer coefficient of hybrid nanofluid is significantly higher in comparison to the basefluid data. Also they confirmed that the heat transfer enhances with the increase of Reynolds number and volume fraction.

Finally based on available research on hybrid nanofluid it can be concluded that the pumping power increases for hybrid nanofluids slightly, but the heat transfer coefficient of hybrid nanofluids was enhanced significantly which makes them a promising candidate for many industrial applications.

2.9. Summary

Water, engine oil and ethylene glycol are commonly used as working fluids for transfer of heat in many industrial equipment such as heat exchangers, evaporators, cooling devices and solar collectors. Small improvement in efficiency of heat exchanger equipment could lead to huge saving in initial and operational costs. One way to achieve this aim is to enhance the effective thermal conductivity of fluids that transfer the heat. Since the thermal conductivity of most liquids is low, there has been interest to use suspended solid particles to enhance the thermal conductivity of the base-fluid. However these earlier attempts have faced obstacles such as, increasing in pressure drop, sedimentation of particles and erosion of equipment. Investigation showed that nanoparticles have the ability to improve the effective thermal conductivity of base fluid and are useful for different industrial applications (Aly, 2014; Chol, 1995; Kasaeian et al., 2015). Nanofluids have attracted researchers since the material in the nanometer size have unique physical and chemical properties. In particular, many nanofluids have shown enhanced thermal conductivity, which makes them suitable for use as working fluids. Experimental studies also revealed that addition of nanoparticles to base fluid not only enhances thermal conductivity but also augments convective heat transfer compared to the pure base fluids.

In the recent years, significant investigations on the use of carbon-based nanomaterials such as, single-wall carbon nanotube, multi-wall carbon nanotube, graphene oxide and graphene nanoplatelets (GNP) to make nanofluids were reported in the literature. New

research indicates that graphene nanofluids could provide higher thermal conductivity enhancement in comparison to other tested nanofluids. Graphene particles have better thermal conductivity and also higher mechanical strength, and electrical conductivity. Favourable thermo-physical properties of graphene has made it an excellent candidate for use in the synthesis of nanofluids.

Majority of earlier investigation on nanofluid regarding thermos-physical properties and heat transfer coefficient were done on single nanoparticles; based on that, the graphene based nanofluids provided the best heat transfer coefficient. Synthesis of nanocomposite and preparation of nanofluid based on nanocomposite are very new and interesting topic for researcher. Even though, there has been a lot of literature reported on the preparation, stability and heat transfer performance in the various flow regime of nanofluids, the study on graphene and/or hybrid graphene based nanofluids in the turbulent flow regime is an excellent research interest.

CHAPTER 3: METHODOLOGY

3.1. Characterization methods

Since structure and morphology of nanoparticle have significant influence on thermal conductivity and heat transfer of nanofluids, it is important to fully determine the structural of nanopowders. The perfect characterization of nano powder is very important and essential for understanding the enhancement behavior of nanofluids. Information of characterization methods are briefly explained in the following sections.

3.1.1. XRD

X-ray powder diffraction (XRD) is a unique technique mostly used for component identification of crystalline materials. The examined material was excellently homogenized, grounded and average bulk composition was determined. Phase compositions were determined using an X-ray diffractometer (XRD, EMPYREAN, PANALYTICAL) with $Cu-K_{\alpha}$ radiation over a 2θ range from 10° to 70° . The "PANalytical X'Pert HighScore" software was employed to compare the XRD profiles with the standards compiled by the Joint Committee on Powder Diffraction and Standards (JCPDS) which involved card # 01-087-0718.

3.1.2. FESEM

Nano science has powerfully driven the improvement of latest electron microscopy, with needs not only for higher resolution but also for more structural detail from the nanopowders. FESEM is a very beneficial equipment for surface images with high resolution in the field of nanomaterial research. A beam with energetic electron employ to probe very fine objects. A highly focused tiny beam of electrons is skimmed over a slim sample, and the electrons that go through the fine specimen are gattered on a collector under the specimen, making the high resolution images. FESEM tool has

become more important because of suitability for the observation of carbon –based hybrid nanomaterials where there is no need of high beam energy, since material which are light atom based can easily scanned by low energetic electrons.

In this research, investigation of the morphological characteristics and the particle size estimation of synthesized doped and un-doped powders were performed by emission scanning electron microscopy (FESEM, SU8000, Hitachi).

3.1.3. TEM

Transmission electron microscopy (TEM) is the preliminary tool to verify agglomerations of particles and to identify single particle dimensions. The beam can be able to scan topography on the nanometre scale. A main disadvantage of using TEM is that the specimens have to be dried out and then attached to the carbon plate and put in a vacuum chamber of the TEM; thus the nanoparticles are not perfectly in the suspension form and agglomeration may happen during the drying procedure. Another drawback of TEM is the time and cost which is required to prepare the samples. Nevertheless, combination of TEM and dynamic light scattering can be employed to obtain the exact size of the nanofluid samples. Only few initial images were taken by TEM as a feasibility study. Transmission electron microscope (TEM) analysis was performed by HT 7700 (Hitachi) machine.

3.1.4. FTIR

Fourier transform infrared spectroscopy (FTIR) is a technique which is used to indicate functional groups on the surface of nanopowders. Very fine sample prepared by grinding of low concentration of dry powder with potassium bromide and then compacted into a very thin pallet. Then the infrared spectra of the prepared samples are studied by a Fourier transform infrared spectroscopy (Bruker IFS 66/S) in the region 400–4000 cm^{-1} .

3.1.5. Raman

Raman spectroscopy is a type of vibrational spectroscopy, more similar infrared (IR) spectroscopy. Though IR bands rise because of change in the dipole moment of molecule due to an interface between molecule and light but Raman bands rise due to change of polarizability of the molecule with the same interaction. It means that these detected bands arise from particular molecular vibration and then the energies of this transition is plotted like a spectrum. The mentioned plot can be used to determine the molecule as it provides a “molecular fingerprint” of the molecule being scanned. Raman spectra data were collected using a Renishaw Invia Raman Microscope with laser excitation at 514 nm.

3.2. Thermos-physical measurement equipment

3.2.1. Rheometer

Viscosity is one of the important property of fluid flow. Pressure drop, pumping power and heat transfer capability of fluid is directly dependent on the viscosity. Furthermore, the dynamic viscosity of nanofluid is investigated at various shear rate to find the rheological behavior of suspension, whether the suspension has Newtonian or Non-Newtonian behavior. The viscosity of distilled water and different weight fraction of nanofluids were measured by rheometer Physica, MCR, Anton Paar, Austria. The rotational rheometer consists of a moving cylindrical plate and a stationary cylindrical surface which are parallel with a small gap. Viscosity of distilled water and nanofluid samples at various concentrations and temperatures in the range of 20–40 °C at a shear rate of 500/s had been investigated. The measured viscosity of distilled water at 20 °C is 1.10 (mPa sec), which is in good agreement with the previously reported data.

3.2.2. DSC

Differential scanning calorimetry (DSC) is an appropriate device to investigate the specific heat capacity of nanofluids. The change in the amount of heat flow needed for heating up a sample reference pan and sample pan are measured as a function of temperature. In this study, a differential scanning calorimeter (DSC 8000, Perkin Elmer, USA), which is calibrated using indium (99.999%) with an accuracy of $\pm 1.0\%$, is used to find the specific heat capacity of all nanofluid samples directly. It is armed with a cooling accessory in a nitrogen environment. A prepared sample mass of 15-20 mg is kept in an aluminium pan, and the temperature is raised from $-50\text{ }^{\circ}\text{C}$ to $+50\text{ }^{\circ}\text{C}$ at the rate of $5\text{ }^{\circ}\text{C}/\text{min}$. Several experiments had been conducted to find the DSC thermograms based on minimizing the error for the average measured values. All the specific heat capacities had been measured under the same conditions.

3.2.3. Density meter

Volumetric behaviour of nanofluid samples obtained from experimental measurements of density as a function of nanoparticles weight fraction and temperature. The densities of the prepared nanofluids were measured experimentally by Mettler Toledo DE-40 density meter. The accuracy of density measurement is $10^{-4}\text{ g}/\text{cm}^3$. For each temperature and sample the measurements have been recorded 3 times. For validation purpose the density of distilled water has been measured and confirmed that the accuracy of the tool is adequate.

3.2.4. Thermal and Electrical conductivity

The most important property of nanofluid which must be measured is thermal conductivity. Thermal conductivities of nanofluids were measured by the KD-2 pro device (Decagon, USA) where KS-1 probe sensors were used having 6 cm and 1.3 mm length and diameter, respectively. The accuracy of the measured thermal conductivity is 5%. To ensure the equilibrium of nanofluids, an average of 16 measurements were

recorded during 4 hours for each temperature and weight concentrations. Calibration of instrument with DI water was performed before starting of the measurements of nanofluids. Thermal conductivity of DI water at 30 °C was measured and a value of 0.61 W/mK found, which is in agreement with the previous investigations (Duangthongsuk & Wongwises, 2009b; X Zhang et al., 2006). A photograph of the KD2 pro setup is shown in Figure 3.1.



Figure 3.1: Photograph of the thermal properties analyzer (KD2 pro).

Electrical conductivity of stable suspensions were measured by an AB200 pH/Conductivity Meter (Fisher Scientific) as a functions of temperature and weight fraction. The device has a resolution of 0.1% and measuring range of 0 to 500 mS/cm. The calibration of the conductivity meter was performed before starting the measurement with three buffer solutions of known electrical conductivities. Measurements were completed using ~40 ml of the samples in a beaker which was placed in an isothermal bath, with the conductivity probe dipped in it. For each temperature, the measurements were repeated 4 times, and the average value has been reported.

3.3. Experimental setup

Figure 3.2 represents the schematic and photograph of the experimental setup which includes the flow loop, heater, chiller (for cooling) and a unit for measurement and control. The flow loop contains a pump, a tank, a test section, flow meter system, chiller and a storage tank. A square stainless steel pipe with 1.4 m length, 10 mm inner width and 12.8 mm outer width was installed as a test section. A DC power supplier with a thick isolator layer surrounding the test section provides the constant heat flux boundary condition for the entire testing part. Five thermocouples (T-type) were installed on the test section to record the surface temperatures at different axial positions; the axial distances of thermocouples from the inlet of the test section are 200,400, 600,800 and 1000 mm. The bulk temperatures of the flow is measured by 2 thermocouples which are inserted into the fluid flow at the inlet and outlet of the test section, the resolution of all the thermocouples is ± 0.2 °C and is calibrated before installation. The nanofluids from the storage tank is pumped into the flow loop and circulated through the test section and finally discharged back into the same storage tank. The hydrodynamic entrance length, $l=140d$ was maintained to ensure that the flow is fully developed. A flow meter was installed at the discharge of the pump to measure the nanofluids flow rate. The stainless steel storage tank capacity was 14L. With the aid of the chiller, the outlet temperature of nanofluids was reduced to become equal to the inlet temperature to help reaching the steady state condition in shorter time.

Pressure drop cross the test section was measured to determine the friction factor of hybrid nanofluids. For this purpose, the Differential Pressure Transmitter (DPT) was connected to the ends of the test section. First sets of experimental runs were conducted with the base fluid for calibration purposes. Then a series of tests were performed for different nanofluids. The nanofluids with various weight fraction were used for investigating the friction factor and the heat transfer parameters for Reynolds numbers in

the range of 5000 to 17500. When steady state condition was achieved, the wall, inlet, and outlet temperatures as well as mass flow rate of nanofluids were recorded for each case. Typically, 3 hours was needed for reaching the steady state condition. The properties of nanofluid such as viscosity, thermal conductivity, specific heat capacity and density were considered at the mean bulk temperature. Brief explanation of each part is written in this section.

University of Malaya

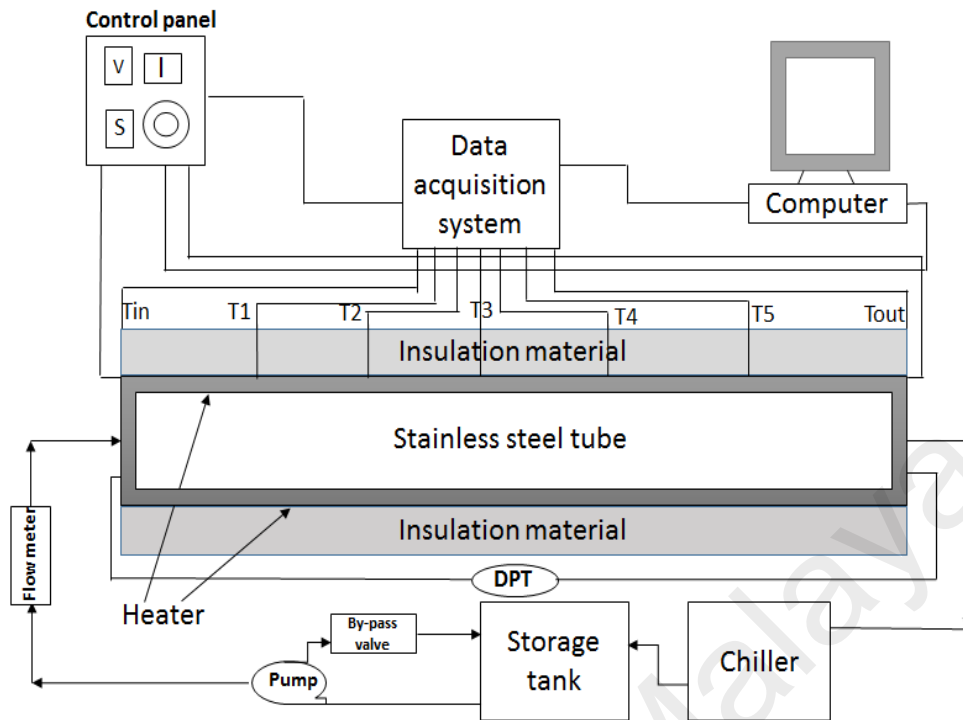


Figure 3.2: Schematic and photograph of the experimental setup.

3.3.1. Test section

Most important part of heat transfer experimental set up is test section and it is manufacture by Baolai Steel Group Co., China. The schematic of the test section is shown in Figure 3.3.

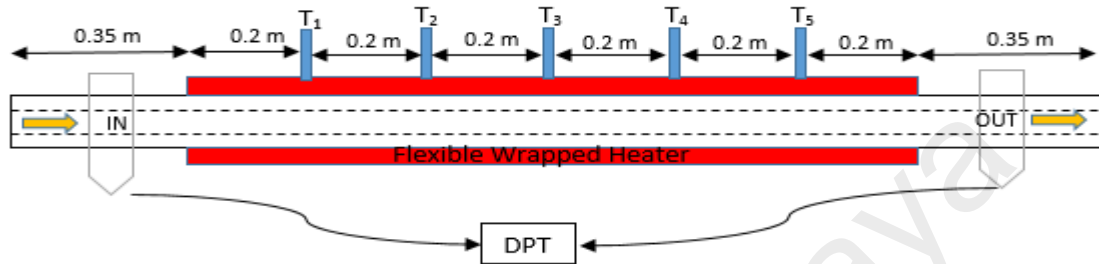


Figure 3.3: Schematic of the test section.

The test section is a square stainless steel 316 tube with a 10 mm inner width, a 12.8 mm outer width and length of 1200 mm. The test section has been divided into five equal sections for placing the thermocouples. The grooves for holding the thermocouples were cut at five equal distances and as deep as possible with the guarantee of not fully penetrating the wall thickness of the test tube. The thermos-wells were installed first with epoxy at the contact points with the test section. After drying epoxy the wells are rigidly installed. Thermocouples then inserted inside the wells until it touches the surface for measuring the surface temperatures at the test section.

3.3.2. Heater

The square tube is warmed up by a high temperature heating tape (Omega, STH052-120 – samox heavy insulated tape). The heater was wrapped around the tube with the similar slope in each turn. This heater was made from acceptable measurement stranded resistance cords that are dual isolated with knitted Samox and braided into flat tapes for more flexibility. A heavy insulated tape is prepared by taking a normal tape and knitting it between layers of Samox yarn. Flexible Heater and wires are made of high quality resistance braided insulation and wire.

3.3.3. Thermocouple

Two different types of thermocouples are needed for the monitoring of the temperature of this experimental set up. The thermocouples used for monitoring the surface temperature of pipe are type-T from Omega (TJ36-CASS-116U-6-CC-XCIB). This type of thermocouple has 1.5 mm case diameter and 300 mm length. The manufacturer confirmed that thermocouples have $\pm 1^\circ\text{C}$ accuracy. Another kind of thermocouples employed for the monitoring of inlet and outlet bulk temperatures of fluid from Omega (Model: PR-12-2-100-1/8-6-E-RP) with Temperature Range of 50- 250°C. This is a RTD sensor thermocouple (PT-100) with 100mm length and 3mm casing diameter. Since heat transfer result has strongly been related to the temperature measurements, so the thermocouples were tested and calibrated before being installing on the experimental set up.

3.3.4. Tank

The capacity of the tank is 14 liters and made of stainless steel with cylindrical shape. It is placed at 30 cm upper than pump to obtain enough pressure and avoid cavitation effect. At the top of the tank a return line, bypass line and stirrer for homogeneous mixing of nanofluid inside the tank are attached. Tank is connected to the pump from the bottom with a pipe.

3.3.5. Chiller

A chiller with bath circulator (DAIHAN-brand, WCR- P30) was needed to maintain the inlet and outlet temperatures of the tank. This chiller containing strong pump for uniform circulation of coolant. Stainless steel Bath (#304) with high thermal efficiency and longer durability and digital remote monitoring and controller system was installed.

3.3.6. Power supplier

Power supplied by a success electronics & transformer manufacturer SDN. BHD, Model: VT2-1 variac auto power transformer. The voltage rang is 0~260V and highest output of 10A. The Variac is a well-known kind of transformer which has a single winding and a single layer. The upper sector of the winding is flattened and machined to remove the insulation and provide a smooth surface for the sliding brush that is used to set the voltage required. Contrasting the common voltage transformer which has two electrically insulated windings (primary and the secondary), an Autotransformer has only one single voltage winding which is joint at both the sides. This single winding is “tapped” at various points along its length to provide a percentage of the primary voltage supply across its secondary load. The autotransformer has the typical magnetic core but only has single winding.

3.3.7. Pump

A liquid flow sealed pump which is used for this study. The maximum head is 6M and highest flow of 64 LPM. The pump has the ability to work at different speed but the maximum speed is 3200 rpm. The suction section of the pump is coupled to the tank. The maximum fluid temperature is 70 °C because of shaft seal limitation. Based on our design and inner hydraulic diameter of pipe, it is confirmed that the pump able to provide turbulent flow up to Reynolds number of 17500. Thus, this pump is suitable for the experiment.

3.3.8. Data logger, clamp meter and multi-meter

Two models of data logger are required for this experimental study. Scada (TK4H) and Graphtec (midi logger gl220) and both linked to a computer for non-stop monitoring and logging. All the type-T thermocouples are linked to the Graphtec data logger channels. Maximum 10 thermocouples can be attached to the data logger and also four

more channels for pulse inputs and discrete logic. Flow meter, RTD thermocouples and pressure transducer are connected to a PID controller (Scada Autonics, Model: TK4H).

The clamp meter and digital multi-meter are purchased from Agilent. All the current and voltage for power supply and heater are measured by these tools, they calibrated by the manufacturer before using.

3.3.9. Others

The fluid flow rate was measured by an Electromagnetic flow meter (Schmieder SEA). It has no moving section and low maintenance and low pressure drop. Electromagnetic flow meters are also ideal for waste water applications. It works on the simple law of Faraday's which says that the voltage induced through conductor as it travels right angles across a magnetic field is related to velocity of the conductor. The device has been calibrated from the manufacturer. The viscosity of fluid is a big issue for this kind of device, if the viscosity of the sample is very far from viscosity of water the reading is not accurate. Since the viscosity of nanofluid which used in experimental loop is always near to the viscosity of water, thus the flow meter measurement is correct.

The smart pressure transducer with correctness of $\pm 0.075\%$ of span connected to the outlet and inlet of the test section was applied in this test (Model ADP9000 Series). Also an inverter was needed to change and control the speed of the pump (Hoffman Muller, HM-V8A11P5B).

3.4. Lab equipment

High power ultrasonication probe (Sonics Vibra Cell, Ningbo Kesheng Ultrasonic Equipment Co., Ltd. China) having 20 kHz frequency power supply, 1200W output power and bath ultrasonication (Powersonic, Digital Ultrasonic, UB-410) was used for preparation of nanofluid. In addition, an industrial hot plate (HTS-1003 Hotplate Stirrer, LMS) is essentially needed for synthesis process. Different size of magnetic stirrer

is employed for stirring the samples during the time of data logging. There is an industrial oven for drying the samples in Advanced Heat Transfer Lab, University of Malaya. Advanced Heat Transfer Lab and Mechanical, Chemical Engineering and Chemistry Department, University of Malaya have procured all other general lab equipment'

3.5. Data reduction

Calibration of the experimental set up was initially performed with water (base fluid). The amount of heat supplied to the test section and the amount of heat absorbed by the flowing fluid, respectively, are

$$P = V \times I \quad (3.1)$$

$$Q = \dot{m} \times C_p \times (T_o - T_i) \quad (3.2)$$

A maximum deviation of $\pm 3\%$ was observed between the measured amount of energy supplies and energy absorbed, which confirms negligible amount of heat transfer to the surrounding of the test section.

The Newton law for heat transfer is used to estimate the experimental heat transfer coefficient. That is,

$$h = \frac{q}{A(T_w - T_b)} \quad (3.3)$$

Where $T_w = \frac{\sum T}{5}$ (T_w is average temperature of five thermocouples), $T_b = \frac{T_o + T_i}{2}$ and

$$A = \pi DL$$

The Nusselt number is defined as

$$Nu = \frac{h \times D_h}{k} \quad (3.4)$$

Where, $D_h = \frac{4A_c}{P}$, A_c is the cross-sectional area and P is the perimeter of the square pipe.

The available Nusselt number correlations for single-phase fluids are listed in this section.

Dittus and Boelter (1930) presented equation for evaluation of Nusselt number for water:

$$Nu = 0.023 Re^{0.8} Pr^{0.4} \quad (3.5)$$

Equation (5) is applicable for the range of $Re > 10^4$, $0.6 < Pr < 200$.

Petukhov (1970) presented equation for evaluation of Nusselt number for water :

$$Nu = \frac{\left(\frac{f}{8}\right) Re Pr}{1.07 + 12.7 \left(\frac{f}{8}\right)^{0.5} (Pr^{2/3} - 1)} \quad (3.6)$$

Equation (3.6) is applicable for the range of $0.5 < Pr < 2000$ and $3000 < Re < 5 \times 10^6$.

Gnielinski (1975) presented equation for evaluation of Nusselt number for water:

$$Nu = \frac{\left(\frac{f}{8}\right) (Re - 1000) Pr}{1 + 12.7 \left(\frac{f}{8}\right)^{0.5} (Pr^{2/3} - 1)} \quad (3.7)$$

Where, $f = (0.79 \ln Re - 1.64)^{-2}$. Equation (3.7) is for the range $2300 < Re < 10^6$, $0.5 < Pr < 2000$.

Because the single-phase fluid Nusselt number correlations underestimate the heat transfer of nanofluids, the researchers have developed new Nusselt number correlations for nanofluids. Some of the available Nusselt number correlations are outline here:

Maïga et al. (2006) presented equation for evaluation of Nusselt number for Al_2O_3 / water nanofluids as a function of Re and Pr:

$$Nu = 0.085 Re^{0.71} Pr^{0.35} \quad (3.8)$$

$10^4 < Re < 5 \times 10^5$, $6.6 < Pr < 13.9$ and $0 < \varphi < 10$

Pak and Cho (1998) presented equation for evaluation of Nusselt number for Al_2O_3 / water and TiO_2 /water nanofluids as a function of Re and Pr:

$$Nu = 0.021 Re^{0.8} Pr^{0.5} \quad (3.9)$$

$10^4 < Re < 10^5$, $6.54 < Pr < 12.33$, $0 < \varphi < 3.0\%$

Sundar et al. (2014a) presented equation for evaluation of Nusselt number for MWCNT- Fe_3O_4 / water hybrid nanofluids as a function of Re, Pr and volume fraction:

$$Nu = 0.0215 Re^{0.8} Pr^{0.5} (1 + \varphi)^{0.78} \quad (3.10)$$

$3000 < Re < 22000$, $0 < \varphi < 0.3\%$, $4.50 < Pr < 6.13$

The friction factor of nanofluids was measured experimentally from the recorded pressure loss data across the test section. That is,

$$f = \frac{\Delta P}{\left(\frac{L}{D}\right)\left(\frac{\rho V^2}{2}\right)} \quad (3.11)$$

The available friction factor expression for water and nanofluids are represented by equations (3.12)-(3.14):

Blasius (1908) presented equation for evaluation of friction factor for water flow;

$$f = 0.3164 Re^{-0.25} \quad (3.12)$$

Where, $3000 < Re < 10^5$

Petukhov (1970) presented equation for evaluation of friction factor for water flow;

$$f = (0.790 \ln(Re) - 1.64)^{-2} \quad (3.13)$$

Where, $2300 < Re < 5 \times 10^6$

Sundar et al. (2014a) presented equation for evaluation of friction factor for nanofluid flow;

$$f = 0.3108 Re^{-0.245} (1.0 + \varphi)^{0.42} \quad (3.14)$$

Where, $3000 < Re < 22000$, $0 < \varphi < 0.6\%$

According to the previous studies (Amiri, Sadri, Shanbedi, Ahmadi, Kazi, et al., 2015; Samira et al., 2014), applying base-fluids including nanoparticles can be imposed heat transfer equipment with an enhancement in both of the pressure drop (negative effect) and heat transfer coefficient (positive effect). To investigate these issue exactly, performance index (ϵ) can be selected as an appropriate parameter to clarify the range of temperature and velocity that can be used by synthesized coolant:

$$\epsilon = \frac{h_{nf}/h_{bf}}{\Delta P_{nf}/\Delta P_{bf}} = \frac{R_h}{R_{\Delta P}} \quad (3.15)$$

R_h is the ratio of the heat transfer enhancement in the presence of the nanoparticles to the base-fluid and $R_{\Delta P}$ is the ratio of pressure drop of synthesized coolant to the base-

fluid. In the turbulent region, the pumping power can be measured by Eq. 3.16 to study energy saving (R. B. Mansour et al., 2007).

$$\frac{W_{nf}}{W_{bf}} = \left(\frac{\mu_{nf}}{\mu_{bf}} \right)^{0.25} \left(\frac{\rho_{bf}}{\rho_{nf}} \right)^2 \quad (3.16)$$

3.6. Optimization method

Response surface methodology (RSM) is a strong method for prediction of a relation between some explanatory variables and one or more response variables. The principal concept of RSM is to find a sequence of experimental data to gain an optimum response. RSM contains a cluster of statistical and mathematical methods that are based on the fitting of the empirical models to the experimental data. The RSM method employed to find the developed correlation from available experiment data of the Nusselt number and friction factor. Minitab#17 software has been used to do data analysis and prediction of the developed correlation.

CHAPTER 4: PREPARATION, CHARACTERIZATION AND THERMOS- PHYSICAL PROPERTIES OF NANOFLUIDS

4.1. Introduction

Homogeneous and stable suspension of nanoparticles in a conventional working fluid such as water or ethylene glycol is discussed in this chapter. Researchers have investigated various method for preparation of nanofluid, but in this research covalent functionalization procedure is chosen for making stable nanofluid. Also, in this section nanoparticle surface characterization and thermo-physical properties of nanofluid investigated.

4.2. Functionalized GNP water based nanofluid

4.2.1. Preparation

Graphene nanoplatelets (GNPs) with purity $\sim 99.5\%$, maximum particle diameter of $2 \mu\text{m}$ and specific surface area $500 \text{ m}^2/\text{g}$ were purchased from, XG Sciences, Lansing , MI , USA. The chemicals such as HNO_3 (nitric acid) and H_2SO_4 (sulphuric acid) were purchased from Sigma-Aldrich Co., Selangor, Malaysia.

Since graphene nanoplatelet is naturally hydrophobic and it cannot be dispersed in any solvent which is polar like distilled water. Functionalization by acid treatment is a suitable way to make GNPs hydrophilic. This functionalization process helps to introduce functional groups such as carboxyl and hydroxyl groups on the surface of GNPs. Acid treatment process was performed by dispersing GNPs in a solution of HNO_3 and H_2SO_4 at 1:3 ratio (strong acid medium) (Baby & Ramaprabhu, 2010; Baby & Ramaprabhu, 2011), for 3 hours under bath-ultrasonication. After 3 hours, GNPs were washed several times with DI water and then the prepared rich sample was used in the next step to make nanofluids at different concentrations with the addition of the specific amounts of distilled

water. The resulting nanofluids were stable and no sedimentation of particles were found for a long time. Figure 4.1 shows the schematic of functionalization procedure and nanofluid preparation.

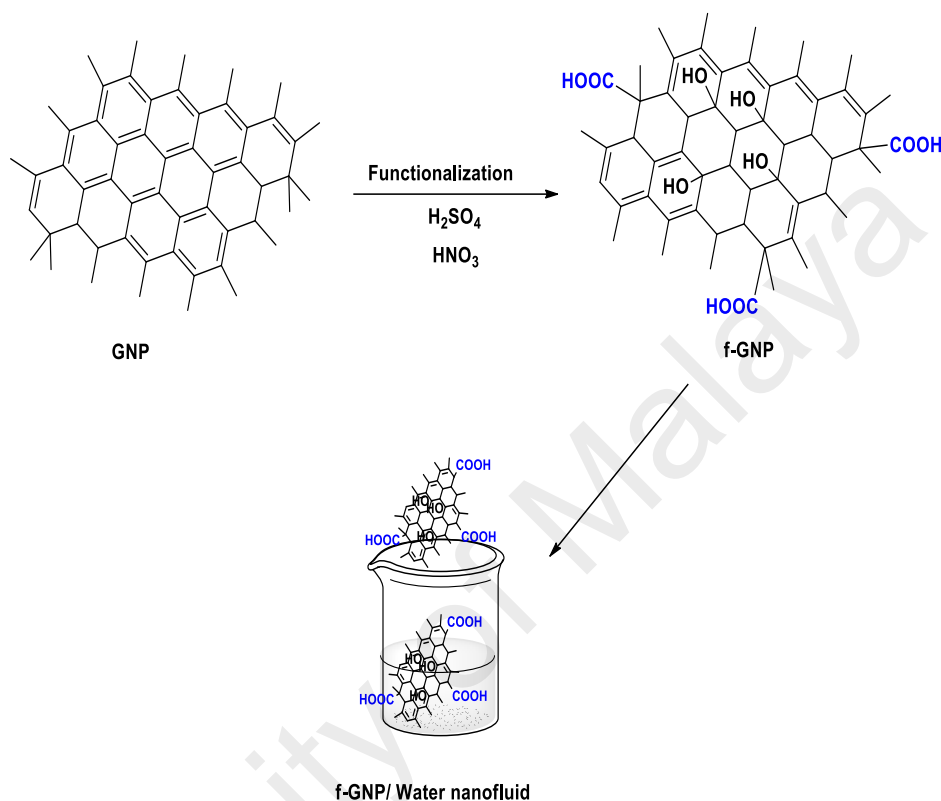


Figure 4.1: Schematic of functionalization process and making of nanofluid

4.2.2. Characterization of f-GNP nanoparticles

Surface modification of GNP by functional groups becomes necessary in order to achieve a proper dispersion. Figure 4.2 (a) shows a comparison of the FTIR spectra of GNP and functionalized GNP (f-GNP). The broad peak centred around 3430 cm^{-1} attributes to stretching vibrational modes of the hydroxyl group ($-OH$) (Gharehkhani, Sadeghinezhad, et al., 2015). The appearance of two new bands around 2915 and 2845 cm^{-1} in the FTIR results of f-GNP are due to asymmetric and symmetric $-CH$ stretching modes. The peak intensity of the C-OH and epoxide groups (C-O-C) at 1440 and 1020 cm^{-1} respectively, confirm the attachment of functional groups to GNP (Kumar et al., 2013). The typical peaks of carbonyl and ionised carboxyl groups belonging to

functionalization of GNP appear to have the strength at around 1600 cm^{-1} (Baby et al., 2010; Kaniyoor et al., 2009).

Figure 4.2 (b) presents the D and G bands of functionalized and untreated GNP in Raman spectra. D-band (sp^3) at around 1360 cm^{-1} is due to the defects, disorder, impurities etc., present in the samples while G-band (sp^2) at 1580 cm^{-1} corresponds to the characteristic peak of most of the carbonaceous materials due to the in-plane vibration of carbon atoms (Gharehkhani, Shirazi, Jahromi, et al., 2015; Shirazi et al., 2015). The G-band of f-GNP is shifted that attributes to the disturbing of GNP sheets due to the acid treatment (Baby & Sundara, 2011). The intensity ratios of D- and G-bands (ID/IG) calculated for GNP and f-GNP are 0.19 and 0.43 respectively. The dramatic increase of D-band intensity is interpreted as the presence of defects and disorder formed in the sample after vigorous mechanical and chemical process of acid treatment.

Figure 4.2 (c) shows the XRD patterns of functionalized GNP. The peaks of plane (0 0 2) at around 26.6° and plane (0 0 4) at 55° represent the structure of GNP. The results show that the functionalizing of GNP did not affect the crystalline structure of GNP.

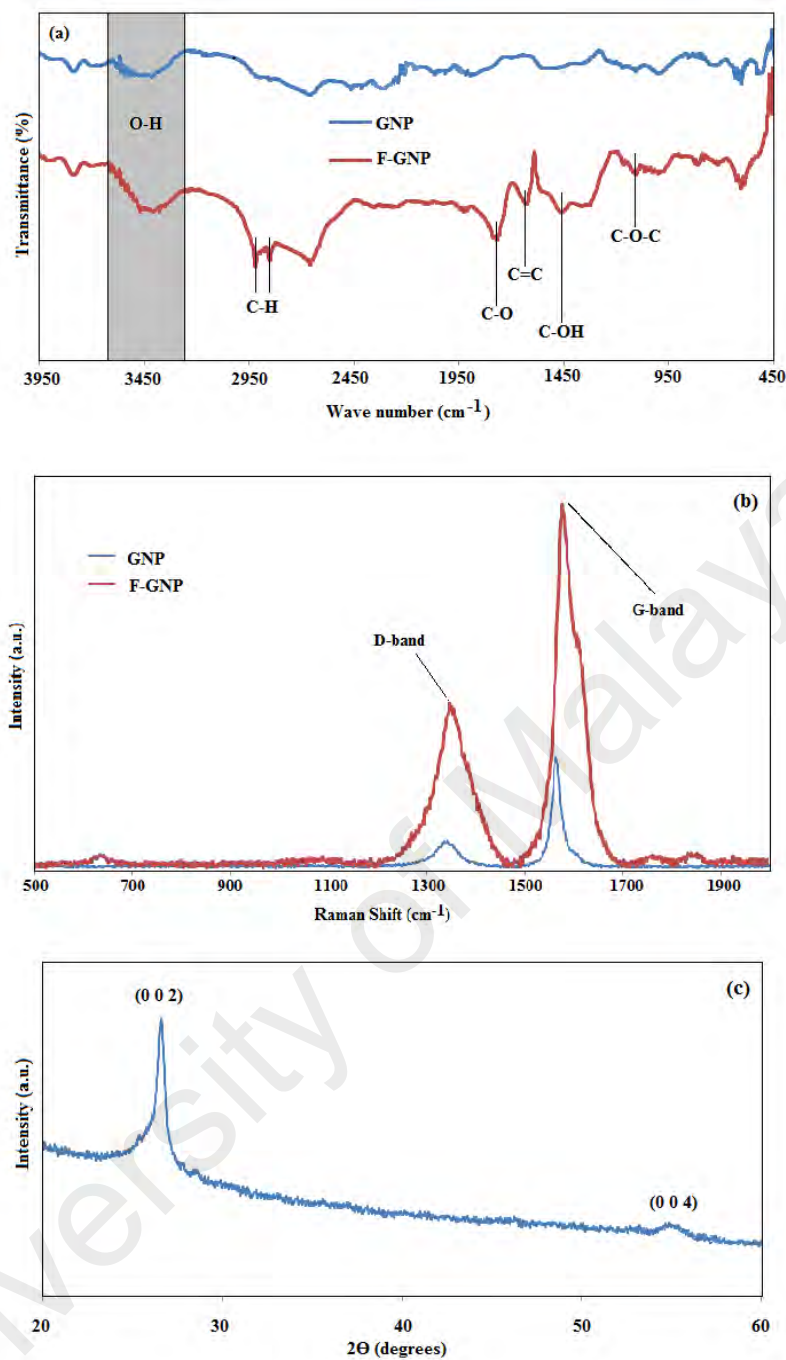


Figure 4.2: (a and b) FTIR and Raman spectra of GNP and f-GNP and (c) XRD pattern of f-GNP

Figure 4.3 (a-d) shows the morphology of f-GNP materials. The effect of fictionalization can be obviously observed in TEM image that the functionalizing treatment resulted in breaking the smooth surface layers of GNP into very small sheets (Figure 4.3 (a and b)). This may also explain the reason why ID/IG of f-GNP in Raman spectra is significantly higher than that of untreated GNP. FESEM images also confirm that fictionalization of GNP results in the broken sheets of GNP (Figure 4.3 (c and d)).

However, the presence of small sheets provides better dispersion stability of nanofluid, it may cause a tiny decrease of the thermal conductivity (Munkhbayar et al., 2013).

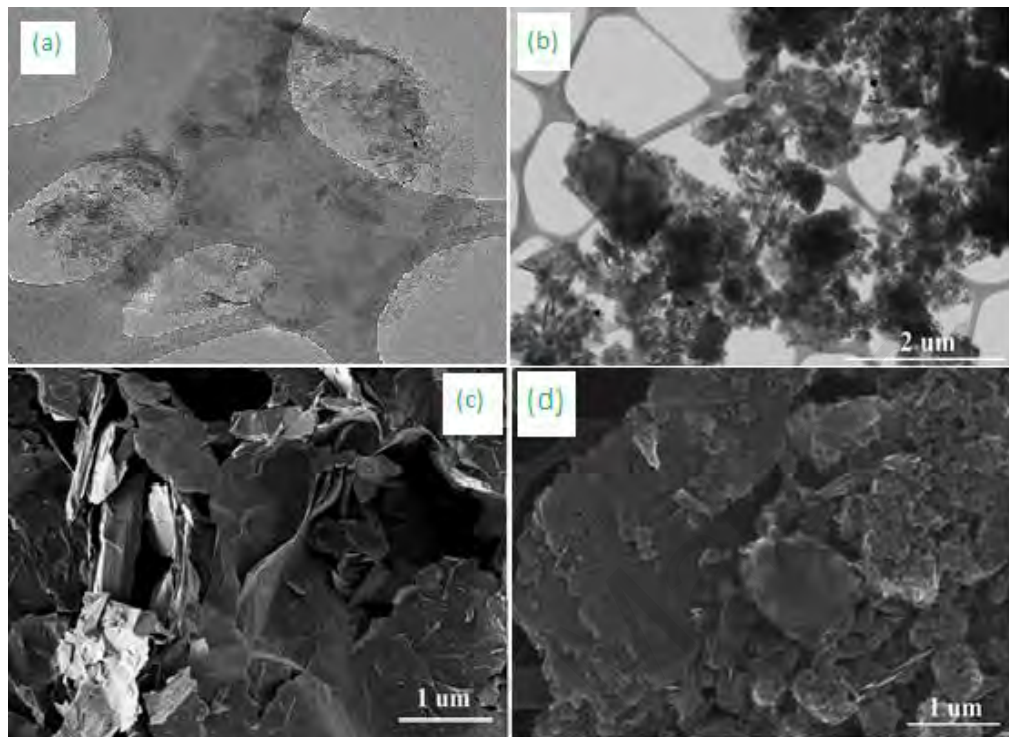


Figure 4.3: (a and b) TEM images and (c and d) FESEM images of pristine GNP and f-GNP

4.2.3. Stability and particle size distribution

The particle size distribution change is analysed using the dynamic light scattering (DLS) method to check the aggregate size with time. Dynamic light scattering (DLS) is a method in physics that can be used to define the size distribution profile of small particles in suspension or polymers in solution. When light hits small particles, the light scatters in all directions as long as the particles are small compared to the wavelength (below 250 nm). If the light source is a laser, and thus it is monochromatic and coherent, the scattering intensity fluctuates over time. Figure 4.4 presents the graphs of the particle size distributions for pristine- and functionalized GNP-based water nanofluids. The difference between pristine and functionalized GNP-based water nanofluids is significant, showing a movement to the smaller particle size when the distribution of the carboxylated GNP in water is compared with that of pristine GNP in the same media. While pristine GNP was completely sedimented after 24 hr to reach particle size distribution of 309.478

nm, the functionalized GNP material has shown the particle size distribution of 204.811 nm, indicating stable and homogenous colloidal system of them in aqueous media (Amiri, Shanbedi, et al., 2015; Q. He et al., 2013; X. Li et al., 2007).

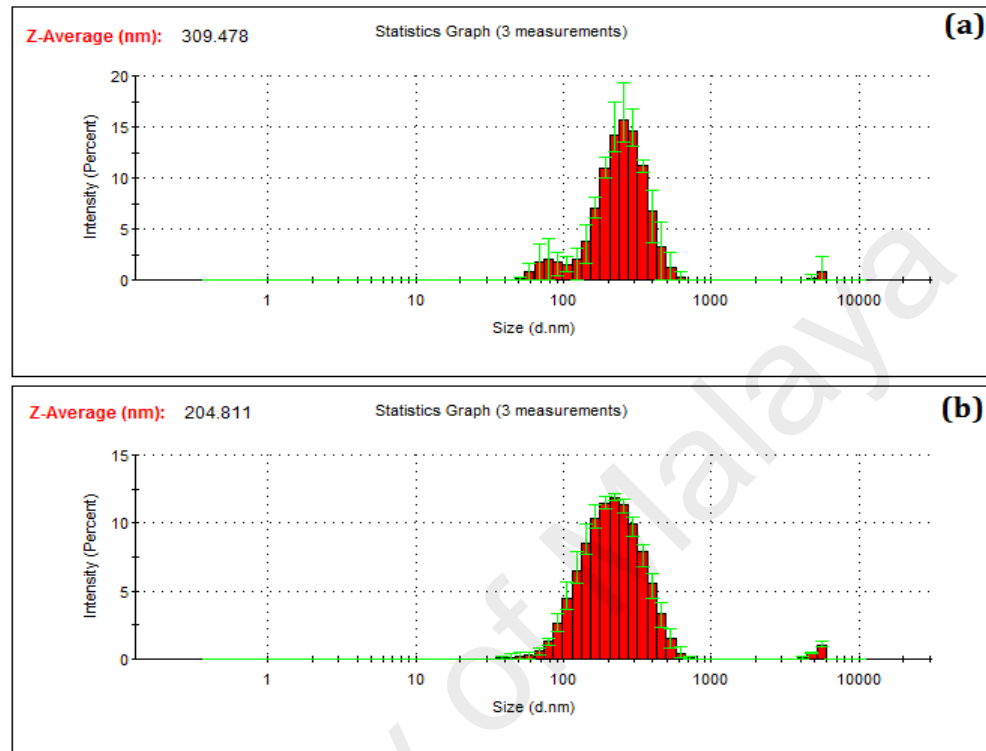


Figure 4.4: Particle size distribution of (a) pristine GNP-based water nanofluid and (b) functionalized GNP-based water nanofluid.

Regarding the uniformity of mixing these nanoparticles with water, UV-vis can be utilized to show that the homogeneity of suspension. Figure 4.5 (a) illustrates the UV-vis spectrum of the functionalized GNP-based water nanofluids. UV-Vis spectroscopy is commonly applied for the investigation of the stability of coolant including solid nanoparticles and is able to measure the sedimentation time. According to the Beer-Lambert's law, the absorbance of a solution is directly proportional to the concentration of the absorbing species such as particles in the solution. As a raw spectrum of functionalized GNP-based water nanofluid, a sharp peak at 263 nm is attributed to the presence of GNP.

Also, quantitative analysis of the dispersion state and the long-term stability of the functionalized GNP-based water nanofluid can be performed in the UV-Vis

spectroscopy, as shown in Figure 4.5 (b). Thus, the absorbance at the wavelength of 263 nm was measured during 240 hours for all weight concentrations. It can be seen that the concentration of loaded GNP in aqueous media decrease insignificantly over time. As a result, the maximum sediment of 7% was obtained for highest weight concentration of 0.1 wt. %, which confirmed the suitable dispersibility of functionalized GNP in distilled water.

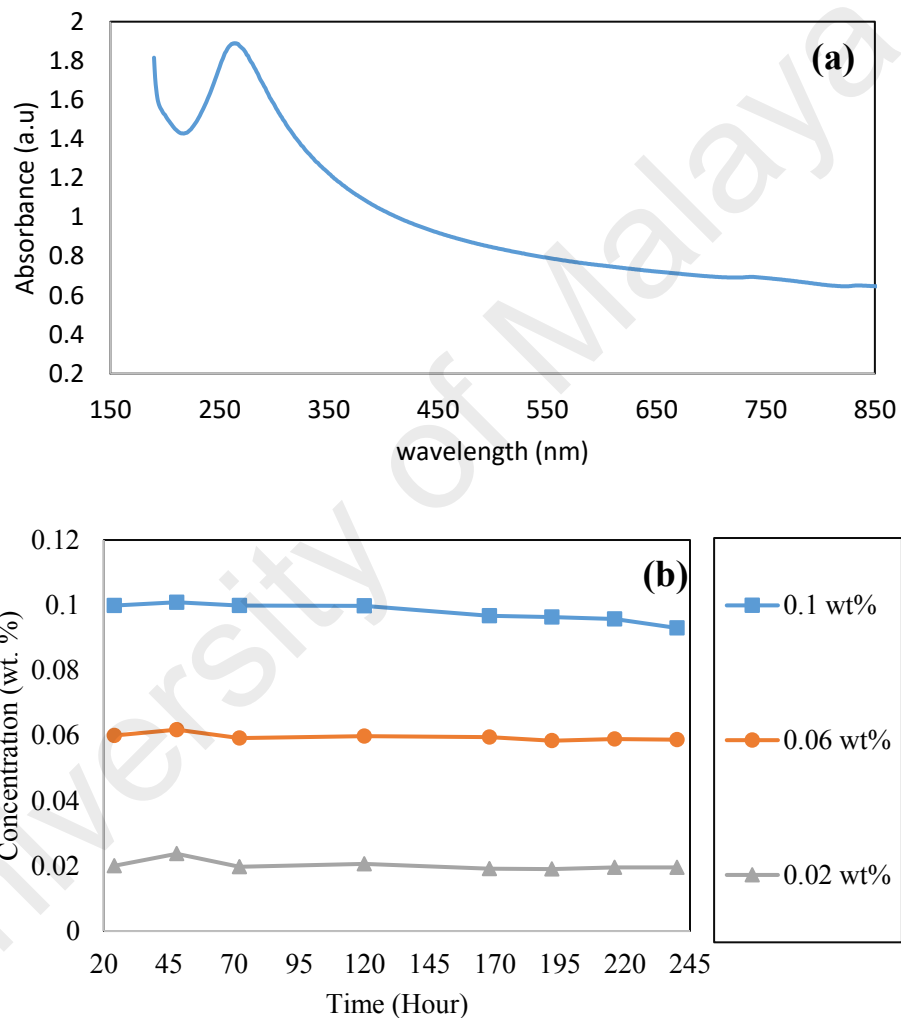


Figure 4.5: (a) UV-vis spectrum of functionalized GNP-based water nanofluid and (b) the colloidal stability of functionalized GNP-based water nanofluid as a function of time.

4.2.4. Thermo-physical properties of f-GNP nanofluids

Thermal conductivity of three different weight percentages (0.02, 0.06 and 0.1 wt %) of functionalized GNP nanofluid samples are recorded in the range of 20 °C to 40 °C. Tinny amounts of weight percentages are chosen to avoid sedimentation and increase of

effective viscosity. Figure 4.6 presented the thermal conductivity of water and f-GNP nanofluids at different temperatures for various volume concentrations. It is shown that the thermal conductivity of nanofluids rises with the increase of weight fraction of nanoparticles and fluid temperature. For 0.1% weight fraction of f-GNP, the enhancement of thermal conductivity is 13.56% at 20 °C and nearly 15.87% at 40 °C. Enhancement in the effective thermal conductivity is due to the high thermal conductivity of GNP nanoparticles. With the increasing of nanoparticles weight fraction the particles distance (free path) decreases. This fact is because of the percolation effect. More particles are in contact with each other, which increases the frequency of lattice vibration (Baby & Sundara, 2011). The increase of thermal conductivity of carbon based nanofluids with the increase of weight fraction has also been reported by other researchers (Amiri, Shanbedi, et al., 2015; Baby & Sundara, 2011; Das et al., 2003).

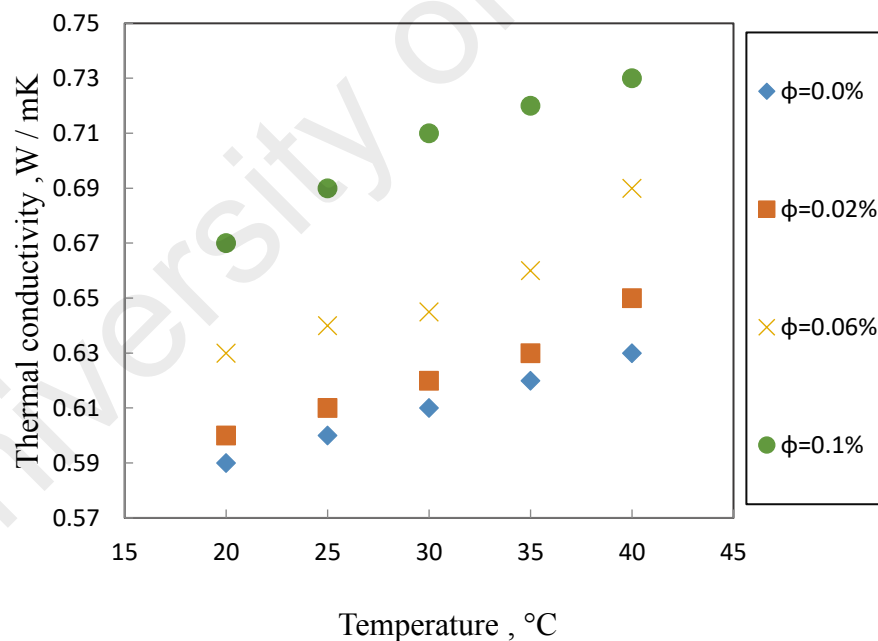


Figure 4.6: Thermal conductivity of f-GNP nanofluids as a function of temperature for different weight fractions.

Figure 4.7 indicates the viscosity of base fluid (distilled water) and f-GNP nanofluids at different weight fractions and at temperatures in the range of 20 °C to 40 °C for a shear rate of 500/s. The measured viscosity of distilled water at 20 °C is 1.10 (m Pa.sec), which

is good match with the existing reported data. It is found that with the increase of nanofluids weight fraction, the viscosity of nanofluids rises as the increase in concentration would have a direct influence on the fluid internal shear stress (Nguyen, Desgranges, Roy, Galanis, Mare, Boucher, & Angue Mintsa, 2007). The viscosity decreases with the increment of temperatures, for the weakening of inter-molecular and inter-particle adhesion forces (Nguyen, Desgranges, Roy, Galanis, Mare, Boucher, & Angue Mintsa, 2007). Viscosity increase of about 24% is noticed at 0.1% weight fraction of nanofluid compared to the viscosity of the distilled water at 40 °C.

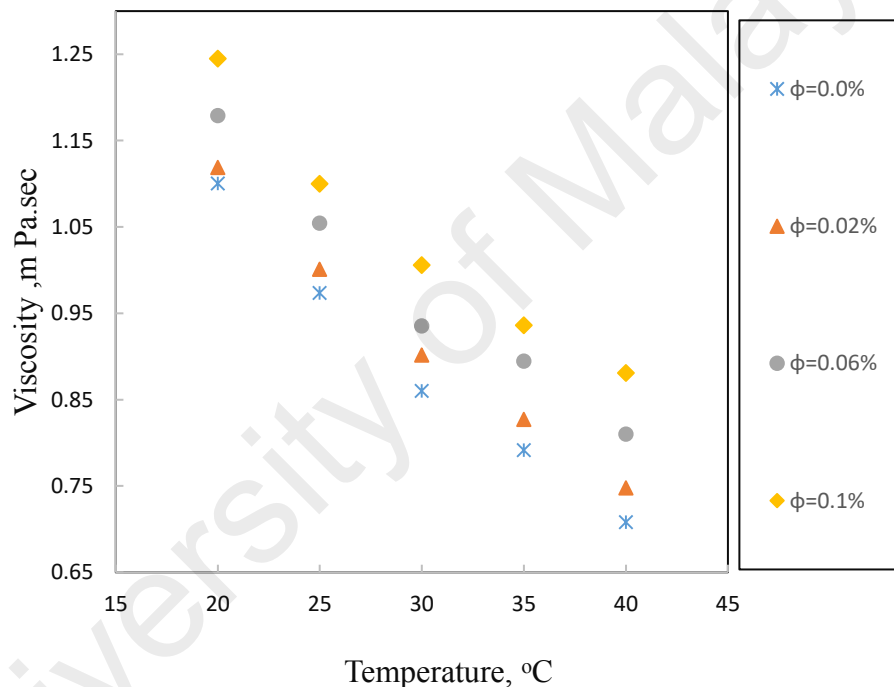


Figure 4.7: Viscosity of f-GNP nanofluids as a function of temperature at different weight fractions.

Figure 4.8 shows the densities of base fluid and f-GNP nanofluids at different weight concentrations and at temperatures in the range of 20 °C to 40 °C. It is seen that with the rise of nanoparticle weight fraction, the density of the nanofluid enhances slightly. Actually the density is linearly proportional to the nanoparticles weight fraction and its deviation from each other is proportional to the order of nanoparticles weight fraction. The density enhancement over the density of base fluid at 40 °C, is about 0.06% for 0.1%

volume fraction of nanoparticles. The density increase is trivial, which could be considered insignificant.

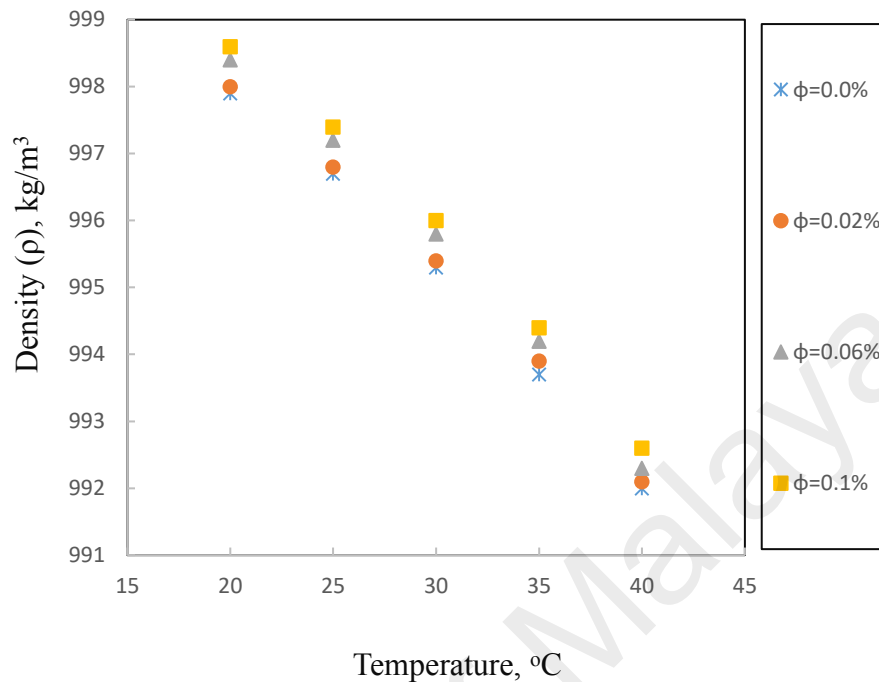


Figure 4.8: Density of f-GNP nanofluids as a function of temperature for different weight fractions.

However the specific heat capacity has important effect on heat transfer performance of nanofluids, but only a few literature are available about the effect of nanoparticle weight fraction on the specific heat of nanofluids (Shin & Banerjee, 2014; Vanapalli & ter Brake, 2013; L.-P. Zhou et al., 2010). Table 4.1, indicates the specific heat capacity of functionalized GNP nanofluids as a function of nanoparticle concentrations and temperatures. It can be seen that the specific heat capacity of nanofluid samples are lower than those of the base fluids. With the increasing of particles weight fraction the specific heat capacities are decreased. As per Table 4.1, when temperature gradually increases from 20 °C to 50 °C the specific heat capacity of samples are enhanced. The measured nanofluid specific heat capacities show the specific heat of nanofluid is about 1.53% and 6.09 % lower than that of the base fluid for 0.02 and 0.1 wt% of nanoparticles respectively at 45 °C.

Table 4.1: Specific heat capacity of water and f-GNP water based nanofluids at different weight fraction and temperature.

Temp	Water			
	0.00%	0.02%	0.06%	0.10%
20	4.099	4.057	4.02	3.8
25	4.104	4.046	4.023	3.794
30	4.105	4.042	4.012	3.815
35	4.1	4.041	3.997	3.827
40	4.101	4.037	4.014	3.84
45	4.106	4.043	4.007	3.856

Convective heat transfer coefficient and friction factor of the samples are experimentally evaluated at the mean bulk temperature. Also the obtained data of the summarized thermal conductivity, density, viscosity and specific heat capacity of the samples at the mean bulk temperature are presented in table 4.2.

Table 4.2: Thermo-physical properties of water and f-GNP water based nanofluid at mean bulk temperature.

Thermo-Physical properties	water	0.02%	0.06%	0.10%
Thermal conductivity, K (W / mK)	0.61	0.62	0.645	0.71
Viscosity, μ (m Pa.sec)	0.860420	0.901783	0.935683	1.00596 4
Density, ρ (kg/m ³)	995.3	995.4	995.8	996
Specific heat capacity, Cp (J/g K)	4.105	4.042	4.012	3.815

4.3. Functionalized GNP- Ag water based hybrid nanofluid

4.3.1. Synthesis of GNP-Ag nanocomposite

Above-mentioned procedure employed for making the functionalized GNP. Later the functionalized GNP were decorated with silver (Ag) by a chemical reaction method. The brief procedure of synthesis is stated for reference. The solution of ammonia-silver was prepared by adding drop wise ammonia (1 wt %) to 0.01 L silver nitrate solution (0.05

M) until fully reacted and silver colour disappeared. The $\text{Ag}(\text{NH}_3)_2\text{OH}$ solution (0.04 M) was mixed with 120 ml functionalized GNP (1mg/mL) solution, at a weight ratio of 1: 6. The irradiation of final solution was done under vigorous stirring for 4 hours. After that, GNP-Ag nanocomposites were collected after centrifuge at 11000 rpm for 40 min. The obtained composite was washed well with distilled water several times to remove reactants. The prepared rich sample was used in the next step to make nanofluids at different concentrations by adding specific amounts of distilled water. The resulting nanofluids were stable and no sedimentation of particles was found for up to 60 days. Figure 4.9 shows the schematic of molecular structure of synthesised GNP-Ag nanocomposite.

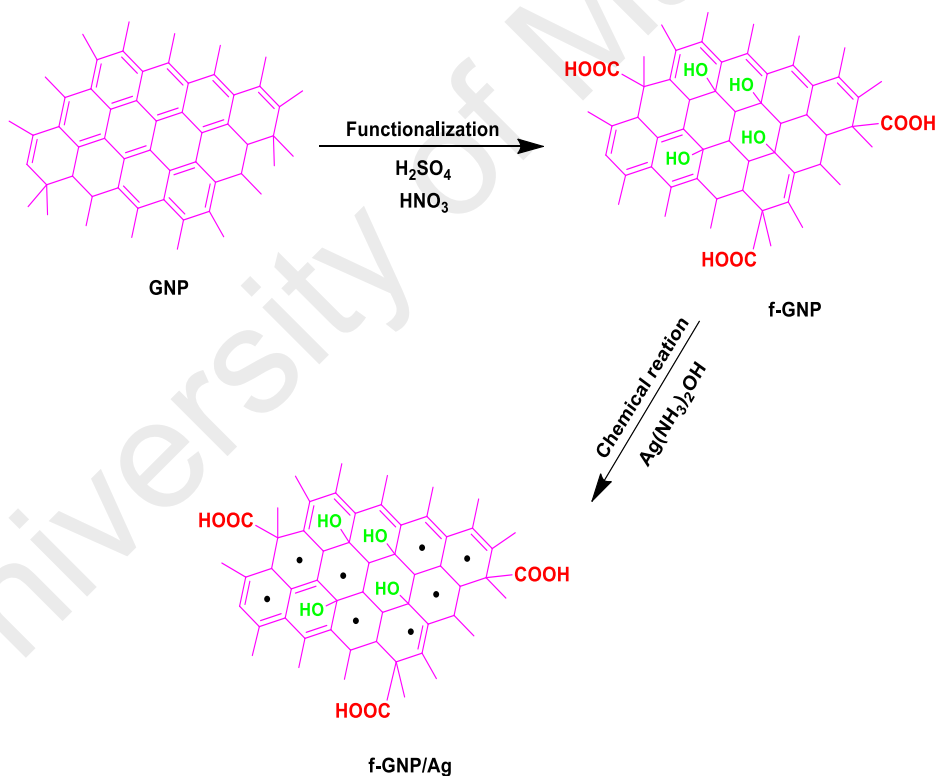
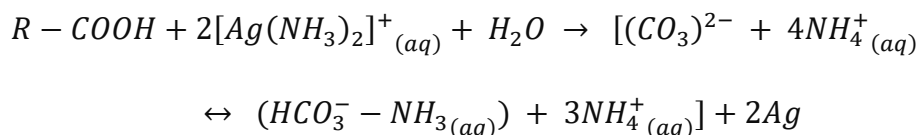


Figure 4.9: Schematic of molecular structure of GNP-Ag nanocomposite

The molecular structure of carboxylic acids on the basal plane of the GNP flakes with a hydrogen atom directly bonded to an ammoniacal silver nitrate solution to illustrate reducing properties as a result. In fact, carboxylic acid will reduce the ammoniacal silver

nitrate solution (i.e. the diamine silver (I) ion found in the Tollen's reagent) to metallic silver and resulted in the formation of the silver nanoparticles. Due to the acidic condition, the resulting metallic silvers were dispersed in the aqueous media homogenously.

The interaction is as follow:



4.3.2. Characterization of GNP-Ag nanocomposite

Figure 4.10 shows the XRD patterns of Ag coated GNP. The peak at around 26.6° represents the structure of GNP. The peak at 38.2° attributes to the face centred cubic Ag nano-particles decorated on the GNP (plane of (1 1 1)). Peak of (2 0 0) plane at around 44.4° is also corresponded to the present Ag decorated on GNP. Moreover the peaks at 64.6° and 77.6° ((2 2 0) and (3 1 1)) are both related to Ag nano-particles decorated on GNP. XRD patterns confirm that no unexpected reaction happened during acid treatment, chemical reduction and Ag coating processes.

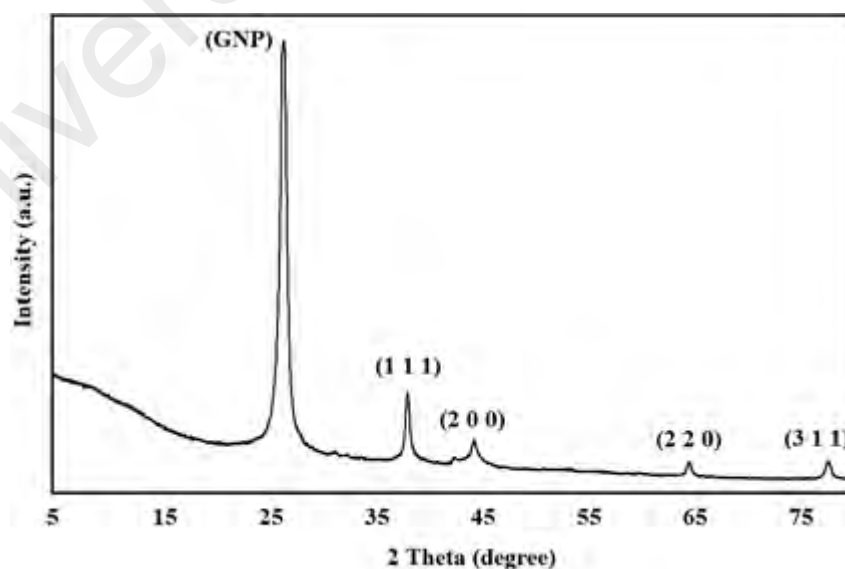


Figure 4.10: XRD pattern of GNP-Ag nanocomposite.

Figure 4.11 presents the D and G bands of coated and uncoated GNP in Raman spectra. D-band (sp^3) at around 1360 cm^{-1} is due to the defects, disorder, impurities etc., present in the samples while G-band (sp^2) at 1580 cm^{-1} corresponds to the characteristic peak of most of the carbon related materials due to the in-plane vibration of carbon atoms (Shirazi et al., 2015) and (Gharehkhani, Shirazi, Pilban-Jahromi, et al., 2015). After acid treatment and coating process, it is obvious that G peak shifted to higher energy of 1597 cm^{-1} . This blue-shift position could be corresponded to the disturbing of GNP sheet and also Ag coated GNP. The intensity ratios of D- and G-bands (I_D/I_G) calculated for pure GNP and Ag coated are 0.05 and 0.79 respectively. The dramatic increase of D-band Raman intensity is interpreted as the presence of defects and disorder formed in the sample after vigorous mechanical and chemical process of acid treatment and Ag coating.

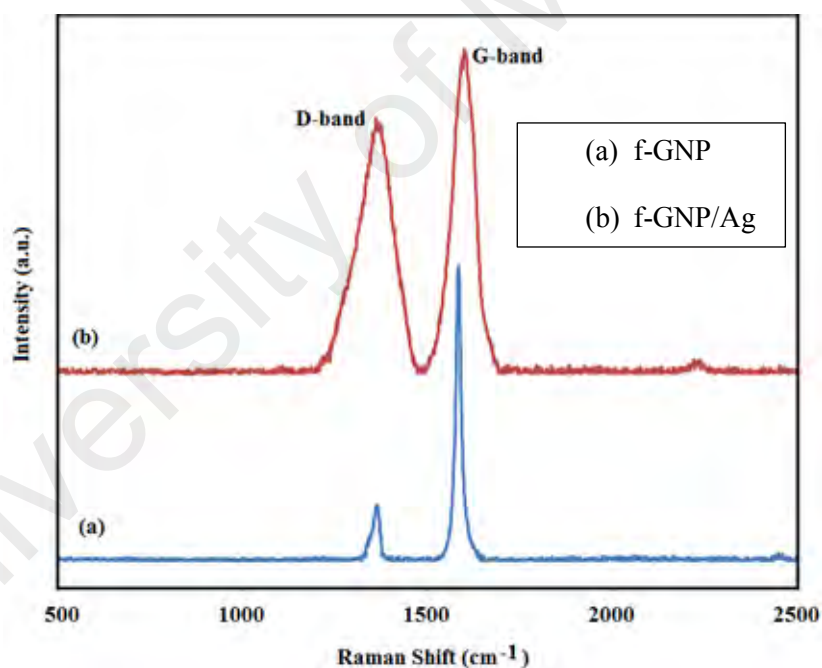


Figure 4.11: Raman spectra of GNP-Ag nanocomposite.

The Morphological characterizations of the Ag coated GNP nano-powders are shown in Figure 4.12. The uniform distribution of Ag coating on the graphene sheets can be clearly seen in FESEM image. Ag nano-particles coated GNP can be the evidence of a

perfect acid treatment resulting in functional groups reduction which finally led to appropriate coating of Ag on GNP sheets.

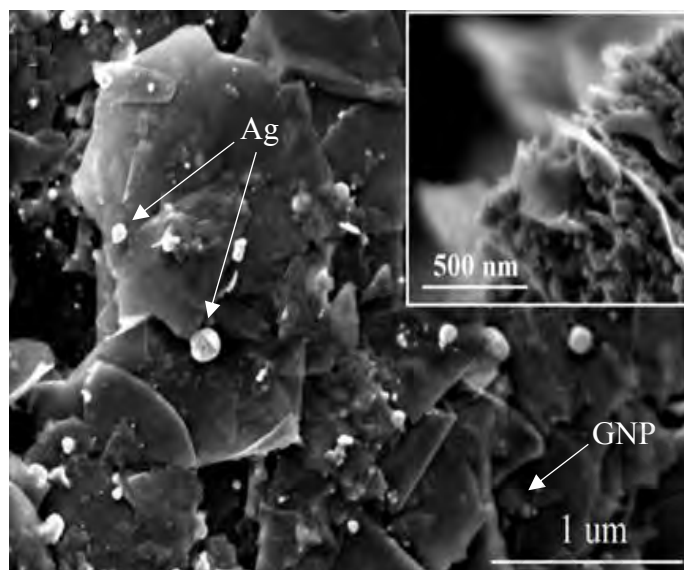


Figure 4. 12: FESEM image of GNP-Ag nanocomposite.

Figure 4.13 indicates the TEM image of Ag coated GNP sheet. The uniformity of Ag nano-particles distribution is more visible in TEM images that are due to proper functionalization of GNP. It also could be figured out from the TEM images that the wrinkled surface and folding at the edges of GNP sheets happened through the acid treatment and probably Ag coating.

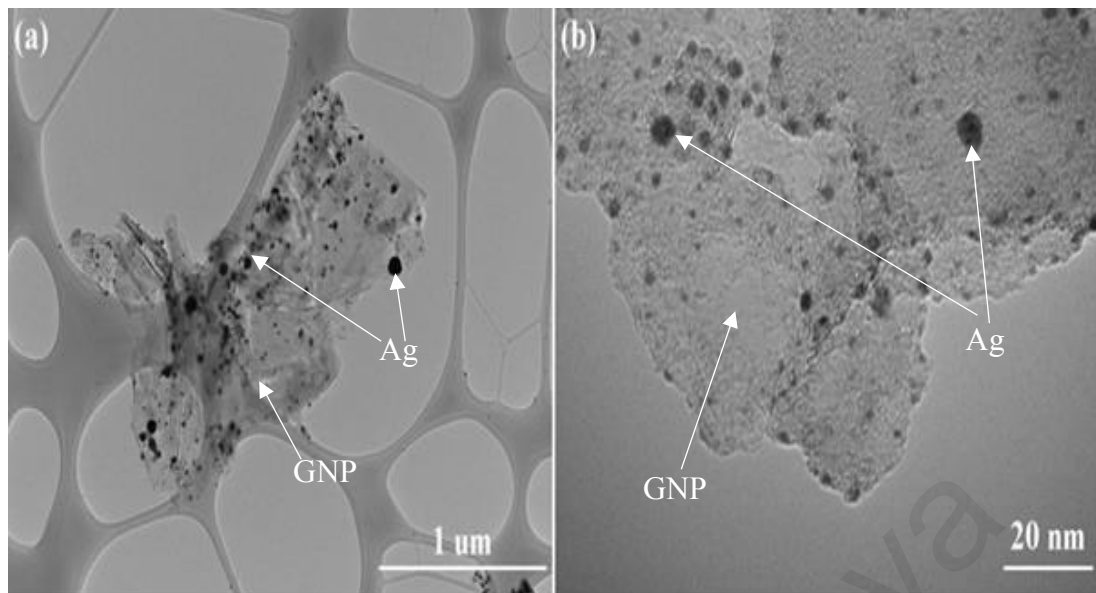


Figure 4.13: TEM images of GNP-Ag nanocomposite.

4.3.3. Thermo-physical properties of GNP-Ag hybrid nanofluids

Thermal conductivities of the nanofluids are measured for weight concentrations in the range of 0.02% to 0.1% and the temperature variation from 20 °C to 40 °C. Low values of particle concentrations are selected to avoid increase of effective viscosity. Figure 4.14 presented the thermal conductivity of distilled water based GNP-Ag nanofluids at different temperatures for various concentrations. It is seen that the thermal conductivity of nanofluids increases with the increase of weight fraction of nanoparticles and/or temperature. For 0.1% weight concentration of GNP-Ag, the enhancement of thermal conductivity is 16.94% at 20 °C and nearly 22.22% at 40 °C for the same concentration. The increase in the effective thermal conductivity is due to the high thermal conductivity of GNP as well as Ag nanoparticles. With increasing of weight concentration, the particles distance (free path) decreases. This is due to the percolation effect. Percolation refers to the movement of fluids through porous materials, describes the behaviour of connected clusters in a random graph. With increasing of nanoparticle weight fraction in the base fluid the percolation effect enhanced and led to improvement of thermal performance of the suspensions.

More particles are in contact with each other, which increases the frequency of lattice vibration (Baby & Sundara, 2011). The increase in thermal conductivity is linear with the rise of both the temperature and weight fraction. The enhancement of thermal conductivity of carbon based nanofluids was already reported by other researchers (Baby & Sundara, 2011; Das et al., 2003).

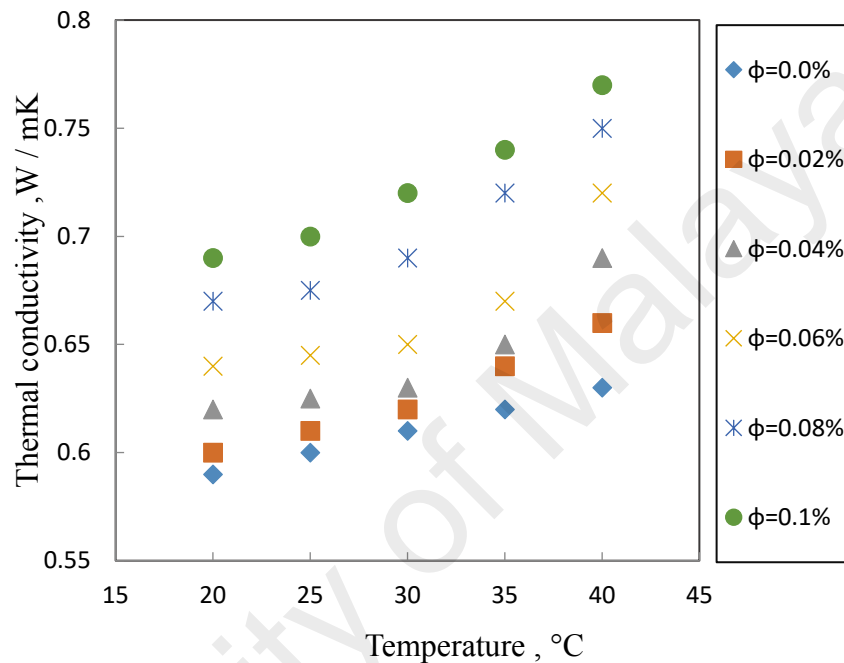


Figure 4.14: Variation of experimental data for thermal conductivity of GNP-Ag hybrid nanofluids with the effect of temperatures and particle concentrations.

Figure 4.15 shows the viscosity of distilled water and GNP-Ag nanofluids for various concentrations and at temperatures in the range of 20 °C to 40 °C for a shear rate of 500/s. The measured viscosity of distilled water at 20 °C is 1.10 (m Pa.sec), which is in good agreement with the previously reported data. It is found that with the increase of nanofluids solid volume concentrations, the viscosity of nanofluids increases due to the fact that increasing concentration would have a direct effect on the fluid internal shear stress (Nguyen, Desgranges, Roy, Galanis, Mare, Boucher, & Angue Mintsas, 2007). The viscosity decreases with the increase of temperatures, which is due to a weakening of inter-particle and inter-molecular adhesion forces (Nguyen, Desgranges, Roy, Galanis,

Mare, Boucher, & Angue Mintsa, 2007). Viscosity increase by about 30% for 0.1% weight concentration of nanofluids compared to the viscosity of the base fluid at 40 °C.

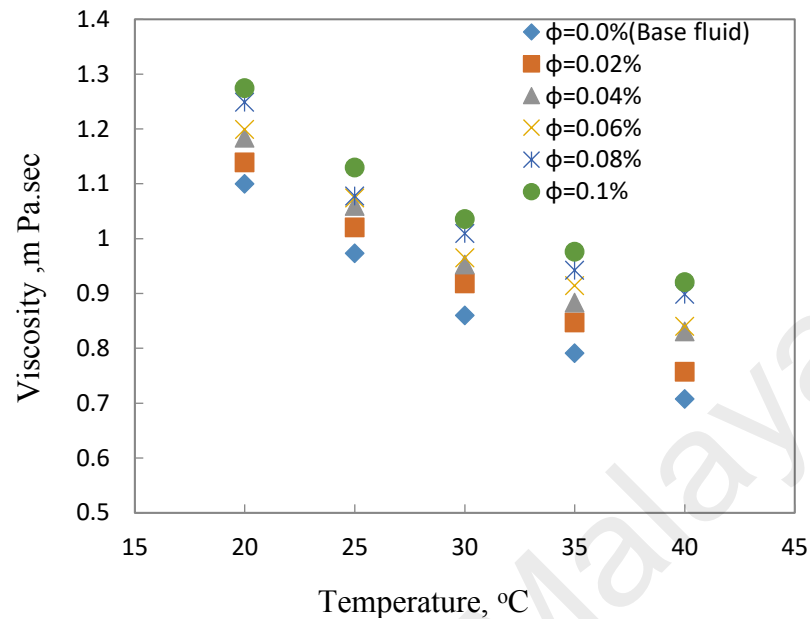


Figure 4.15: Variation of experimental data for viscosity of GNP-Ag hybrid nanofluids with temperatures and particle concentrations.

Figure 4.16 represents the densities measurement of distilled water and hybrid nanofluids for different weight concentrations at the temperatures in the range of 20 °C to 40 °C. It is seen that with the increase of nanoparticle fraction the density increases slightly. Actually the density is linearly proportional to the solid fraction and its variation is of the same order as the solid weight fraction. The density increase compare to the density of base fluid at 40 °C, is about 0.09% for 0.1% fraction of nanoparticles. The density increase is very small, which could be considered negligible.

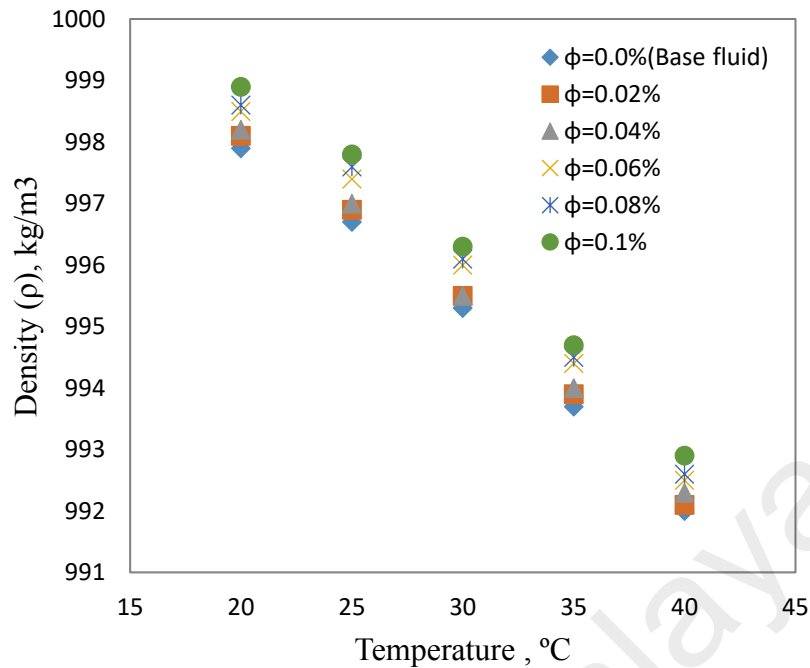


Figure 4.16: Variation of the experimental data for density of GNP-Ag hybrid nanofluids with temperatures and particle concentrations.

4.4. Activated Hybrid of Biomass Carbon/Graphene Oxide Ethylene Glycol based nanofluid

4.4.1. Synthesis of hybrid nanocomposite and nanofluid preparation

Graphite flakes were purchased from Ashbury Inc. and the rest of the chemicals and materials such as nitric acid (HNO_3), sulphuric acid (H_2SO_4), phosphoric acid (H_3PO_4 , 98%), potassium permanganate (KMnO_4 , 99.9%), hydrogen peroxide (H_2O_2 , 30%), hydrochloric acid (HCl , 37%), potassium hydroxide (KOH) and ethylene glycol (EG, 98%) were purchased from Sigma-Aldrich Co., Selangor, Malaysia. The EFB fibers were prepared from the Forest Research Institute of Malaysia.

GO was prepared using graphite flakes by a simplified Hummer's method (Hummers Jr & Offeman, 1958). Typically, graphite flakes (1 g) were mixed with 120 mL of H_2SO_4 and 13 mL of H_3PO_4 at room temperature. After that, 6 g of KMnO_4 was gradually added to the mixture. After three days of continues stirring, the mixture was diluted with 250

mL of ice water. Afterwards, H_2O_2 was added until the gas evolution ceased. The suspension was then washed with HCl (1 M) and deionised water until the pH of the solution reached 5. Finally, the product (GO) was separated from the solution using a centrifuge.

A simple heat treatment route was adopted to produce the final sample. The carbon prepared via pyrolysis of empty fruit bunch (EFB) fiber at 500 °C with 10 °C /min increment within 2 hr in N_2 atmosphere. The acceptable tiny powders of carbon were prepared by ball milling (5 min). The GO (3 wt% of carbon) dispersed in distilled water (50 ml) by sonication for 30 min. GO and carbon samples added to two beakers containing 100 mL aqueous KOH solution separately and were stirred for 2 hours (500 rpm). The mass ratio of KOH/carbon and KOH/GO was 4:1. The carbon sample and GO sample were mixed together, and stirred for 3 hours and finally dried at 50 °C. The mixture was put in a ceramic boat and placed in a tube furnace. The mixture was heated at a rate of 5 °C up to 430 °C under N_2 flow and held for 30 minutes, after that heated up to 800 °C and retained for 75 minutes. The obtained nanocomposite was washed with distilled water and HCl (0.1 M) several times to remove the impurities and then dried at temperature of 60 °C. This sample was denoted as hybrid of Activated Carbon/Graphene Oxide (ACG) and used to make nanofluid.

Since ACG nanocomposite is naturally hydrophobic, it cannot be dispersed in any polar solution like EG. Functionalization by acid treatment is a suitable way to ensure the proper dispersion of ACG in EG. Acid treatment process was performed by dispersing ACG in a 1:3 ratio of HNO_3 and H_2SO_4 solution (strong acid medium) for 3 hours under bath-ultrasonication. After 3 hours, ACG nanopowder was washed several times with DI water and then dried in an oven at the temperature of 70 °C for more than 24 hours. The prepared ACG functionalized sample was used in the next step to make nanofluids at different concentrations. A calculated amount of ACG was dispersed in the EG by

ultrasonication. The optimized ultrasonication time was 45 min. The nanofluids prepared by the above-mentioned method was stable and no sedimentation of particles was found up to 24 hours.

4.4.2. Characterization of ACG nanocomposite

Figure 4.17 (a and b) shows the FESEM images of Activated Carbon (AC) and ACG respectively. The image presents an appropriate contribution of GO in the carbon structure which is confirmed further by TEM image (Figure 4.17 (c)). Moreover, the chemical composition of the ACG sample is contained Carbon (63.331%), hydrogen (2.006%), nitrogen (0.290%) and oxygen (34.373%).

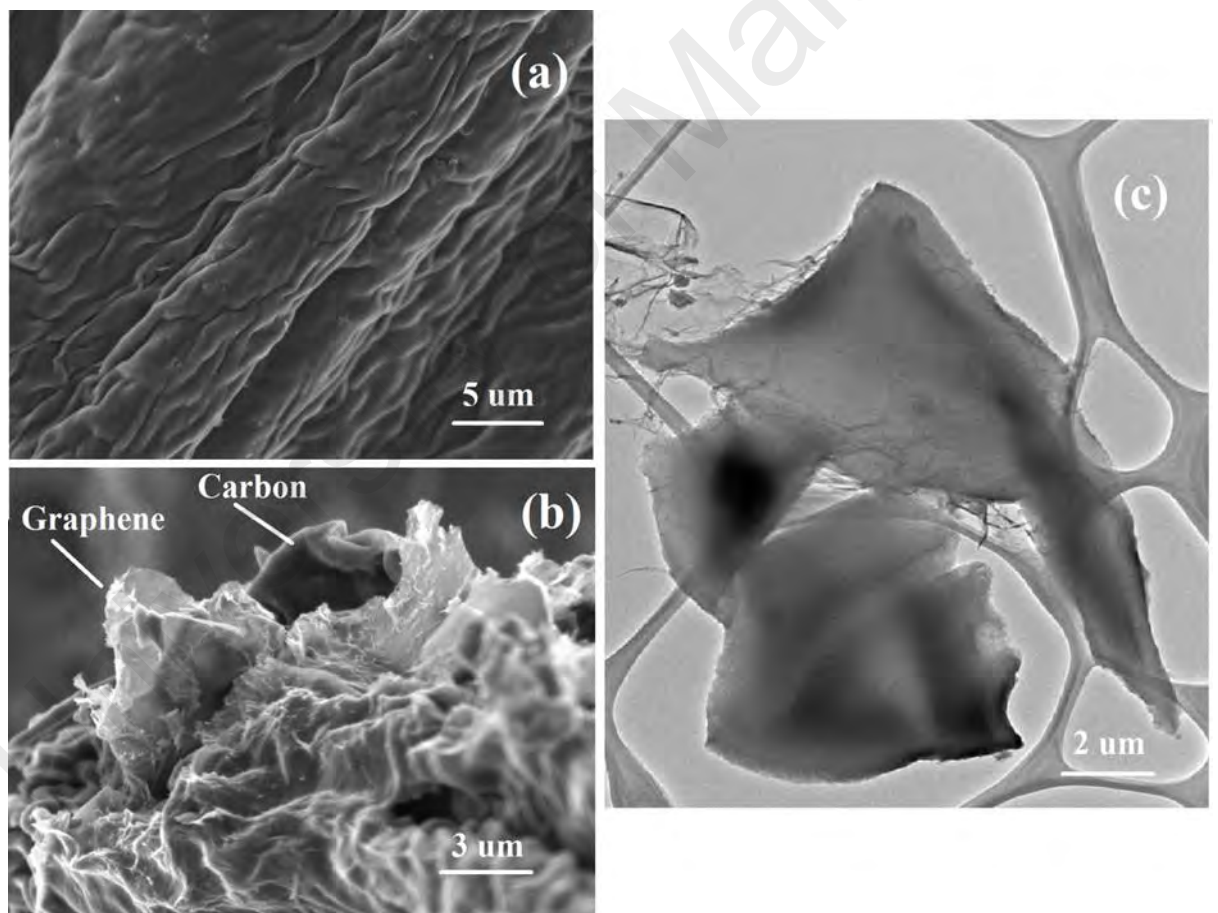


Figure 4.17: FESEM images of (a) pure AC, (b) ACG and (c) TEM image of ACG

Raman and XRD analysis of the carbon materials are two powerful methods for structural characterization. XRD analysis results for AC and ACG are shown in Figure 4.18 (a). The samples exhibit a very weak and broad peak in the range of 20°-30°,

indicating that the samples are in amorphous state. The Raman spectra of ACG and AC are presented in Figure 4.18 (b). Raman spectrums of the prepared sample display the D-band at $\sim 1340\text{ cm}^{-1}$ and the G-band at $\sim 1598\text{ cm}^{-1}$. One of the important parameters in the Raman studies is the peak intensity ratio of the D and G bands, (I_D/I_G) which is attributed to the disordered crystal structures of the carbon. The I_D/I_G value is 0.51 for ACG, and 0.36 for AC. The D_band and G_band around 1340 and 1598 cm^{-1} are respectively associated to the intensity ratios for disordered and graphitic bands in the samples. In fact, the intensity ratio of I_D/I_G is known to describe the proportion of sp^3 hybridized carbon to sp^2 hybridized carbon. It is known that the presence of functional groups such as carboxyl groups could change hybridization of some sp^2 carbons to sp^3 ones, leading to an increase in I_D/I_G ratio. As could be seen in Figure 4.18(b), the I_D/I_G ratio of acid-treated sample (ACG) is larger than that of AC. In functionalization studies of carbon nanostructures, the higher intensity ratio of I_D/I_G indicates the higher disruption of aromatic $\pi - \pi$ electrons, implying the partial damage of graphitic carbon in AC, implying the successful oxidation of AC for preparing hydrophilic COOH branches.

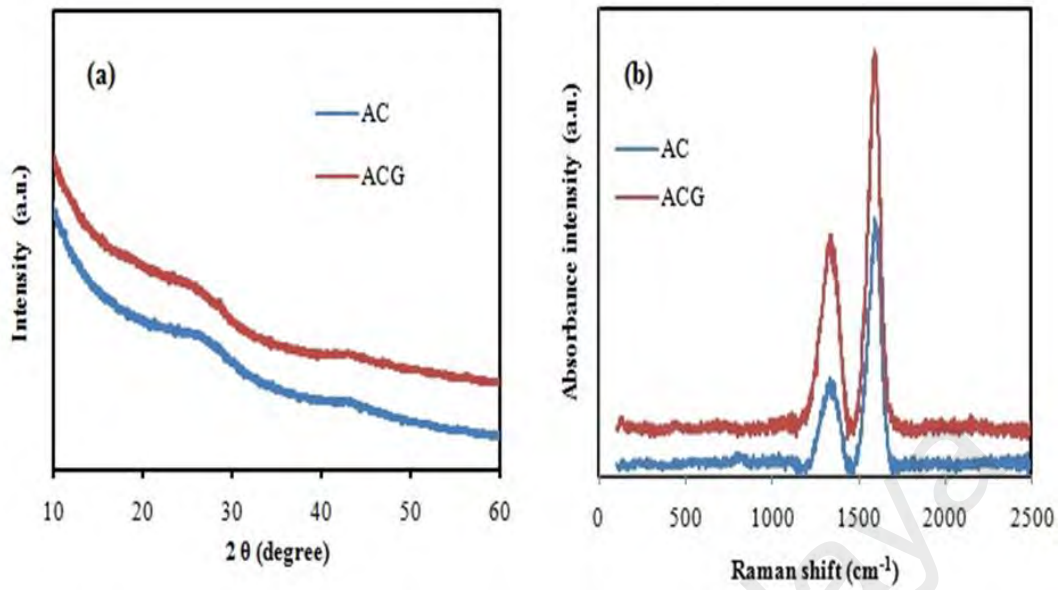


Figure 4.18: (a) X-ray diffraction analysis of samples and (b) Raman spectra of AC and ACG.

4.4.3. Thermo-physical properties of ACG hybrid nanofluids

Thermal conductivity of three different ACG/EG weight percentage nanofluid samples are measured in the range of 20 °C to 40 °C temperature. Low values of weight percentage are selected to avoid increase of effective viscosity and sedimentation. Figure 4.19(a) presents the thermal conductivity of EG based ACG nanofluids at different temperatures for various weight concentrations. It is found that the thermal conductivity of nanofluids enhances with the increase of weight percentage of nanoparticles and/or temperature. Enhancement of the thermal conductivity is nonlinear both for weight percentage and temperature. The nonlinearity/linearity of thermal conductivity with respect to volume fraction relates to the nature of the nanoparticle as well as the EG. It is notable that the particle weight percentage has governed the enhancement in thermal conductivity which can be attributed to the percolation mechanism being confirmed by the optical images (see Figure 4.20) (PM Sudeep et al., 2014) .

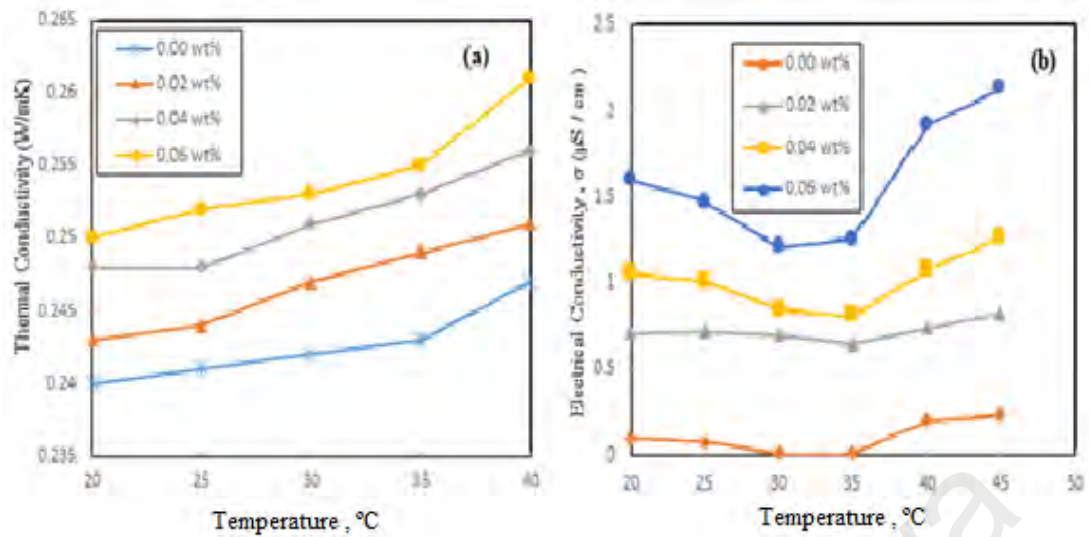


Figure 4.19: (a) Thermal conductivity and (b) electrical conductivity of EG and ACG hybrid nanofluids.

Moreover, the percentage enhancement of thermal conductivity is calculated by using the equation (4.1) as shown below:

$$Enhancement (\%) = \frac{[(k_{nf} - k_b) \times 100]}{k_b} \quad (4.1)$$

Where, k_b is the thermal conductivity of the base fluid and k_{nf} is that of the nanofluid.

For 0.06% weight percentage of ACG in EG, the enhancement of thermal conductivity is 4.17% at 20°C and 6.47% at 40°C for the same concentration. The increase in the effective thermal conductivity is due to the high thermal conductivity of activated carbon as well as graphene nanoparticles. This behaviour of enhancement and nonlinearity was already reported by previous researchers (Shirazi et al., 2015).

Figure 4.19(b) shows the effective electrical conductivity of ACG/EG nanofluids at different temperatures for various concentrations. The experimental data reveals an improvement in electrical conductivity with the increase of nanoparticles weight fraction and temperature in the case of ACG/EG nanofluids. The electrical conductivity of 0.06% nanofluid was obtained 2.13 $\mu\text{S/cm}$ at 45 °C, which is 787.5% higher than the electrical conductivity of the base fluid.

Figure 4.20 presented the optical images of ACG nanofluid samples at different concentrations after drop casting on glass slide. Figure 4.20 (a-c) show; (1) the uniform

dispersion of ACG samples in EG, and (2) the enhanced percolation channels made by nanoparticles concentration enhancement.

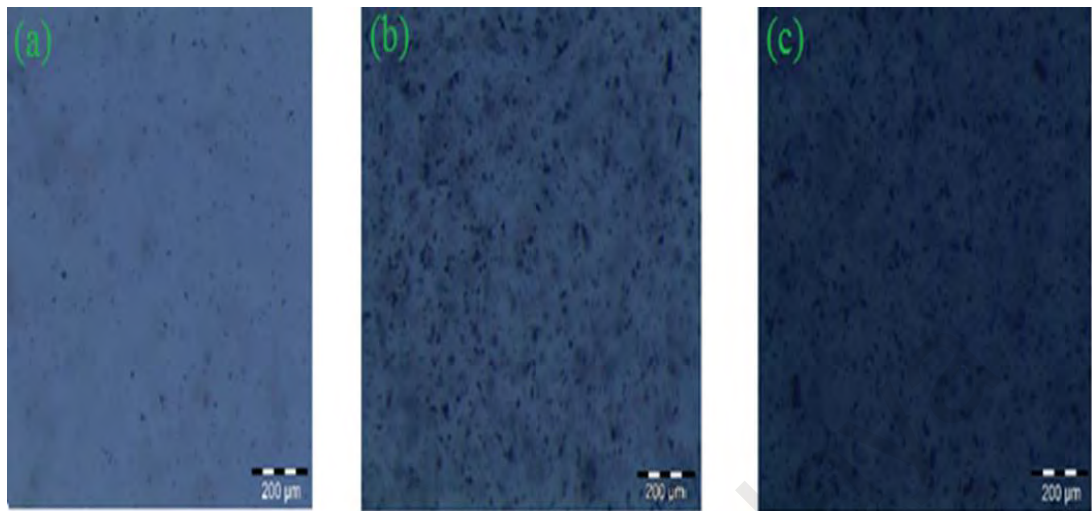


Figure 4.20: Optical images of ACG/EG hybrid nanofluids at (a) 0.02 wt%, (b) 0.04 wt% and (c) 0.06 wt%.

The viscosity of nanofluids is one of the important factors in different types of heat transfer applications as it has directed effect on the design of heat transfer equipment. Fig.5 shows the viscosity of pure ethylene glycol (EG) and various weight concentrations of ACG/EG nanofluids as a function of shear rate at temperature of 20 °C, the range of shear rates are from 20/s to 500/s. EG and various concentrations of ACG/EG nanofluids have shown independent behaviour within the range of investigation, which qualifies Newtonian performance of ACG/EG nanofluids. The measured viscosity of pure ethylene glycol is 0.0179 (Pa.s) at 20 °C which is very close to others theoretical and experimental standards (Mariano et al., 2015). Figure 4.21 Shows the link between the viscosity of the hybrid nanofluids and the temperature for different weight concentrations of the ACG at shear rate of 500/s. The viscosity increases nonlinearly with increase of ACG weight concentration, With the increase of the nanoparticle weight fraction in the base fluid the internal shear stress increased and as well amplification of internal shear stress happened (Kumaresan & Velraj, 2012). The compound structure of ACG enhances the surface interactions, when it is dispersed in EG. A very low weight percentages of nanoparticles was added to avoid sedimentation and the rises of viscosity is just a little. Highest amount

of viscosity incensement at 0.06 wt% is around 4.16%. For all the weight concentrations, viscosity decreases gradually with the increase of temperature, similar trend have been observed for pure EG, Which is due to weakening of the inter-particle and inter-molecular adhesion forces(Nguyen, Desgranges, Roy, Galanis, Mare, Boucher, & Mintsa, 2007). At a higher temperature range, particularly at 45°C, the viscosity enhancement is low for all the nanofluids, which makes it appropriate for heating applications with minimum penalty in the pumping power.

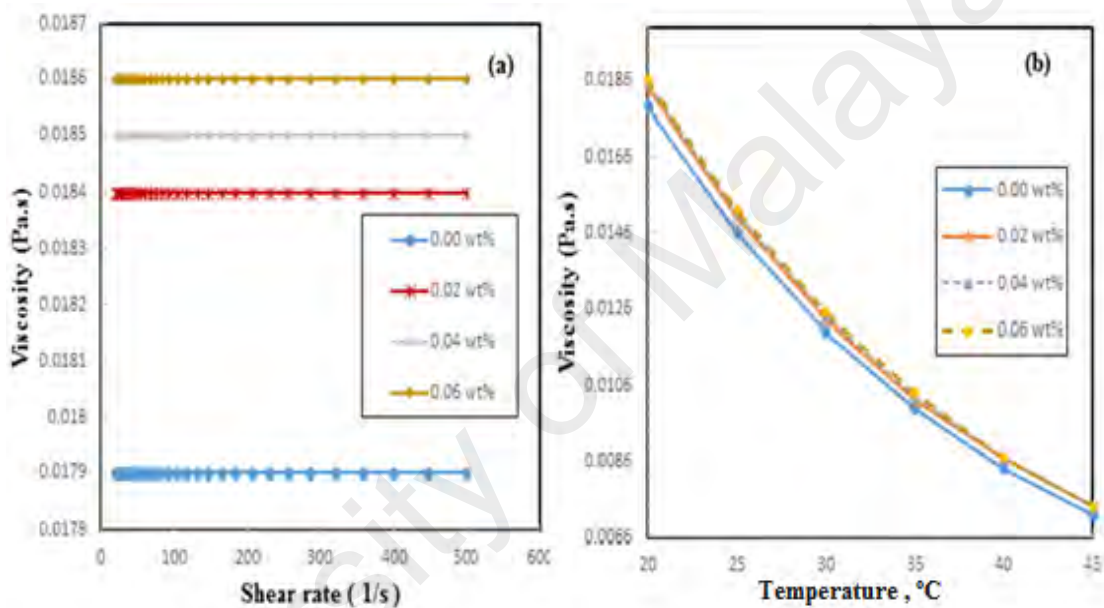


Figure 4.21: (a) Viscosity versus shear rate and (b) dynamic viscosity versus temperature of ACG/EG hybrid nanofluids at different weight concentrations and shear rate of 500/s.

Volumetric behaviour of hybrid samples obtained from experimental measurements of density are presented here. Figure 4.22 shows the density of pure ethylene glycol and hybrid nanofluid samples as a function of temperature and weight fraction. The data with particle weight percentages of 0.02%, 0.04% and 0.06% were measured from 20 to 50 °C at 5 °C steps. The instrument was calibrated with distilled water and found as, 0.997 kg/m³ which is very near to the literature value (0.998 kg/m³). The density of ACG/EG hybrid nanofluids increases with the increase of nanoparticle concentrations, and decreases when temperature increases. Some other experimental result with other base fluid and

nanoparticles showed the same trend (Kumaresan & Velraj, 2012; Mariano et al., 2015). The highest amount of density enhancement is 0.09% for 0.06 wt% at 20 °C. This insignificant density enhancement might be attributed to the interface effects on the bulk fluid properties produced by the solid nanoparticle surface, and to the interactions among the nanoparticles themselves, which is usually considered negligible.

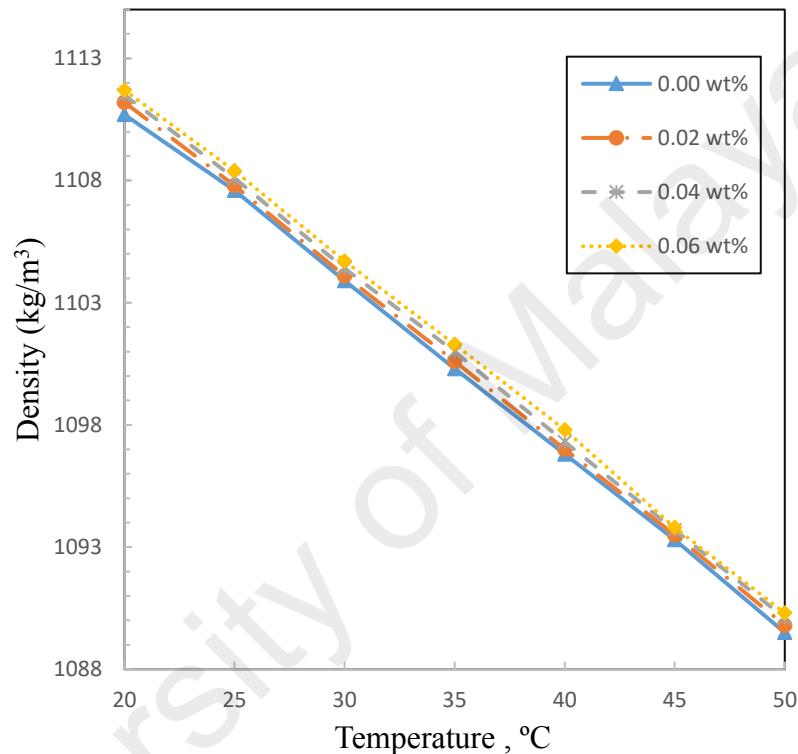


Figure 4.22: Density of EG and ACG hybrid nanofluids at different temperatures.

Despite importance of the specific heat capacity on heat transfer performance of nanofluids, only a limited literature are available about the effect of nanoparticle concentrations on the specific heat of nanofluids. Figure 4.23 shows the specific heat capacity of ACG/EG nanofluids as a function of nanoparticle concentrations and temperatures. It can be seen that the specific heat capacity of nanofluid samples are higher than those of the base fluids. With the increasing of particles weight percentage the specific heat capacities are enhanced. Figure 4.23 illustrates when temperature gradually increases from 20 °C to 50 °C the specific heat capacity of samples are also improved. The measured nanofluid specific heat capacities show the specific heat of nanofluid at

0.06 wt % fraction is about 2.25 % higher than that of the base fluid at 50 °C. There is a little increase in specific heat capacity of hybrid nanofluids with the increase of loading of ACG. However, most of the previous investigations reported that specific heat capacity decreases with the addition of nanoparticle but some unexpected results are also observed (Shahrul et al., 2014). Ghazvini et al. (2012) found that, specific heat of all nanodiamond-engine oil fluids increases with the increase of weight fractions and Mohebbi (2012) also reported the same trend for specific heat results. It seems that specific heat capacity of both the basefluid and nanoparticles have influence on the nanofluids heat capacity and also the interfacial free energy of solid–liquid is changed with the alteration of suspended nanoparticles. Due to the greater surface area of nanoparticles, its surface free energy has a superior influence on the system capacity, which affects the specific heat of composite materials (Q. He et al., 2012; Shahrul et al., 2014).

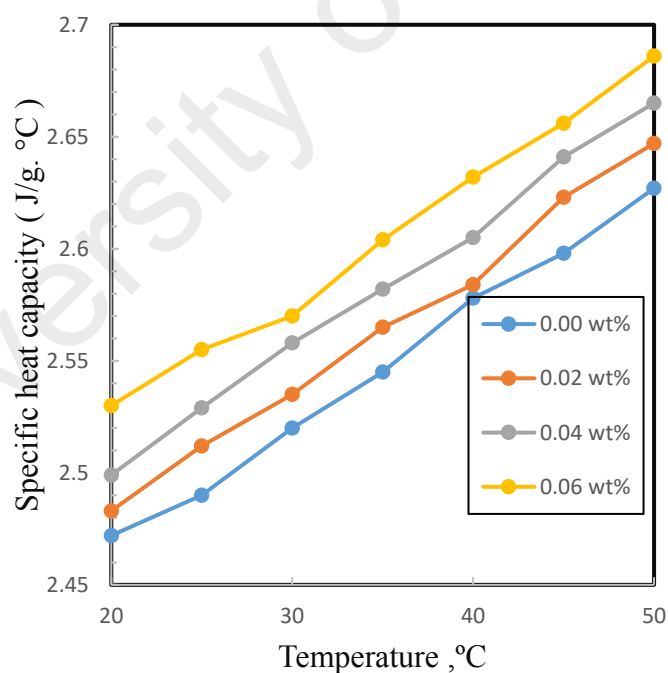


Figure 4.23: Specific heat capacity of ACG/EG nanofluids at different temperature.

4.5. Functionalized GNP-Pt water based hybrid nanofluid

4.5.1. Synthesis of GNP-Pt nanocomposite

Graphene nanoplatelet (GNP) with purity $\sim 99.5\%$, maximum particle diameter of 2 μm and specific surface area of 500 m^2/g were purchased from, XG Sciences, Lansing, MI, USA. The rest of the chemicals such as potassium tetrachloroplatinate II (K_2PtCl_4), nitric acid (HNO_3), sulphuric acid (H_2SO_4) and Sodium borohydride (NaBH_4) were purchased from Sigma-Aldrich Co., Selangor, Malaysia.

As mentioned earlier, since GNP is not naturally hydrophilic and it cannot be dispersed in distilled water and acid treatment required to make it dispersible (the procedure of acid treatment has been explained in section 4.3.1). then, the functionalized GNP was decorated with platinum by a chemical reaction process. The functionalized GNP (30 mg) was dispersed into 10 mL of distilled water. This process was continued by the addition of 0.035 M K_2PtCl_4 to the dispersed functionalized GNP suspension with continuous stirring for 2 h at room temperature, then 2 mL of Sodium borohydride (0.1M) was added to the solution drop wisely at 60 $^\circ\text{C}$. The irradiation of final solution was done under vigorous stirring for 4 h. Then GNP–Pt nanocomposites were collected after centrifuge at 11,000 rpm for 40 min. The obtained composite was washed well with distilled water several times to remove reactants. The prepared rich sample was used in the next step to prepare nanofluids at different concentrations by adding specific amounts of distilled water. The resulting nanofluids were stable and the sedimentation of GNP-Pt hybrid nanofluid was less than 5.7% after 22 days. Figure 4.24 shows the schematic of molecular structure of synthesised GNP–Pt nanocomposite.

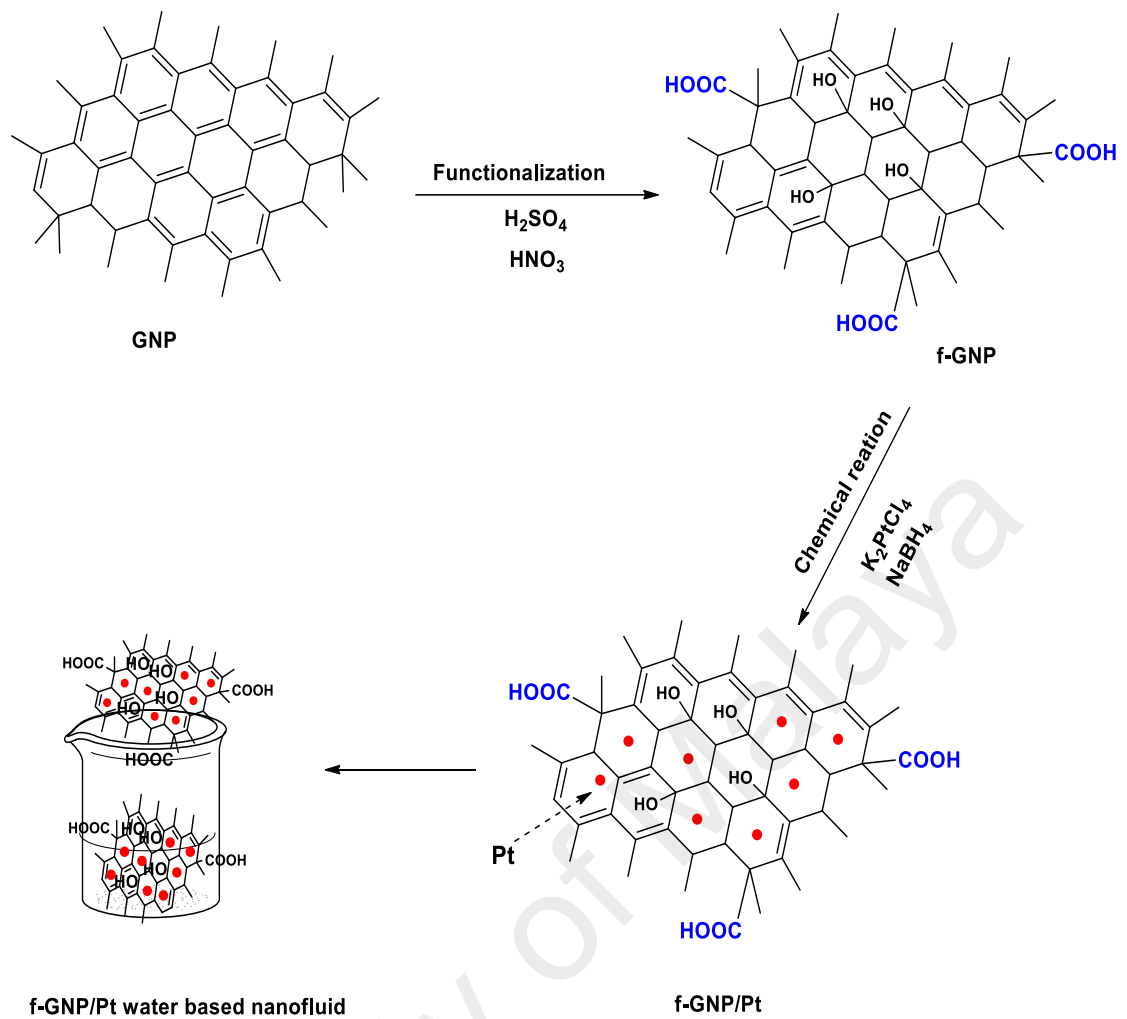
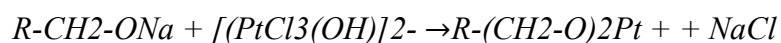
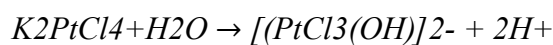
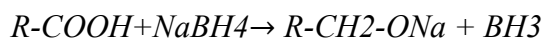


Figure 4.24: Schematic of the synthesis of GNP-Pt nanocomposite and then making of nanofluid.

The interactions are as follows:



4.5.2. Characterization of GNP-Pt nanocomposite

Figure 4.25 shows the XRD patterns of Pt coated GNP. The peak at around 26.6° represents the structure of GNP. The XRD profile of the sample shows three diffraction peaks at 40° , 46.5° and 67.8° , which are attributed to the (111), (200) and (220) lattice planes of cubic Pt (JCPDS card no. 00-001-1194). XRD patterns confirm that no unexpected reaction happened during acid treatment, chemical reduction and Pt coating

processes. Moreover it can be clearly concluded that Pt nanoparticles has been successfully decorated on the GNPs.

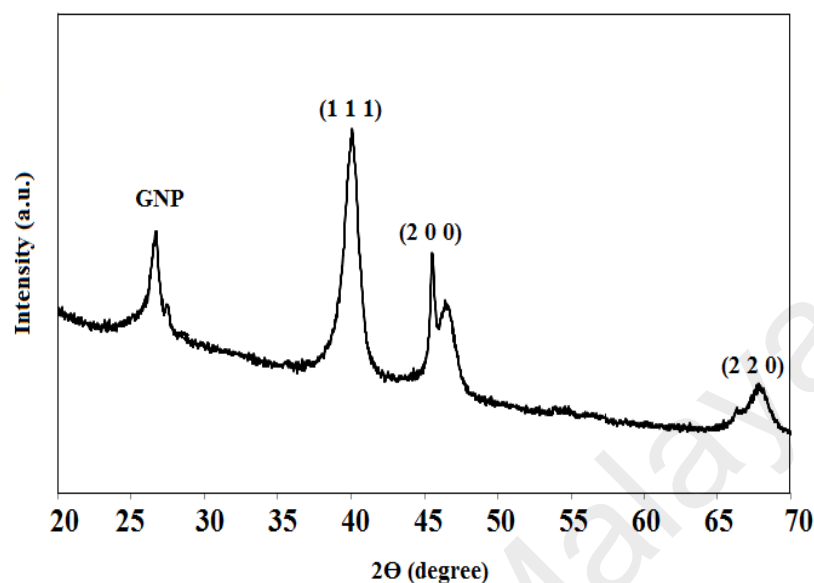


Figure 4.25: XRD pattern of GNP–Pt nanocomposite

The morphological characterizations of the Pt coated GNP nano-powders are presented in Figure 4.26. The uniform distribution of Pt attachment on the graphene sheets can be noticed in FESEM image (Figure 4.26). Pt nano-particles attachment with GNP can be the evidence of a successful acid treatment ensuring reduction of functional groups which finally provides appropriate uniform attachment of Pt on GNP sheets.

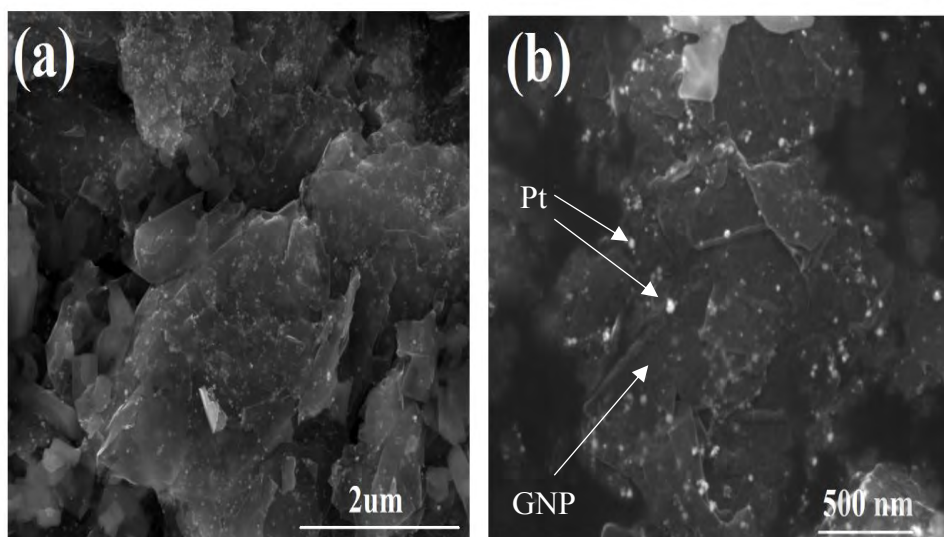


Figure 4.26: FESEM images of GNP–Pt nanocomposite; (a) low and (b) high magnifications.

Figure 4.27 shows the TEM image of Pt coated GNP sheet. The uniformity of Pt nanoparticles distribution due to proper functionalization of GNP is more visible in TEM images. From the image it could also be figured out that the wrinkled surface and folding at the edges of GNP sheets are produced during the acid treatment and the attachment of Pt particles.

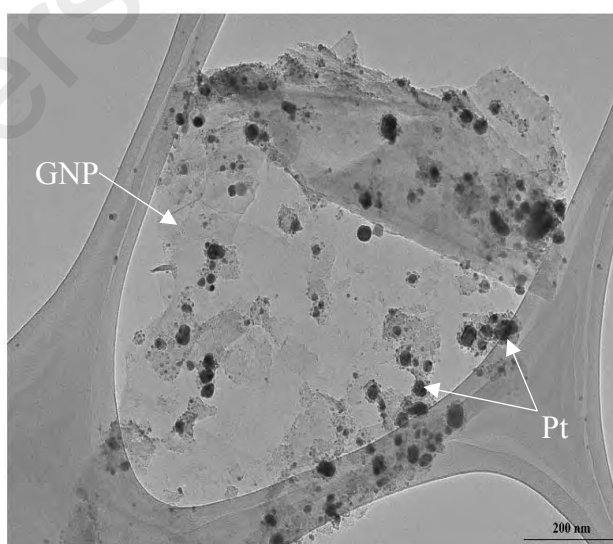


Figure 4.27: TEM image of GNP-Pt nanocomposite.

The uniformity of nanoparticles dispersion in water could be observed by a UV-visible Spectrophotometer which could correlate the absorbance with the homogeneity of

suspension. Figure 4.28 (a) illustrates the UV–vis spectrum of the functionalized GNP-Pt based water nanofluids. UV–Vis spectroscopy is generally considered for the investigation of the stability of the coolant and the sedimentation with time as estimated from the change of absorbance of the suspension with time. According to the Beer–Lambert’s law, the absorbance of a solution is directly proportional to the concentration of the absorbing species such as particles in the solution. As a raw spectrum of functionalized GNP-Pt based water nanofluid, a sharp peak at 263 nm is attributed to the presence of GNP and a broad peak at 730 nm is due to the existence of Pt nanoparticles. Also, quantitative analysis of the dispersion state and the long-term stability of the functionalized GNP-Pt based water nanofluid can be performed in the UV–Vis spectroscopy, as shown in Figure 4.28 (b). Thus, the absorbance at the wavelength of 263 nm was measured during 528 hours for all the weight concentrations. It can be seen that the concentration of the loaded nanocomposite in the aqueous media had decreased insignificantly over time. As a result, the maximum sediment of 5.7% was obtained for the highest weight concentration of 0.1 %, which confirmed the suitable dispersibility of the functionalized GNP-Pt nanocomposite in distilled water.

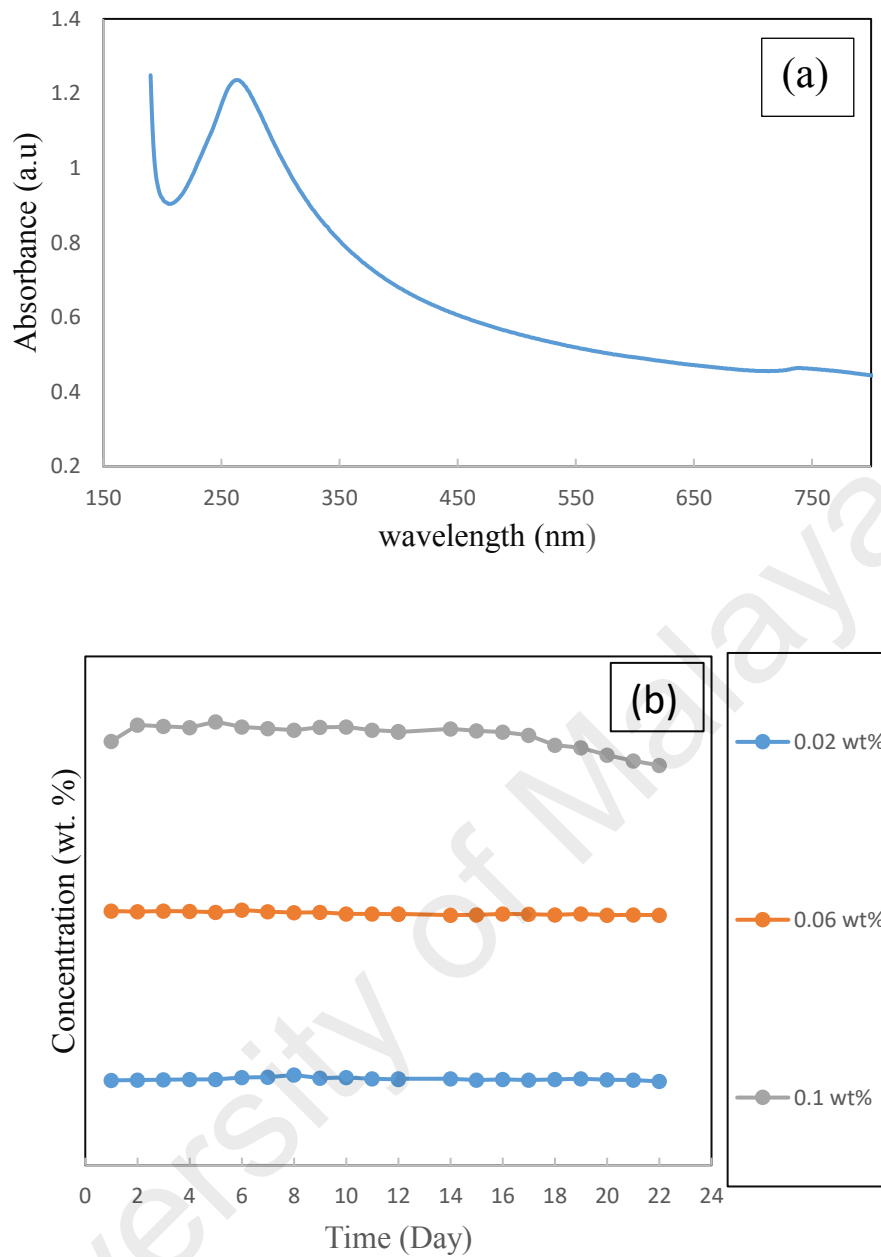


Figure 4.28: (a) UV-vis spectrum of functionalized GNP-Pt based water nanofluid and (b) the colloidal stability of functionalized GNP-Pt based water nanofluid as a function of time.

4.5.3. Thermo-physical properties of GNP-Pt hybrid nanofluids

Thermal conductivity of three different weight percentages GNP/Pt water based hybrid nanofluid. Samples are experimentally examined in the range of 20 °C to 40 °C temperature. Low values of weight percentages are selected to avoid increase of effective viscosity and sedimentation. Figure 4.29 presents the thermal conductivity of water based functionalized GNP-Pt nanofluids at different temperatures and various weight

concentrations. It is found that the thermal conductivity of nanofluids enhances with the increase of weight percentage of nanoparticles and/or temperature. Enhancement of the thermal conductivity is nonlinear with the changes of both the weight percentage and the temperature. The nonlinearity/linearity of the variation of the thermal conductivity with respect to volume fraction relates to the nature of the hybrid nanoparticle as well as the base fluid. At 0.1% weight concentration of GNP-Pt nanofluid, the enhancement of thermal conductivity is 14.91% at 20 °C and nearly 17.77% at 40 °C. Enhancement in the effective thermal conductivity is due to the high thermal conductivity of GNP as well as Pt nanoparticles. With the increasing of nanoparticles weight concentration the distance between particles (free path) decreases. It happens due to the percolation effect. The rise of thermal conductivity of carbon-based water nanofluids with the increase of weight concentration has also been stated by other researchers (Amiri, Shanbedi, et al., 2015; Baby & Sundara, 2011; Das et al., 2003).

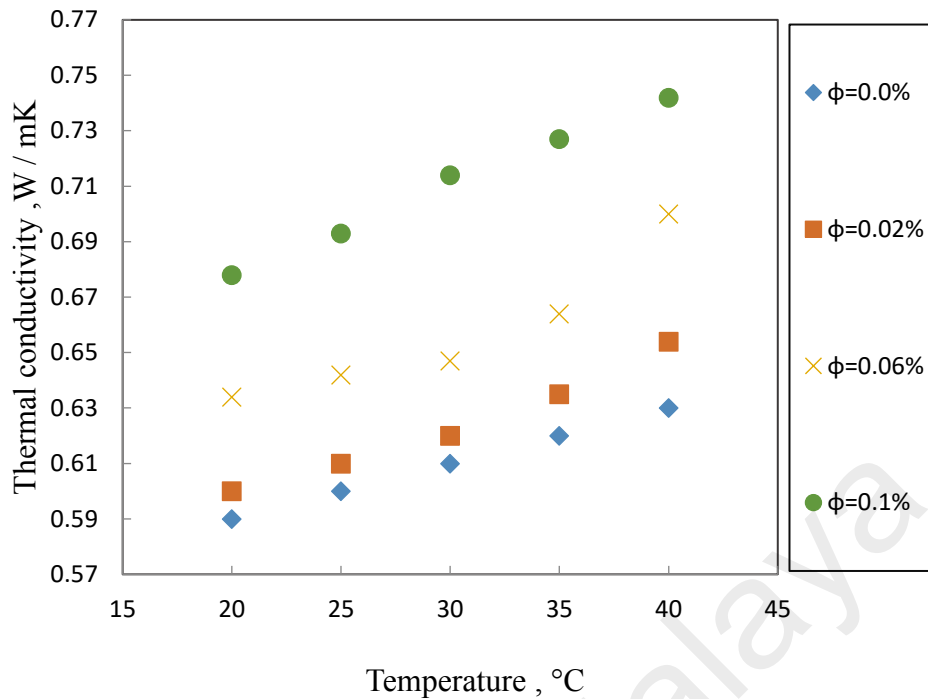


Figure 4.29: Thermal conductivity of functionalized GNP-Pt hybrid nanofluids as a function of temperature at different weight concentrations.

Figure 4. 30 represents the viscosity of distilled water (base fluid) and functionalized GNP-Pt hybrid nanofluids at different weight concentrations and at various temperatures from 20 °C to 40 °C for a shear rate of 500/s. The measured viscosity of base fluid (distilled water) at 20 °C is 1.10 (m Pa.sec), which has a good match with the available literature data. It is established that with the rise of nanofluids weight concentration, the viscosity of nanofluids increases as the increase in concentration would have a direct influence on the fluid internal shear stress (Nguyen, Desgranges, Roy, Galanis, Mare, Boucher, & Angue Mintsa, 2007). The viscosity decreases with the increment of temperatures, for the weakening of inter-molecular and inter-particle adhesion forces (Nguyen, Desgranges, Roy, Galanis, Mare, Boucher, & Angue Mintsa, 2007). There is about 33% increase of viscosity at 0.1% weight concentration of nanofluid compared to the viscosity of the distilled water at 40 °C.

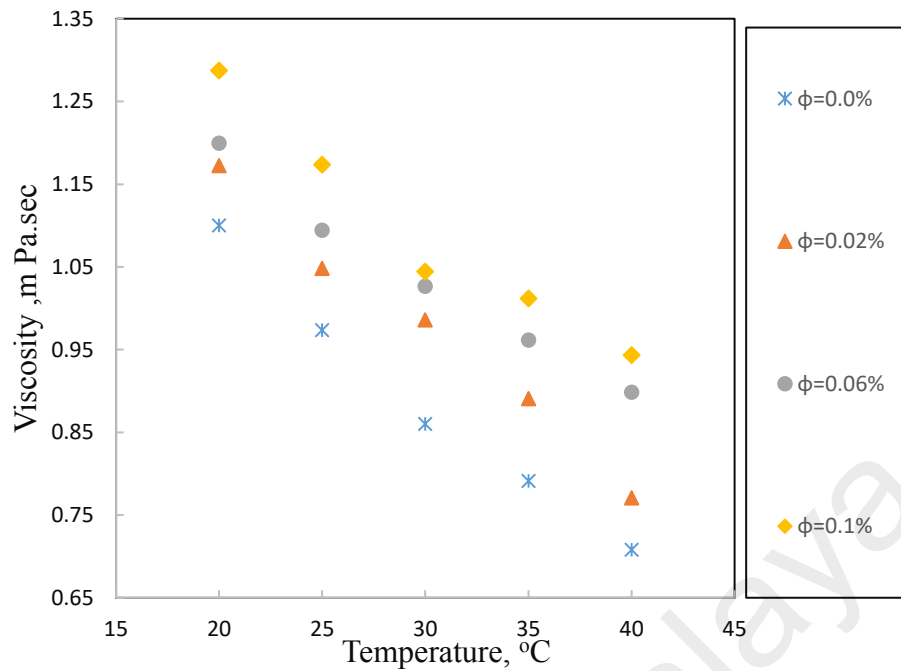


Figure 4.30: Viscosity of functionalized GNP-Pt hybrid nanofluids as a function of temperature at different weight concentrations.

Volumetric behaviour of functionalized GNP-Pt hybrid nanofluids has investigated from experimental measurements. Figure 4.31 shows the density of distilled water and hybrid nanofluid samples as a function of weight fraction and temperature. The data with particle weight percentages of 0.02%, 0.04% and 0.06% were measured at 20 to 40 °C and at 5 °C steps. The density of GNP-Pt water based hybrid nanofluids has increases with the increase of nanoparticle concentrations, and decreases when the temperature increases. Some other experimental results with various base fluid and nanoparticles have shown the same tendency (Kumaresan & Velraj, 2012; Mariano et al., 2015). The highest amount of density enhancement is 0.11% for 0.1 wt% at 40 °C. This trivial density improvement might be attributed to the interface effects on the bulk fluid properties produced by the solid nanoparticle surface, and to the interactions among the nanoparticles themselves, which is usually considered negligible.

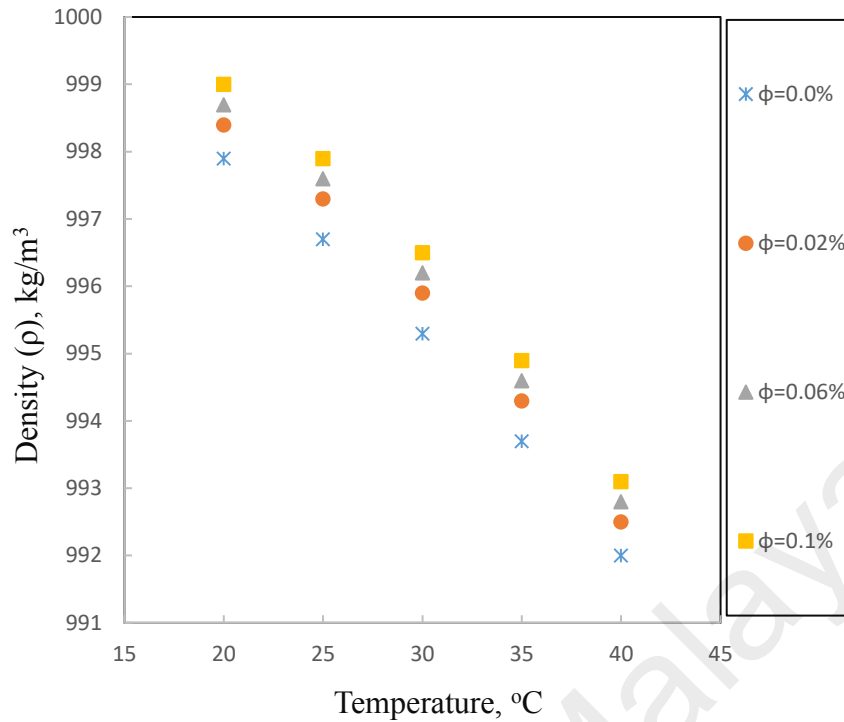


Figure 4.31: Density of functionalized GNP-Pt hybrid nanofluids as a function of temperature for different weight concentrations.

There are available limited investigations about the influence of nanoparticle concentrations on the specific heat of nanofluids (Shin & Banerjee, 2014; Vanapalli & ter Brake, 2013; L.-P. Zhou et al., 2010). Table 4.4, shows the specific heat capacity of functionalized GNP-Pt hybrid nanofluids as function of nanoparticle concentrations and temperatures. It can be seen that the specific heat capacity of nanofluid samples are lower than those of the distilled water. With the increasing of particles weight concentration the specific heat capacities are decreased. The measured nanofluid specific heat capacities show the specific heats of nanofluids are about 1.77% and 6.26 % lower than those of the base fluid for 0.02 and 0.1 wt% of nanoparticles respectively at 45 °C. However, most of the earlier investigations have stated that the specific heat capacity decreases with the addition of nanoparticles but some unexpected results are also observed (Shahrul et al., 2014). It seems that the specific heat capacity of both the nanoparticles and basefluid have effect on the nanofluids heat capacity and also the interfacial free energy of solid–liquid is changed with the alteration of suspended nanoparticles. Due to the greater surface area

of nanoparticles, its surface free energy has a superior impact on the overall heat capacity, which affects the specific heat of nanocomposite materials (Amiri et al., 2012; Shahrul et al., 2014).

Table 4.3: Specific heat capacity of water and functionalized GNP-Pt hybrid water based nanofluids at different weight concentration and temperature.

Temp	Water	GNP-Pt nanofluid		
	0.00%	0.02%	0.06%	0.10%
20	4.099	4.053	4.019	3.796
25	4.104	4.042	4.02	3.789
30	4.105	4.039	4.017	3.801
35	4.1	4.036	3.995	3.812
40	4.101	4.034	4.012	3.81
45	4.106	4.033	4.001	3.849

The comparison study of thermal conductivity enhancement for various samples has been shown in table 4.4. All of the samples revealed significant improvement but the GNP-Ag hybrid nanofluid shows the highest enhanced.

Table 4.4: Comparison study for thermal conductivity enhancement of the various samples at 0.1% weight concentration.

Type of nanofluids	20 °C	40 °C
f-GNP	13.56%	15.87%
f-GNP/Ag	16.94%	22.22%
ACG	4.17%	6.47%
f-GNP/PT	14.91%	17.7%

4.6. Summary

The present chapter highlights the synthesise and surface characterization of the nanocomposite and also the investigation of the thermos-physical property of the functionalized and hybrid nanofluid. Functionalized graphene, graphene based hybrid

nanocomposite (GNP-Pt and GNP-Ag) and hybrid of activated carbon/Graphene were synthesized and the surface characterizations were experimentally studied with various instruments. All the nanocomposite were made perfectly and homogeneously. Then, based on aforementioned nanoparticles new types of nanofluids had been prepared. All the samples showed well stability and no sedimentation. Finally, thermos-physical property measurements of the as prepared sample were performed. The experiment revealed that enhancement of thermal conductivity of hybrid nanofluid is higher than single phase nanofluid. Among hybrid nanofluids, GNP-Ag nanofluid showed the higher improvement in thermal conductivity which is due to the better thermal ability of the guest nanoparticles (Ag). The much higher increase in thermal conductivity in comparison to viscosity provides a strong signal of its possible use in thermal transport application which ideally needs liquid substance with high thermal property and low pumping resistance.

CHAPTER 5: HEAT TRANSFER AND FRICTION FACTOR OF NANOFLUIDS

5.1. Introduction

In this chapter, experimental investigation of turbulent forced convection heat transfer in square and round heated pipe (with same hydraulic diameter) was carried out. The emphasis was given on the heat transfer enhancement and friction factor resulting from various parameters which include different types of carbon based and hybrid nanofluids, volume fraction of nanoparticles in the range of $0.02\% < \varphi < 0.1\%$ and the Reynolds number in the range of $5000 < Re < 17500$.

5.2. Validation of experimental heat transfer set up

For the validation of experimental data, a preliminary set of tests were accomplished with water as the working fluid. Comparison of the experimentally measured Nusselt number for water with those from the existing correlations of Dittus-Boelter (Dittus & Boelter, 1930) and Petukhov (Petukhov, 1970) are shown in Figure 5.1. This figure confirmed that the obtained data are in good agreement with the evaluated values from the empirical correlations for turbulent flows. In particular, the correlation of Dittus-Boelter (Dittus & Boelter, 1930) seem to agree with the present measurement pretty well for Reynolds numbers (Re) lower than 15,000. For the whole range of considered Re, the model of Petukhov (Petukhov, 1970) shows better agreement with the present measurements. The average deviation between the present data and the Petukhov correlations for Nusselt number is about 1.55%, which validates the experimental methodology.

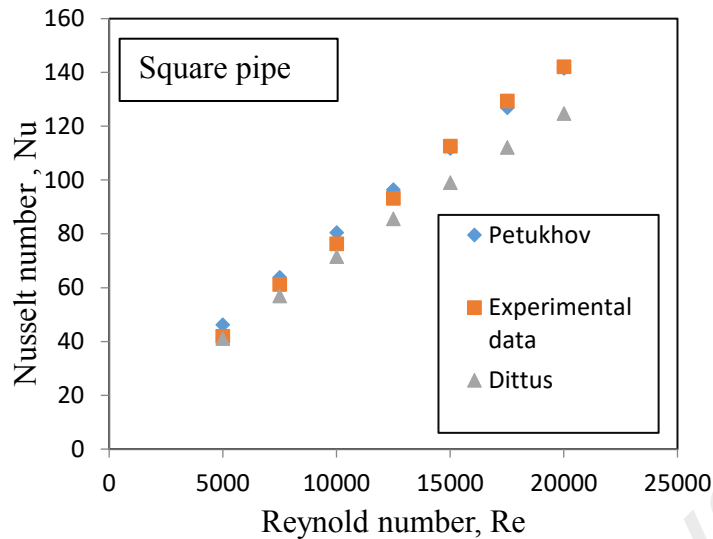


Figure 5.1: Comparison of measured Nusselt number of water with the correlations of Dittus- Boelter and Petukhov.

Figure 5.2 shows the experimental data of friction factor for the distilled water which was evaluated from equation (3.11) along with the numerical data from equations (3.12) and (3.12). Average deviations of 7.86% and 7.60% are obtained between experimental data and data from the two numerical correlations respectively.

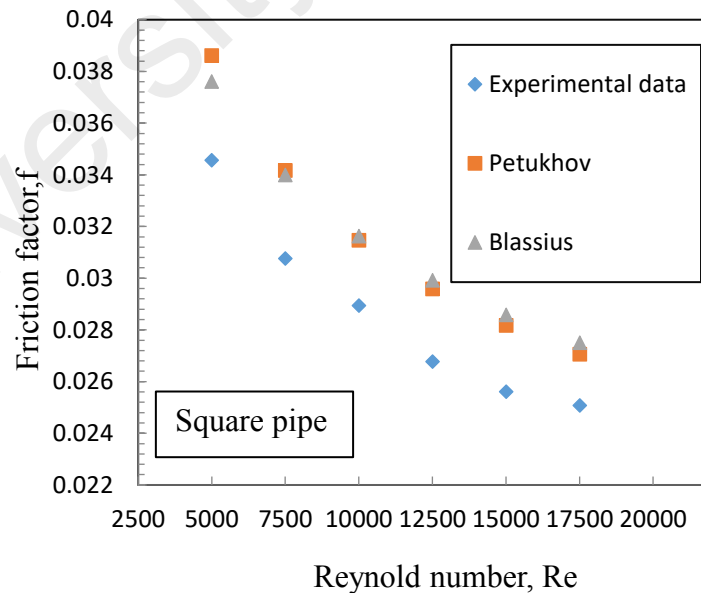


Figure 5.2: Comparison of measured friction factor of water with the correlations of Petukhov and Blasius.

Figure 5.3 shows the cross section effect on the Nusselt number. Two different cross section has been studied with water at a same condition. Both square and round pipe have

been chosen with same hydraulic diameter of 10 mm. the experimental results confirm that at same condition and hydraulic diameter change of cross section do not have influence on the Nusselt number and heat transfer performance of the convective heat transfer loop. An average deviation of 2.26% was found which might be due to the uncertainty of the device.

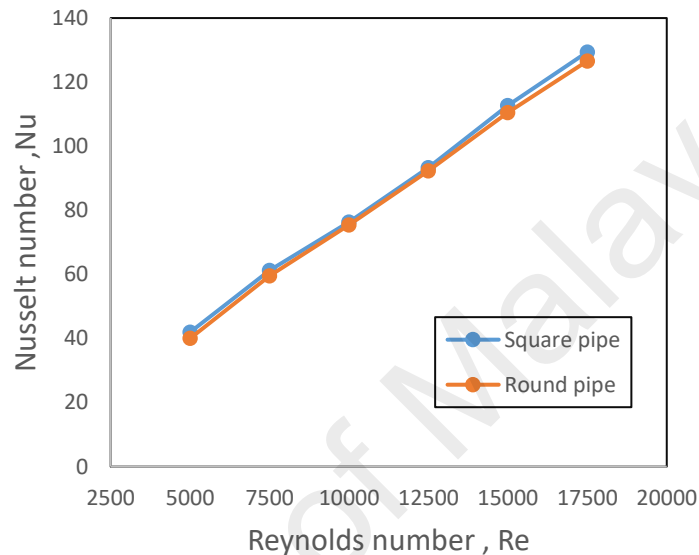


Figure 5.3: effect of test section cross section on the Nusselt number.

5.3. f-GNP/ Water nanofluids

5.3.1. Nusselt number and heat transfer coefficient of f-GNP nanofluids

Nanofluids at various weight fraction of functionalized GNP are then experimentally examined. The experimental data of Nusselt numbers for the nanofluids are calculated by equation (3.4), and the results are shown in Figure 5.4. It is recognised that the Nusselt number enhances with the increase of Reynolds number and also with the increase of nanoparticles weight fraction. This is because the nanofluid contains suspended nanoparticles, which have higher conductivity compared to the base fluid. The Nusselt number enhancement for f-GNP nanofluid is also attributed to the thermo-physical properties of the nanoparticles as well as particle Brownian motion (Sundar et al., 2014a). The enhancement of Nusselt numbers of a nanofluid with particle volume fraction of

0.02% are 3.30% and 4.80% corresponding to the Reynolds number of 5000 and 17500 respectively. Similarly, the enhancement of 12.25% and 26.50% in Nusselt number were obtained at 0.1 wt% nanofluid sample.

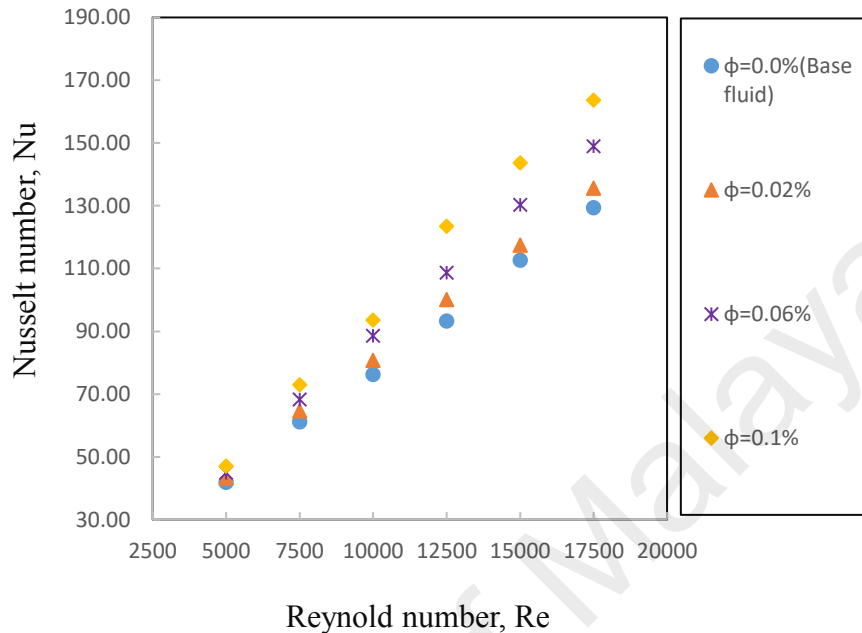


Figure 5.4: Nusselt number of f-GNP nanofluids as a function of Reynolds number for different weight concentrations.

Figure 5.5 indicates convective heat transfer coefficient of water and nanofluids of various weight fractions. For all the samples, convective heat transfer coefficient enhanced with the increases of Reynolds number. Also it is seen that increase of nanoparticles weight fraction has direct effect on heat transfer coefficient of nanofluids. The convective heat transfer improvement is due to the tiny thermal boundary layer at higher Reynolds number, which has reduced the thermal resistance between the inner wall of the tube and the nanofluid supported by the enhanced thermal conductivity of nanofluids. Moreover, improvement of convective heat transfer coefficient is strongly dependent on the specific surface area, Brownian motion and other thermo-physical properties of nanoparticles. The convective heat transfer coefficient is increased nearly 17.72% and 32.68% at the Reynolds number of 5000 and 17500, respectively, at 0.1 wt% nanofluid. This significant improvement is achieved by dispersion of very tiny amount f-GNP nanoparticles to the base fluid.

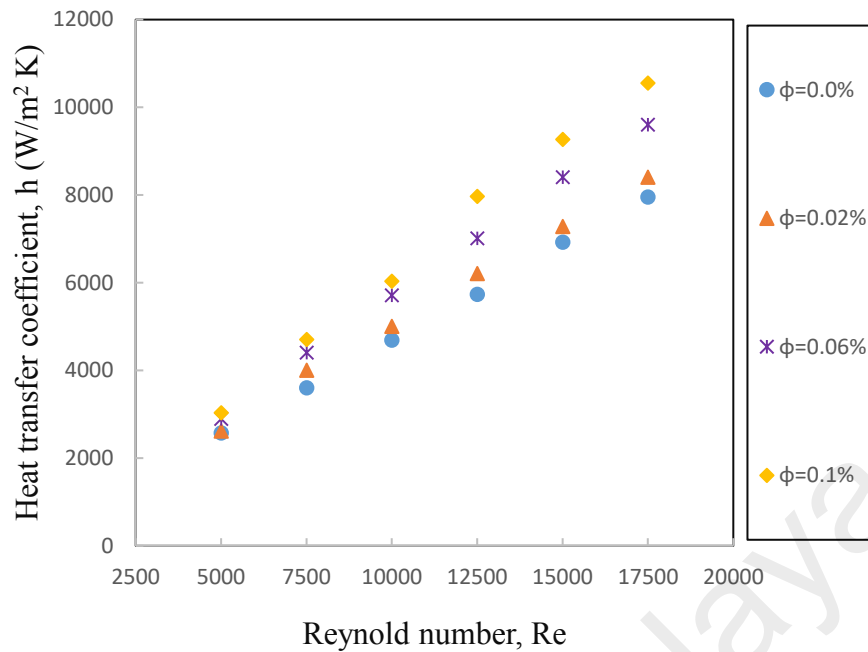


Figure 5.5: Convective heat transfer coefficient of f-GNP nanofluids as a function of Reynolds number at different weight concentrations.

5.3.2. Friction factor of f-GNP nanofluids

Equation (3.11) is used for obtaining the friction factor of f-GNP nanofluids at different weight fractions and the result is shown in Figure 5.6. The enhancement of friction factor for 0.1% weight fraction of f-GNP nanofluid is 9.22% at the Reynolds number of 17500. The augmentation of friction factor due to the suspended f-GNP nanoparticles in the water is not substantial in comparison to the heat transfer enhancement.

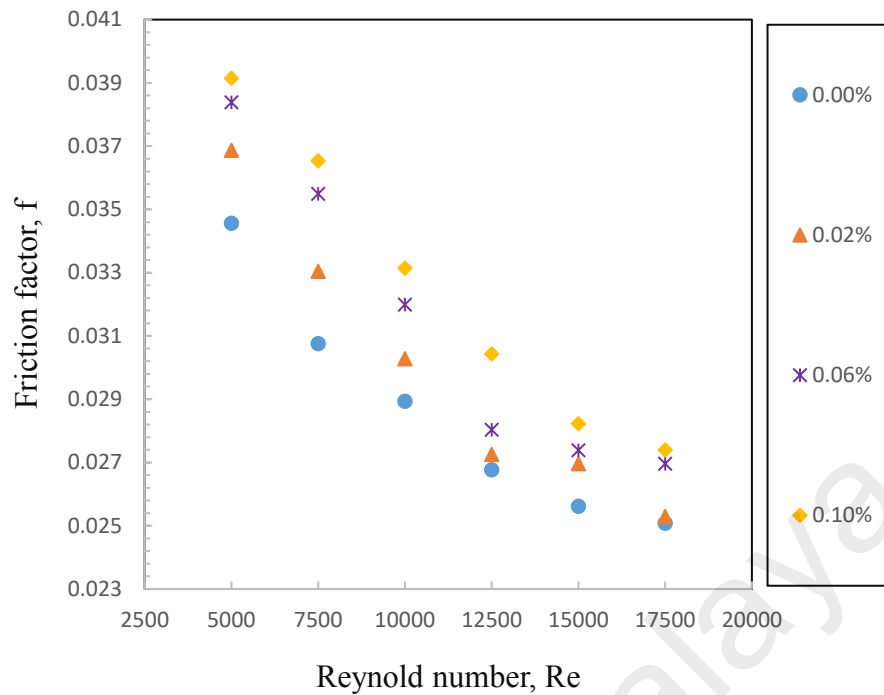


Figure 5.6: Friction factors of f-GNP nanofluids as a function of Reynolds number at different weight concentrations.

5.3.3. Pumping power and performance index

Figure 5.7 (a) presents the performance index of functionalized GNP-based water nanofluids for different weight concentrations and Re numbers. It is noteworthy that the performance index of functionalized GNP-based water nanofluids for all concentrations is greater than 1, except for Re number of 5000, indicating that the prepared nanofluids can be selected as an appropriate alternative coolant for the heat transfer equipment at different flow rates. Also, as the concentration of GNP in basefluid increases, the performance index increases, implying higher effect of heat transfer parameters to rheological factor. The results confirmed that the positive effects of heat transfer triumph over the negative effects of pressure drop in the presence of the prepared nanofluids at different concentrations and Re number, indicating excellent capability of synthesized nanofluid in the heat transfer equipment.

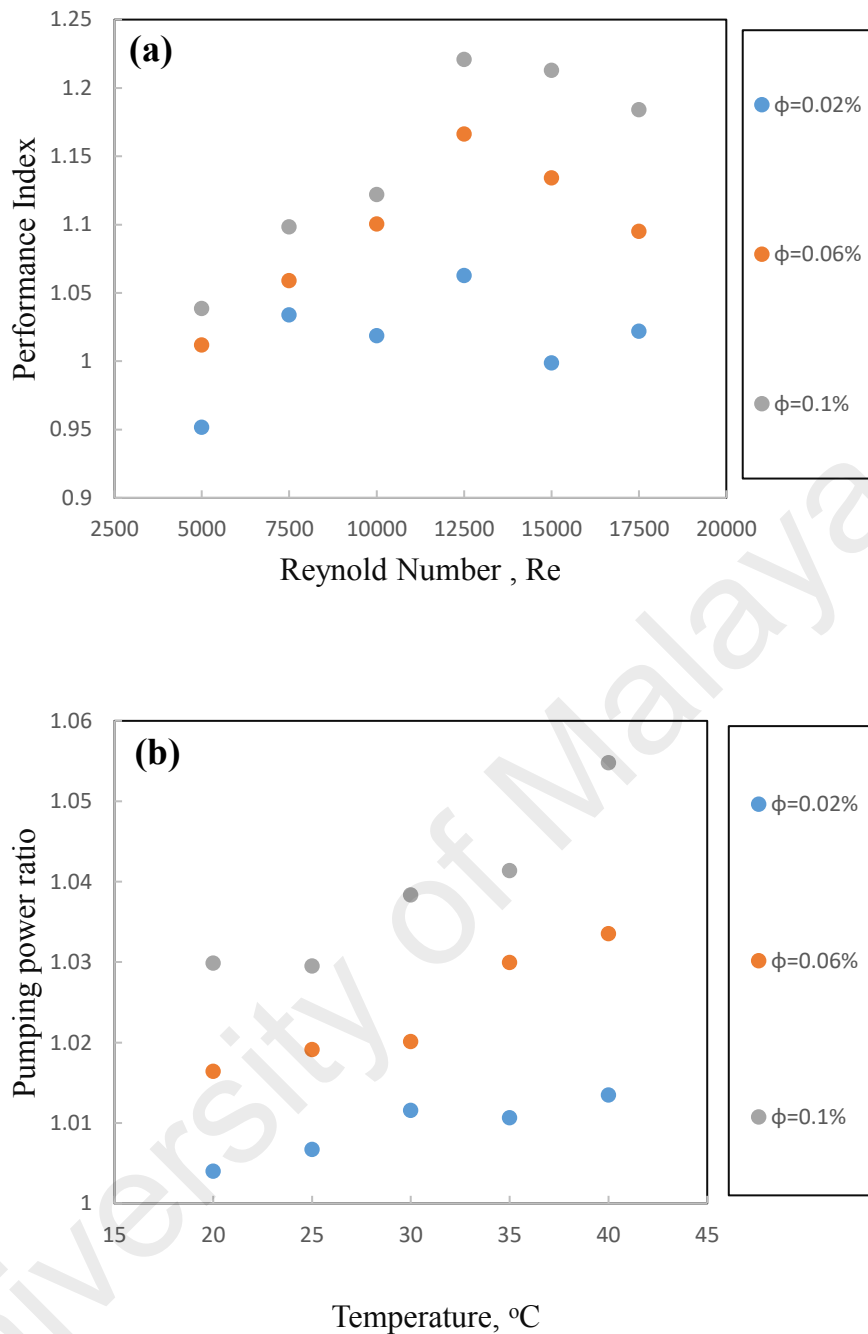


Figure 5.7: (a) Performance index and (b) pumping power ratio of functionalized GNP-based water nanofluids for different weight concentrations.

Optimization of pumping power is also played a key role in determining energy savings of system and can evaluate the performance of system rheologically, which can prepare some basic information about operability of fluid in the heat transfer equipment. Figure 5.7 (b) compares the pumping power of the prepared samples at various weight concentrations of functionalized GNP for different temperatures with that of the base-fluid. Results suggested that there is no significant change in pumping power in the

presence of prepared coolant at different temperatures and concentrations. An insignificant increase in the pumping power (maximum of increase < 6%) with GNP loading can be detected in Figure 5.7 (b), which considered as a positive parameter as compared with other nanofluids (W. Yu et al., 2012).

5.4. GNP-Pt/ Water nanofluids

5.4.1. Nusselt number of GNP-Pt hybrid nanofluids

Different weight concentration of GNP-Pt hybrid nanofluids has been introduced to the heat transfer test rig. The result of experimental data is plotted in Figure 5.8, equation (3.4) has been used for calculation of the Nusselt number. The result confirmed same trend with single phase functionalized GNP nanofluids, Nusselt number improves with the increase of nanoparticles weight fraction and also with the increase of Reynolds number. The Nusselt number enhancement for functionalized GNP-Pt hybrid nanofluid is due to the thermo-physical properties of the nanocomposite nanoparticles.

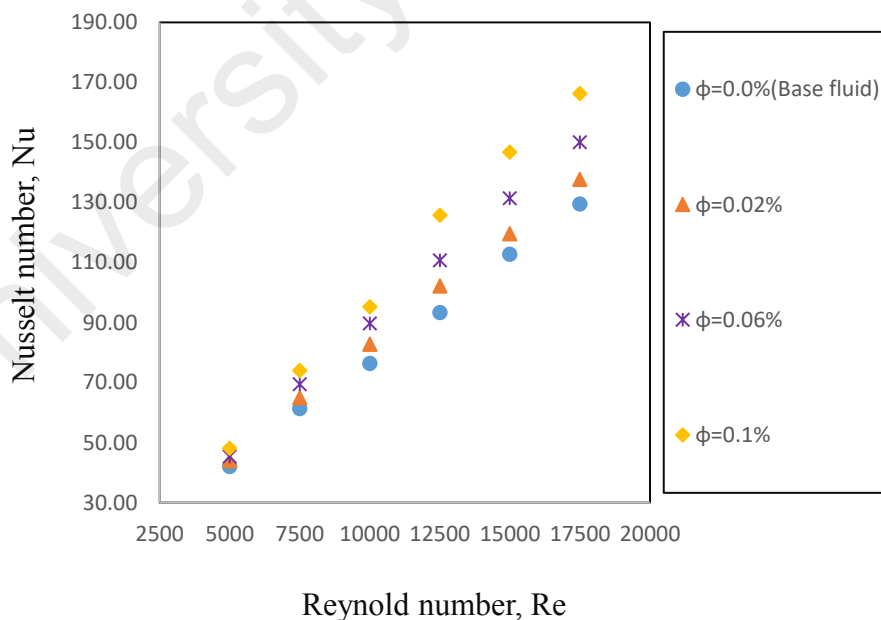


Figure 5.8: Nusselt number of functionalized GNP-Pt hybrid nanofluids as a function of Reynolds number for different weight concentrations.

The enhancement of Nusselt numbers of a nanofluid with particle volume fraction of 0.02% are 4.58% and 6.35% corresponding to the Reynolds number of 5000 and 17500

respectively. Similarly, the enhancement of 14.63% and 28.48% in Nusselt number were obtained at 0.1 wt% nanofluid sample. the amount of enhance of Nusselt number for GNP-Pt hybrid nanofluid is higher than improves of Nusselt number for single phase functionalized GNP nanofluid which is due to the higher thermal conductivity of nanocomposite as well as synergetic effect.

5.4.2. Friction factor of GNP-Pt hybrid nanofluids

Figure 5.9 shows the friction factor of the functionalized GNP-Pt hybrid nanofluids at different weight concentration of nanocomposite. The increase of friction factor for 0.1% weight fraction of functionalized GNP-Pt hybrid nanofluid is 10.98% at the Reynolds number of 17500. The rise of friction factor due to the loading nanocomposite in the base fluid (water) is negligible in comparison to the improving of Nusselt number.

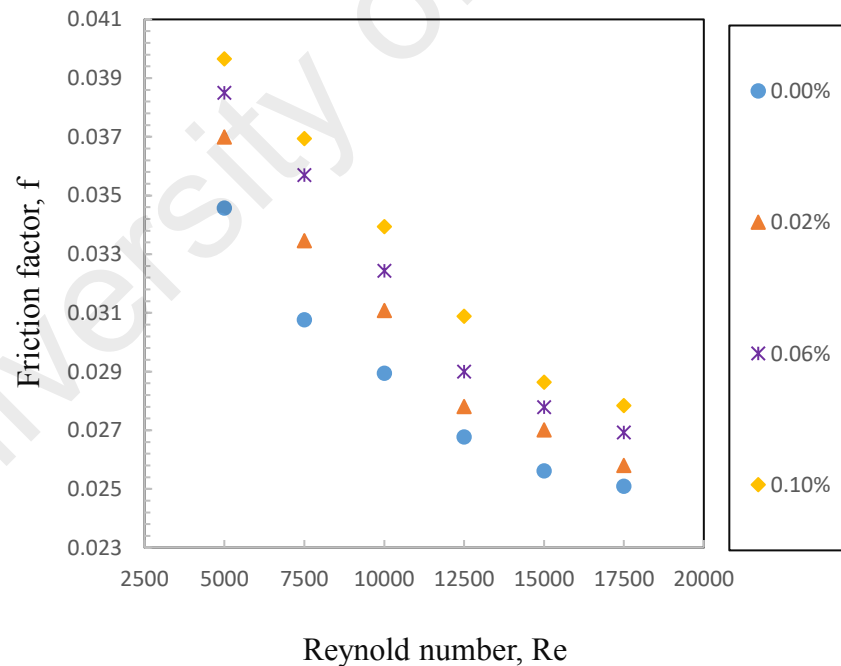


Figure 5.9: Friction factors of functionalized GNP-Pt hybrid nanofluids as a function of Reynolds number at different weight concentrations.

5.5. GNP-Ag/ Water nanofluids

5.5.1. Nusselt number of GNP-Ag hybrid nanofluids

Nanofluids with various weight concentrations of functionalized GNP-Ag are studied in this section. Round heated pipe (test section) with a same hydraulic diameter of 10 mm used for this experiment. The experimental Nusselt numbers for the nanofluids are calculated from equation (3.4), and the results are shown in Figure 5.10. It is seen that the Nusselt number enhances with increase of Reynolds number and also with the increase of nanoparticles concentration. This is because the nanofluid contains suspended nanoparticles, which have higher conductivity compared to the base fluid. The Nusselt number enhancement for GNP–Ag nanofluid is also attributed to thermos-physical properties of the nanoparticles as well as particle Brownian motion (Sundar et al., 2014a). The enhancement of Nusselt number for a nanofluid with particle fraction of 0.02% and 0.1% are, respectively, 8.29% and 10.45%. Similarly, the Nusselt number for nanofluid increases by about 21.89% and 32.70%, respectively, for Reynolds number of 5000 and 17500.

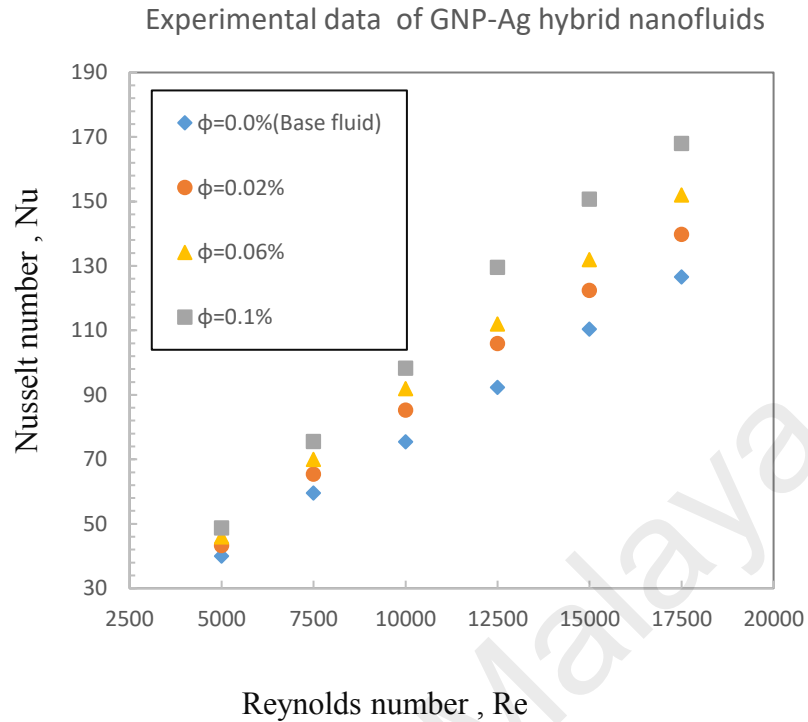


Figure 5.10: Variation of the experimental data for Nusselt number of GNP-Ag hybrid nanofluids with temperatures and particle concentrations.

Comparison of the present experimental Nusselt number with the existing single-phase correlations i.e. Eq. (3.5) of Dittus-Boelter (Dittus & Boelter, 1930), Eq. (3.6) of Petukhov (Petukhov, 1970) and Eq. (3.7) of Gnielinski (Gnielinski, 1975) indicated that the data of Equations (3.5), (3.6) and (3.7) are under predict by 43.73%, 39.31 % and 33.75 % In compared to the experimental data for GNP-Ag nanofluid at 0.1% concentration and at Reynolds number 17500. It can be concluded that the single –phase correlations are not suitable to forecast the correct Nusselt numbers for nanofluids.

According to the presented literature, the available Nusselt number correlations for various nanofluid are employed for evaluation of the present experimental data. Sundar et al. (Sundar et al., 2014a) reported enhancement trend for the Nusselt number for MWCNT-Fe₃O₄ nanocomposite in water. They found that the Nusselt number enhancement is 4% at the Reynold number of 17500. In the present investigation of GNP-

Ag hybrid nanofluid, under the same concentration (0.1%) of particle and the Reynolds number of 17500, the enhancement of Nusselt number is up to 32 % which shows that the prediction of equation (3.10) under-predicts the experimental data by 28% at the Reynolds number of 17500 (Figure 5. 11).

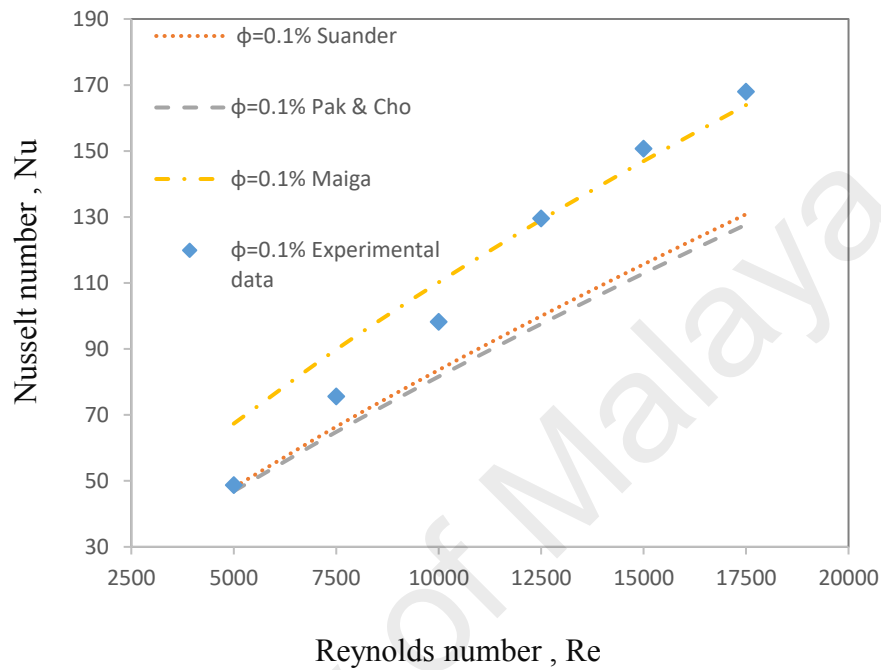


Figure 5.11: Comparison of measured Nusselt numbers of GNP-Ag nanofluids with the correlations of Suander, Pak&Cho and Maiga.

Correlation of Pak and Cho (1998) Nusselt number for TiO_2 and Al_2O_3 nanofluid is also used for comparison with the present data. The predictions of equation (5.9) under-predict the experimental data by 32% for 0.1% nanofluid at Reynolds number of 17500 (Figure 5.11). This is due to the higher enhancement of the thermal properties of nanocomposite based nanofluids. In addition, the correlation presented by Maiga et al.(2006) is used for analyzing the present experimental data. Figure 5.11 clearly showed that however equation (5.9) is under predicted by 3.3% for the same Reynolds number and volume concentration, for the lower Reynolds number it is mismatched between the experimental data and the data of Maiga correlation. Higher thermo-physical properties of GNP-Ag nanocomposite hybrid nanofluids are responsible for more enhancement of heat transfer ability.

In conclude with the above discussion, a new correlation for the Nusselt number based on the experimental data of GNP-Ag hybrid nanofluid with a maximum error of 8.05 % and average error of 4.9% has been introduced by using RSM technique. The equation (5.1) is as the following:

$$Nu_{Reg} = 0.0017066 Re^{0.9253} Pr^{1.29001} \quad (5.1)$$

$$5000 \leq Re \leq 17500, 0 \leq \varphi \leq 0.1\%$$

Figure 5.12 shows the obtained data from Eq. (5.1) along with the experimental data. The developed Eq. (5.1) could be able to predict the Nusselt number of water by considering $\varphi = 0$.

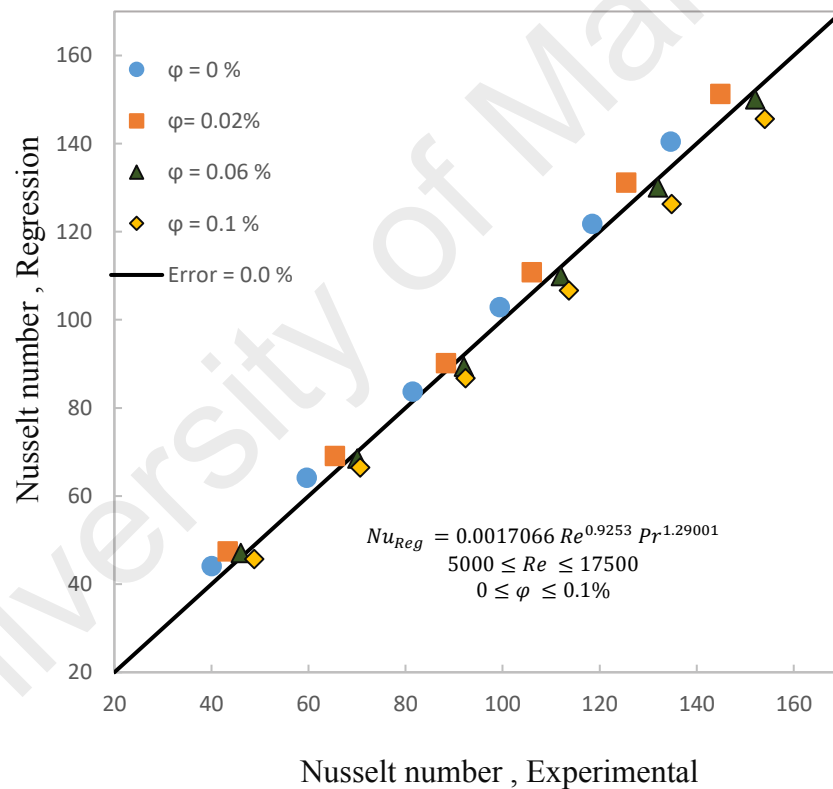


Figure 5.12: Nusselt number of GNP-Ag nanofluid estimated from experimental data is in comparison with the developed Nusselt number correlation of Eq. (5.1)

5.5.2. Friction factor of GNP-Ag hybrid nanofluids

Equation (3.11) is used for estimating the friction factor of GNP-Ag nanofluids at different concentration and the result is illustrated in Figure 5.13. The improvement of

friction factor for 0.1% weight concentration of GNP-Ag nanofluid is 8% at the Reynolds number of 17500, respectively. The enhancement of friction factor due to the suspended of GNP-Ag nanoparticles in the base fluid is not significant in comparison to the heat transfer enhancement.

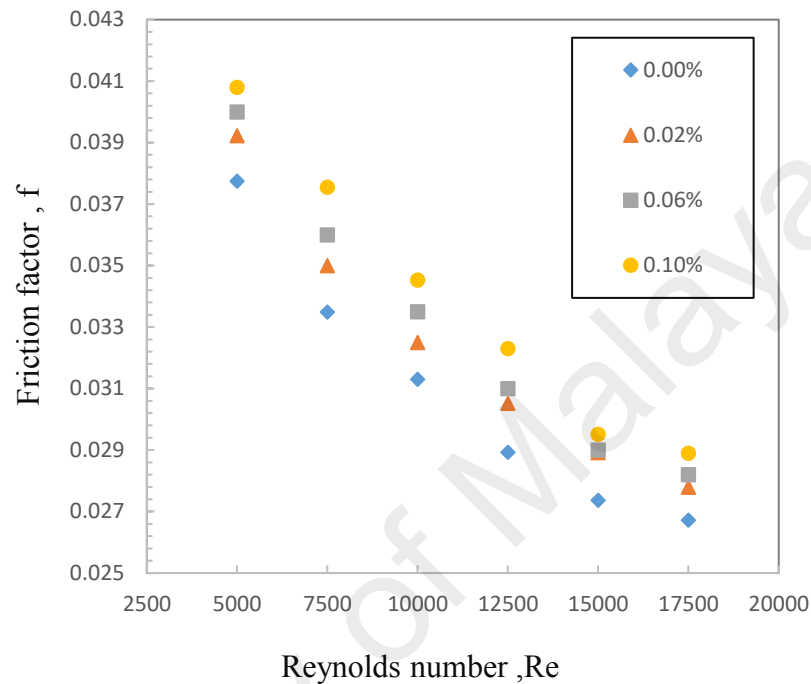


Figure 5.13: Variation of the experimental data for friction factor of GNP-Ag hybrid nanofluids with temperatures and particle concentrations.

The comparison of present experimental data friction factor with the equation (3.14) was shown in Figure 5.14. The Eq. (3.14) is under predicts by 5% and 2% for weight fraction of 0.1% of GNP-Ag nanofluids at Reynolds number of 5000 and 17500, respectively and equation (3.12) is also under predict by 8 % at the same weight concentration with the Reynolds number of 5000.

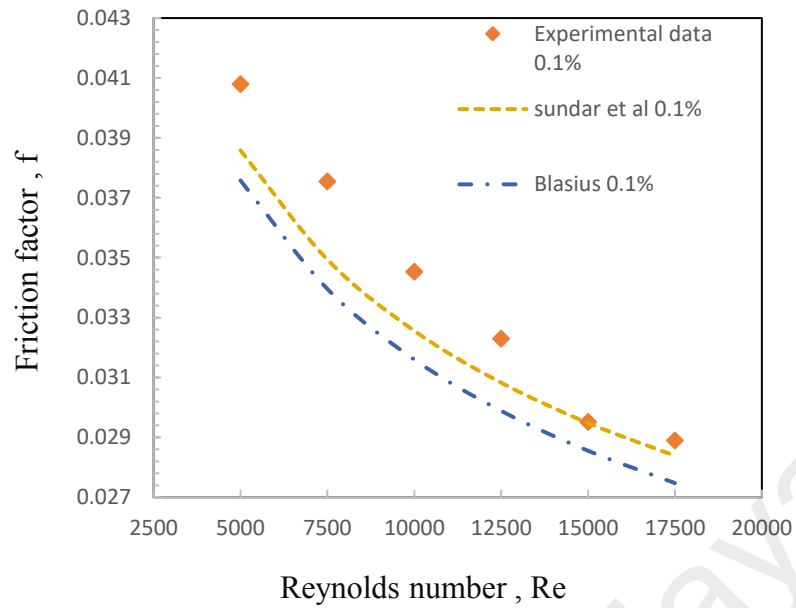


Figure 5.14: Comparison of measured friction factor of GNP-Ag nanofluids with the correlations of Sundar and Blasius.

Based on the experimental data of water and GNP-Ag nanofluid the new correlation for friction factor was proposed with the 0.9 % and 0.51 % of maximum deviation and average deviation, respectively. The expression is written below:

$$f_{Reg} = 0.567322 Re^{-0.285869} \varphi^{0.0271605} \quad (5.2)$$

$$5000 \leq Re \leq 17500, 0 < \varphi \leq 0.1\%$$

Figure 5.15 shows the obtained data from Eq. (5.2) along with the experimental data.

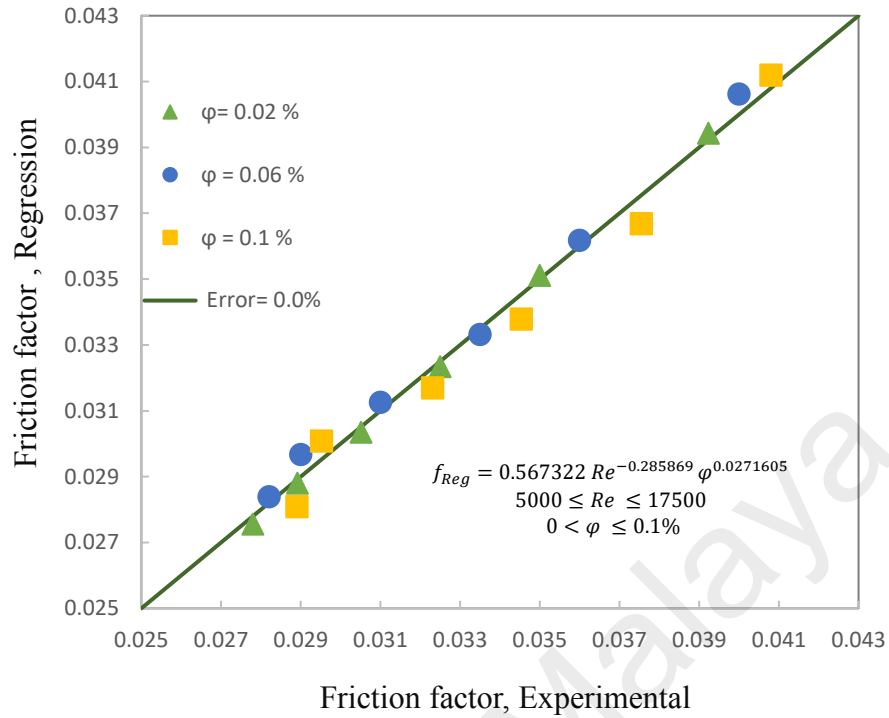


Figure 5.15: Friction factor of GNP-Ag nanofluid estimated from experimental data is in comparison with the developed Nusselt number correlation of Eq. (5.2).

The comparison study of Nusselt number enhancement for various samples has been established in table 5.1. All of the samples revealed substantial improvement but the GNP-Ag hybrid nanofluid shows the highest improved.

Table 5.1: Comparison study for thermal conductivity enhancement of the various samples at 0.1% weight concentration.

Type of nanofluid	Friction loss	Nusselt number (enhance %)
f-GNP	9.22 %	26.57%
f-GNP/Ag	8.3 %	32.7%
f-GNP/PT	10.98%	29.48%

5.6. Summary

In the present chapter, Nusselt number and heat transfer coefficient of the nanofluids for forced convection fully developed turbulent regime at constant Reynold number have been examined. It is confirmed that the Nusselt number and heat transfer coefficient of

the nanofluids are improved in comparison with the base fluid at the same Reynolds number due to the enhancement of the thermal conductivity. In addition, stability study and friction loss of the nanofluids are presented. Since, with the application of the nanofluids in the convective heat transfer set up pumping power and friction loss increases as a negative point, pumping power and performance index of the test rig systemically investigated and found the increase of the pumping power is not too much (as a negative point) but improvement of the performance index (as a positive point) is significant. All samples showed remarkable enhancement for Nusselt number and heat transfer coefficient, GNP-Ag hybrid nanofluid revealed the highest enhancement of heat transfer performance at the same weight concentration. Finally, the developed Nusselt number and friction factor correlation has been proposed the GNP-Ag hybrid nanofluid as the heat exchanging fluid for the next generation.

Further study is needed to observe the effect of adding various nanocomposite and other parameters on the heat transfer coefficient of the working fluids to explore the suitable and higher efficient heat exchanging liquid for the future.

CHAPTER 6: CONCLUSIONS AND RECOMMENDATIONS

Recently many research groups have focused on using nanofluid as a heat exchanger working fluid. Using nanofluids is a promising way to enhance the efficiency of the thermal systems. Many researches have confirmed the enhancement of the heat transfer performance of the thermal system by using nanofluids. The current chapter is a conclusion of the obtained results of this study and suggestion for further research work which is not being able to do in present work due to the time and instrument limitations.

6.1. Conclusions

The aims of the present research are to study the synthesis, preparation and stability, thermos-physical properties, friction loss and heat transfer of the functionalized carbon based and carbon based hybrid nanofluids in a close conduit flow. The following conclusions could be drawn from the obtained experimental results.

- 1- Since Graphene is naturally hydrophobic, so covalent functionalization has a key effect on the stability of graphene hybrid based nanofluids. Thus, selection of a proper functionalization method can make its homogeneous stable suspension. Maximum sediment of less than 10% was noticed for the highest weight concentrations of all the samples, which validates the proper functionalization event.
- 2- Nanocomposite weight concentration and temperature have great influence on the thermal conductivity and viscosity of the as prepared nanofluids. Presence of a small quantity (≤ 0.1 wt. %) of nanocomposite in water resulted in a significant thermal conductivity enhancement, but the influence of adding nanocomposite on the density and specific heat capacity of the nanfluids is not substantial. The maximum enhancement in the thermal conductivity has occurred at the highest weight concentration of the GNP-Ag hybrid nanofluid. however at 0.1% weight concentration of GNP-Ag, the observed enhancement of thermal conductivity is

about 16.94% at 20 °C and nearly about 22.22% at 40 °C for the same concentration. To elucidate the reasons for the strange growth of the thermal conductivity in nanofluids, some potential mechanisms have been studied earlier such as Brownian motion, the nature of heat transport in the nanoparticles and the effects of nanoparticle clustering and also several theoretical models have been investigated by choosing the carbon and carbon based hybrid nanofluids. The thermal enhancement has been attributed to several reasons where more investigations are needed for further clarifications.

- 3- Validation of the data from the test rig with the existing classical correlation for distilled water has confirmed the accuracy of the experiment. Experimental results of Nusselt numbers and convective heat transfer coefficients of all the nanofluids have revealed the remarkable enhancement of heat transfer performance in comparison to the base fluids but it is important to highlight that the improvement for hybrid nanofluids is higher than the case of single phase functionalized carbon based nanofluids due to the synergistic effect. A noticeable enhancement of 26.50% in Nusselt number was obtained at 0.1 wt% of functionalized GNP nanofluid (single phase nanofluid) but for GNP-Ag hybrid nanofluid, it was further escalated to 32.70%.
- 4- In addition, slight increase of the pumping power ($\leq 6\%$) and friction loss ($<10\%$) in comparison to the improvement of performance index (around 20%) and heat transfer coefficient make the hybrid nanofluids as a potential candidate to use as a heat exchanger fluid.

6.2. Recommendations for further works

The research works pointed in this thesis have found some new insights into the thermal and heat transfer performance of hybrid nanofluids. Based on that the following suggestion could be recommended:

Study of the convective heat transfer of hybrid nanofluids in low velocity (laminar) is suggested to find the heat transfer performance in that region. Moreover, investigation of any other types of nanocomposites for making hybrid nanofluid can be proposed to extend the research field. Meanwhile, study of other covalent functionalization group to make a well dispersed suspension could be lead to an interesting result.

In addition, after preparation of another hybrid nanofluids or making with different functional groups, thermal conductivity and viscosity study of them can make a better understanding to figure out the effective mechanisms behind the improvement of thermos-physical properties of the hybrid nanofluid and then developed correlation based on new proposed data. Study of heat transfer and friction loss characteristics in different configurations of heat exchangers could pave the way of improved heat transportation system.

Finally, numerical simulation of functionalized graphene and its hybrid nanofluid can be a very important research topic to a further researcher. Since graphene is not sphere nanoparticle the existing method (single phase and two phase) cannot be used, need to develop a code for graphene based nanofluids. Also, for graphene based hybrid nanofluid the existing method of simulation is not suitable and more research required to simulate the heat transfer behavior of hybrid nanofluids.

References

- Abbasi, S. M., Rashidi, A., Nemati, A., & Arzani, K. (2013). The effect of functionalisation method on the stability and the thermal conductivity of nanofluid hybrids of carbon nanotubes/gamma alumina. *Ceramics International*, 39(4), 3885-3891.
- Aladag, B., Halelfadl, S., Doner, N., Maré, T., Duret, S., & Estellé, P. (2012). Experimental investigations of the viscosity of nanofluids at low temperatures. *Applied energy*, 97, 876-880.
- Allahyari, S., Behzadmehr, A., & Hosseini Sarvari, S. (2011). Conjugate heat transfer of laminar mixed convection of a nanofluid through a horizontal tube with circumferentially non-uniform heating. *International Journal of Thermal Sciences*, 50(10), 1963-1972.
- Aly, W. I. (2014). Numerical study on turbulent heat transfer and pressure drop of nanofluid in coiled tube-in-tube heat exchangers. *Energy Conversion and Management*, 79, 304-316.
- Aminossadati, S., & Ghasemi, B. (2011). Enhanced natural convection in an isosceles triangular enclosure filled with a nanofluid. *Computers & Mathematics with Applications*, 61(7), 1739-1753.
- Amiri, A., Sadri, R., Shanbedi, M., Ahmadi, G., Chew, B., Kazi, S., & Dahari, M. (2015). Performance dependence of thermosyphon on the functionalization approaches: An experimental study on thermo-physical properties of graphene nanoplatelet-based water nanofluids. *Energy Conversion and Management*, 92, 322-330.
- Amiri, A., Sadri, R., Shanbedi, M., Ahmadi, G., Kazi, S., Chew, B., & Zubir, M. N. M. (2015). Synthesis of ethylene glycol-treated Graphene Nanoplatelets with one-pot, microwave-assisted functionalization for use as a high performance engine coolant. *Energy Conversion and Management*, 101, 767-777.
- Amiri, A., Shanbedi, M., Eshghi, H., Heris, S. Z., & Baniadam, M. (2012). Highly dispersed multiwalled carbon nanotubes decorated with Ag nanoparticles in water and experimental investigation of the thermophysical properties. *The Journal of Physical Chemistry C*, 116(5), 3369-3375.
- Amiri, A., Shanbedi, M., Yarmand, H., Arzani, H. K., Gharekhani, S., Montazer, E., . . . Kazi, S. N. (2015). Laminar convective heat transfer of hexylamine-treated MWCNTs-based turbine oil nanofluid. *Energy Conversion and Management*, 105, 355-367.

- Aravind, S. J., & Ramaprabhu, S. (2012). Graphene wrapped multiwalled carbon nanotubes dispersed nanofluids for heat transfer applications. *Journal of Applied Physics*, 112(12), 124304.
- Aravind, S. J., & Ramaprabhu, S. (2013). Graphene–multiwalled carbon nanotube-based nanofluids for improved heat dissipation. *RSC Advances*, 3(13), 4199-4206.
- Assael, M., Metaxa, I., Arvanitidis, J., Christofilos, D., & Lioutas, C. (2005). Thermal conductivity enhancement in aqueous suspensions of carbon multi-walled and double-walled nanotubes in the presence of two different dispersants. *International Journal of Thermophysics*, 26(3), 647-664.
- Baby, T. T., Aravind, S. S. J., Arockiadoss, T., Rakhi, R. B., & Ramaprabhu, S. (2010). Metal decorated graphene nanosheets as immobilization matrix for amperometric glucose biosensor. *Sensors and Actuators B: Chemical*, 145(1), 71-77.
- Baby, T. T., & Ramaprabhu, S. (2010). Investigation of thermal and electrical conductivity of graphene based nanofluids. *Journal of Applied Physics*, 108(12), 124308.
- Baby, T. T., & Ramaprabhu, S. (2011). Experimental investigation of the thermal transport properties of a carbon nanohybrid dispersed nanofluid. *Nanoscale*, 3(5), 2208-2214.
- Baby, T. T., & Sundara, R. (2011). Synthesis and transport properties of metal oxide decorated graphene dispersed nanofluids. *The Journal of Physical Chemistry C*, 115(17), 8527-8533.
- Baby, T. T., & Sundara, R. (2013). Synthesis of silver nanoparticle decorated multiwalled carbon nanotubes-graphene mixture and its heat transfer studies in nanofluid. *AIP Advances*, 3(1), 012111.
- Batmunkh, M., Tanshen, M. R., Nine, M. J., Myekhlai, M., Choi, H., Chung, H., & Jeong, H. (2014). Thermal Conductivity of TiO₂ Nanoparticles Based Aqueous Nanofluids with an Addition of a Modified Silver Particle. *Industrial & Engineering Chemistry Research*, 53(20), 8445-8451.
- Biercuk, M., Llaguno, M. C., Radosavljevic, M., Hyun, J., Johnson, A. T., & Fischer, J. E. (2002). Carbon nanotube composites for thermal management. *Applied Physics Letters*, 80(15), 2767-2769.

- Blasius, H. (1908). Grenzsichten in Flussigkeiten mit kleiner Reibung (German). *Z. Math. Phys*, 56, 1-37.
- Bobbo, S., Fedele, L., Benetti, A., Colla, L., Fabrizio, M., Pagura, C., & Barison, S. (2012). Viscosity of water based SWCNH and TiO₂ nanofluids. *Experimental Thermal and Fluid Science*, 36, 65-71.
- Botha, S. S., Ndungu, P., & Bladergroen, B. J. (2011). Physicochemical properties of oil-based nanofluids containing hybrid structures of silver nanoparticles supported on silica. *Industrial & Engineering Chemistry Research*, 50(6), 3071-3077.
- Buongiorno, J., & Hu, L.-w. (2009). *8. Innovative Technologies: Two-Phase Heat Transfer in Water-Based Nanofluids for Nuclear Applications Final Report*. Retrieved from
- Chandrasekar, M., Suresh, S., & Bose, A. C. (2010). Experimental investigations and theoretical determination of thermal conductivity and viscosity of Al₂O₃/water nanofluid. *Experimental Thermal and Fluid Science*, 34(2), 210-216.
- Chandrasekar, M., Suresh, S., & Chandra Bose, A. (2010). Experimental studies on heat transfer and friction factor characteristics of Al₂O₃/water nanofluid in a circular pipe under laminar flow with wire coil inserts. *Experimental Thermal and Fluid Science*, 34(2), 122-130.
- Chen, H., Ding, Y., He, Y., & Tan, C. (2007). Rheological behaviour of ethylene glycol based titania nanofluids. *Chemical Physics Letters*, 444(4), 333-337.
- Chen, L., Xie, H., Li, Y., & Yu, W. (2008). Nanofluids containing carbon nanotubes treated by mechanochemical reaction. *Thermochimica Acta*, 477(1), 21-24.
- Chen, L. F., Cheng, M., Yang, D. J., & Yang, L. (2014). *Enhanced Thermal Conductivity of Nanofluid by Synergistic Effect of Multi-Walled Carbon Nanotubes and Fe₂O₃ Nanoparticles*. Paper presented at the Applied Mechanics and Materials.
- Cheremisinoff, N. P. (1986). Encyclopedia of fluid mechanics. Volume 2. Dynamics of single-fluid flows and mixing.
- Chevalier, J., Tillement, O., & Ayela, F. (2007). Rheological properties of nanofluids flowing through microchannels. *Applied Physics Letters*, 91(23), 3103.

- Choi, S., Zhang, Z., Yu, W., Lockwood, F., & Grulke, E. (2001). Anomalous thermal conductivity enhancement in nanotube suspensions. *Applied Physics Letters*, 79(14), 2252-2254.
- Choi, S. (1995). Enhancing thermal conductivity of fluids with nanoparticles. *ASME-Publications-Fed*, 231, 99-106.
- Das, S. K., Putra, N., Thiesen, P., & Roetzel, W. (2003). Temperature dependence of thermal conductivity enhancement for nanofluids. *Journal of Heat Transfer*, 125(4), 567-574.
- De Robertis, E., Cosme, E., Neves, R., Kuznetsov, A. Y., Campos, A., Landi, S., & Achete, C. (2012). Application of the modulated temperature differential scanning calorimetry technique for the determination of the specific heat of copper nanofluids. *Applied Thermal Engineering*, 41, 10-17.
- Dias, J., Taylor, M., Thompson, J., Brenkel, I., & Gregg, P. (1988). Radiographic signs of union of scaphoid fractures. An analysis of inter-observer agreement and reproducibility. *Journal of Bone & Joint Surgery, British Volume*, 70(2), 299-301.
- Ding, Y., Alias, H., Wen, D., & Williams, R. A. (2006). Heat transfer of aqueous suspensions of carbon nanotubes (CNT nanofluids). *International Journal of Heat and Mass Transfer*, 49(1), 240-250.
- Dittus, F. W., & Boelter, L. M. K. (1930). Heat transfer for automobile radiators of the tubular type. *University of California Publications in Engineering*, 2.
- Duangthongsuk, W., & Wongwises, S. (2009a). Heat transfer enhancement and pressure drop characteristics of TiO₂-water nanofluid in a double-tube counter flow heat exchanger. *International Journal of Heat and Mass Transfer*, 52(7), 2059-2067.
- Duangthongsuk, W., & Wongwises, S. (2009b). Measurement of temperature-dependent thermal conductivity and viscosity of TiO₂-water nanofluids. *Experimental Thermal and Fluid Science*, 33(4), 706-714.
- Eastman, J., Choi, U., Li, S., Thompson, L., & Lee, S. (1996). *Enhanced thermal conductivity through the development of nanofluids*. Paper presented at the MRS Proceedings.
- Evans, W., Prasher, R., Fish, J., Meakin, P., Phelan, P., & Keblinski, P. (2008). Effect of aggregation and interfacial thermal resistance on thermal conductivity of

nanocomposites and colloidal nanofluids. *International Journal of Heat and Mass Transfer*, 51(5), 1431-1438.

Ferrouillat, S., Bontemps, A., Ribeiro, J.-P., Gruss, J.-A., & Soriano, O. (2011). Hydraulic and heat transfer study of SiO₂/water nanofluids in horizontal tubes with imposed wall temperature boundary conditions. *International Journal of Heat and Fluid Flow*, 32(2), 424-439.

Gangacharyulu, D. (2010). Preparation and characterization of nanofluids and some investigation in biological applications. *Mechanical engineering. Carbondale: Southern Illinois University*, 104.

Ganguly, S., Sikdar, S., & Basu, S. (2009). Experimental investigation of the effective electrical conductivity of aluminum oxide nanofluids. *Powder Technology*, 196(3), 326-330.

Garg, J., Poudel, B., Chiesa, M., Gordon, J., Ma, J., Wang, J., . . . Nanda, J. (2008). Enhanced thermal conductivity and viscosity of copper nanoparticles in ethylene glycol nanofluid. *Journal of Applied Physics*, 103(7), 074301.

Ghadimi, A., Saidur, R., & Metselaar, H. (2011). A review of nanofluid stability properties and characterization in stationary conditions. *International Journal of Heat and Mass Transfer*, 54(17), 4051-4068.

Ghaffari, O., Behzadmehr, A., & Ajam, H. (2010). Turbulent mixed convection of a nanofluid in a horizontal curved tube using a two-phase approach. *International Communications in Heat and Mass Transfer*, 37(10), 1551-1558.

Gharehkhani, S., Sadeghinezhad, E., Kazi, S. N., Yarmand, H., Badarudin, A., Safaei, M. R., & Zubir, M. N. M. (2015). Basic effects of pulp refining on fiber properties—A review. *Carbohydrate polymers*, 115, 785-803.

Gharehkhani, S., Shirazi, S. F. S., Jahromi, S. P., Sookhajian, M., Baradaran, S., Yarmand, H., . . . Basirun, W. J. (2015). Spongy nitrogen-doped activated carbonaceous hybrid derived from biomass material/graphene oxide for supercapacitor electrodes. *RSC Advances*, 5(51), 40505-40513.

Gharehkhani, S., Shirazi, S. F. S., Pilban-Jahromi, S., Sookhajian, M., Baradaran, S., Yarmand, H., . . . Basirun, W. J. (2015). Spongy Nitrogen-Doped Activated Carbonaceous Hybrid Derived from Biomass Material/Graphene Oxide for Supercapacitor Electrodes. *RSC Advances*.

- Ghazvini, M., Akhavan-Behabadi, M., Rasouli, E., & Raisee, M. (2012). Heat transfer properties of nanodiamond–engine oil nanofluid in laminar flow. *Heat Transfer Engineering*, 33(6), 525-532.
- Ghozatloo, A., Rashidi, A., & Shariaty-Niassar, M. (2014). Convective heat transfer enhancement of graphene nanofluids in shell and tube heat exchanger. *Experimental Thermal and Fluid Science*, 53, 136-141.
- Gnielinski, V. (1975). New equations for heat and mass transfer in the turbulent flow in pipes and channels. *NASA STI/Recon Technical Report A*, 75, 22028.
- Godson, L., Raja, B., Lal, D. M., & Wongwises, S. (2010). Experimental investigation on the thermal conductivity and viscosity of silver-deionized water nanofluid. *Experimental Heat Transfer*, 23(4), 317-332.
- Guo, S., Dong, S., & Wang, E. (2008). Gold/platinum hybrid nanoparticles supported on multiwalled carbon nanotube/silica coaxial nanocables: preparation and application as electrocatalysts for oxygen reduction. *The Journal of Physical Chemistry C*, 112(7), 2389-2393.
- Haghshenas Fard, M., Esfahany, M. N., & Talaie, M. (2010). Numerical study of convective heat transfer of nanofluids in a circular tube two-phase model versus single-phase model. *International Communications in Heat and Mass Transfer*, 37(1), 91-97.
- Han, Z., Yang, B., Kim, S., & Zachariah, M. (2007). Application of hybrid sphere/carbon nanotube particles in nanofluids. *Nanotechnology*, 18(10), 105701.
- He, Q., Wang, S., Tong, M., & Liu, Y. (2012). Experimental study on thermophysical properties of nanofluids as phase-change material (PCM) in low temperature cool storage. *Energy conversion and management*, 64, 199-205.
- He, Q., Wang, S., Zeng, S., & Zheng, Z. (2013). Experimental investigation on photothermal properties of nanofluids for direct absorption solar thermal energy systems. *Energy Conversion and Management*, 73, 150-157.
- He, Y., Jin, Y., Chen, H., Ding, Y., Cang, D., & Lu, H. (2007). Heat transfer and flow behaviour of aqueous suspensions of TiO₂ nanoparticles (nanofluids) flowing upward through a vertical pipe. *International Journal of Heat and Mass Transfer*, 50(11), 2272-2281.

- Ho, M. X., & Pan, C. (2014). Optimal concentration of alumina nanoparticles in molten Hitec salt to maximize its specific heat capacity. *International Journal of Heat and Mass Transfer*, 70, 174-184.
- Hong, T.-K., Yang, H.-S., & Choi, C. (2005). Study of the enhanced thermal conductivity of Fe nanofluids. *Journal of Applied Physics*, 97(6), 064311.
- Horrocks, J., & McLaughlin, E. (1963). *Non-steady-state measurements of the thermal conductivities of liquid polyphenyls*. Paper presented at the Proceedings of the Royal Society of London A: Mathematical, Physical and Engineering Sciences.
- Hummers Jr, W. S., & Offeman, R. E. (1958). Preparation of graphitic oxide. *Journal of the American Chemical Society*, 80(6), 1339-1339.
- Hwang, Y., Lee, J.-K., Lee, J.-K., Jeong, Y.-M., Cheong, S.-i., Ahn, Y.-C., & Kim, S. H. (2008). Production and dispersion stability of nanoparticles in nanofluids. *Powder Technology*, 186(2), 145-153.
- Hwang, Y., Lee, J., Lee, C., Jung, Y., Cheong, S., Lee, C., . . . Jang, S. (2007). Stability and thermal conductivity characteristics of nanofluids. *Thermochimica Acta*, 455(1), 70-74.
- Izadi, M., Behzadmehr, A., & Jalali-Vahida, D. (2009). Numerical study of developing laminar forced convection of a nanofluid in an annulus. *International Journal of Thermal Sciences*, 48(11), 2119-2129.
- Jana, S., Salehi-Khojin, A., & Zhong, W.-H. (2007). Enhancement of fluid thermal conductivity by the addition of single and hybrid nano-additives. *Thermochimica Acta*, 462(1), 45-55.
- Jiang, L., Gao, L., & Sun, J. (2003). Production of aqueous colloidal dispersions of carbon nanotubes. *Journal of Colloid and Interface Science*, 260(1), 89-94.
- Kaniyoor, A., Imran Jafri, R., Arockiadoss, T., & Ramaprabhu, S. (2009). Nanostructured Pt decorated graphene and multi walled carbon nanotube based room temperature hydrogen gas sensor. *Nanoscale*, 1(3), 382-386. doi:10.1039/B9NR00015A
- Karthikeyan, N., Philip, J., & Raj, B. (2008). Effect of clustering on the thermal conductivity of nanofluids. *Materials Chemistry and Physics*, 109(1), 50-55.
- Kasaeian, A., Daviran, S., Azarian, R. D., & Rashidi, A. (2015). Performance evaluation and nanofluid using capability study of a solar parabolic trough collector. *Energy Conversion and Management*, 89, 368-375.

- Khoshvaght-Aliabadi, M. (2014). Influence of different design parameters and Al₂O₃-water nanofluid flow on heat transfer and flow characteristics of sinusoidal-corrugated channels. *Energy Conversion and Management*, 88, 96-105.
- Kline, S. J., & McClintock, F. (1953). Describing uncertainties in single-sample experiments. *Mechanical engineering*, 75(1), 3-8.
- Kole, M., & Dey, T. (2010). Viscosity of alumina nanoparticles dispersed in car engine coolant. *Experimental Thermal and Fluid Science*, 34(6), 677-683.
- Kole, M., & Dey, T. (2013). Investigation of thermal conductivity, viscosity, and electrical conductivity of graphene based nanofluids. *Journal of Applied Physics*, 113(8), 084307.
- Kulkarni, D. P., Vajjha, R. S., Das, D. K., & Oliva, D. (2008). Application of aluminum oxide nanofluids in diesel electric generator as jacket water coolant. *Applied Thermal Engineering*, 28(14), 1774-1781.
- Kumar, S. V., Huang, N. M., Lim, H. N., Zainy, M., Harrison, I., & Chia, C. H. (2013). Preparation of highly water dispersible functional graphene/silver nanocomposite for the detection of melamine. *Sensors and Actuators B: Chemical*, 181, 885-893.
- Kumaresan, V., & Velraj, R. (2012). Experimental investigation of the thermo-physical properties of water-ethylene glycol mixture based CNT nanofluids. *Thermochimica Acta*, 545, 180-186.
- Kurt, H., & Kayfeci, M. (2009). Prediction of thermal conductivity of ethylene glycol-water solutions by using artificial neural networks. *Applied energy*, 86(10), 2244-2248.
- Lauder, B. E., & Spalding, D. (1974). The numerical computation of turbulent flows. *Computer methods in applied mechanics and engineering*, 3(2), 269-289.
- Lee, D. (2007). Thermophysical properties of interfacial layer in nanofluids. *Langmuir*, 23(11), 6011-6018.
- Lee, D., Kim, J.-W., & Kim, B. G. (2006). A new parameter to control heat transport in nanofluids: surface charge state of the particle in suspension. *The Journal of Physical Chemistry B*, 110(9), 4323-4328.

- Lee, J.-H., Hwang, K. S., Jang, S. P., Lee, B. H., Kim, J. H., Choi, S. U., & Choi, C. J. (2008). Effective viscosities and thermal conductivities of aqueous nanofluids containing low volume concentrations of Al₂O₃ nanoparticles. *International Journal of Heat and Mass Transfer*, 51(11), 2651-2656.
- Lee, K., Hwang, Y., Cheong, S., Kwon, L., Kim, S., & Lee, J. (2009). Performance evaluation of nano-lubricants of fullerene nanoparticles in refrigeration mineral oil. *Current Applied Physics*, 9(2), e128-e131.
- Li, C. H., & Peterson, G. (2006). Experimental investigation of temperature and volume fraction variations on the effective thermal conductivity of nanoparticle suspensions (nanofluids). *Journal of Applied Physics*, 99(8), 084314.
- Li, H., Ha, C.-S., & Kim, I. (2009). Fabrication of carbon nanotube/SiO₂ and carbon nanotube/SiO₂/Ag nanoparticles hybrids by using plasma treatment. *Nanoscale research letters*, 4(11), 1384-1388.
- Li, X., Zhu, D., & Wang, X. (2007). Evaluation on dispersion behavior of the aqueous copper nano-suspensions. *Journal of Colloid and Interface Science*, 310(2), 456-463.
- Li, X. F., Zhu, D. S., Wang, X. J., Wang, N., Gao, J. W., & Li, H. (2008). Thermal conductivity enhancement dependent pH and chemical surfactant for Cu-H₂O nanofluids. *Thermochimica Acta*, 469(1-2), 98-103.
- Li, Y., Tung, S., Schneider, E., & Xi, S. (2009). A review on development of nanofluid preparation and characterization. *Powder Technology*, 196(2), 89-101.
- Liu, J., Wang, F., Zhang, L., Fang, X., & Zhang, Z. (2014). Thermodynamic properties and thermal stability of ionic liquid-based nanofluids containing graphene as advanced heat transfer fluids for medium-to-high-temperature applications. *Renewable Energy*, 63, 519-523.
- Lotfi, R., Saboohi, Y., & Rashidi, A. (2010). Numerical study of forced convective heat transfer of nanofluids: comparison of different approaches. *International Communications in Heat and Mass Transfer*, 37(1), 74-78.
- Mahmoudi, A. H., Shahi, M., Raouf, A. H., & Ghasemian, A. (2010). Numerical study of natural convection cooling of horizontal heat source mounted in a square cavity filled with nanofluid. *International Communications in Heat and Mass Transfer*, 37(8), 1135-1141.

- Maïga, S. E. B., Nguyen, C. T., Galanis, N., Roy, G., Maré, T., & Coqueux, M. (2006). Heat transfer enhancement in turbulent tube flow using Al₂O₃ nanoparticle suspension. *International Journal of Numerical Methods for Heat & Fluid Flow*, 16(3), 275-292.
- Manca, O., Nardini, S., & Ricci, D. (2012). A numerical study of nanofluid forced convection in ribbed channels. *Applied Thermal Engineering*, 37, 280-292.
- Mansour, M., Mohamed, R., Abd-Elaziz, M., & Ahmed, S. E. (2010). Numerical simulation of mixed convection flows in a square lid-driven cavity partially heated from below using nanofluid. *International Communications in Heat and Mass Transfer*, 37(10), 1504-1512.
- Mansour, R. B., Galanis, N., & Nguyen, C. T. (2007). Effect of uncertainties in physical properties on forced convection heat transfer with nanofluids. *Applied Thermal Engineering*, 27(1), 240-249.
- Mapa, L., & Mazhar, S. (2005). *Heat transfer in mini heat exchanger using nanofluids*. Paper presented at the Conference of American Society for Engineering Education, DeKalb, IL, Apr.
- Mariano, A., Pastoriza-Gallego, M. J., Lugo, L., Mussari, L., & Piñeiro, M. M. (2015). Co₃O₄ ethylene glycol-based nanofluids: Thermal conductivity, viscosity and high pressure density. *International Journal of Heat and Mass Transfer*, 85, 54-60.
- Masuda, H., Ebata, A., & Teramae, K. (1993). Alteration of thermal conductivity and viscosity of liquid by dispersing ultra-fine particles. Dispersion of Al₂O₃, SiO₂ and TiO₂ ultra-fine particles.
- Minea, A. A., & Luciu, R. S. (2012). Investigations on electrical conductivity of stabilized water based Al₂O₃ nanofluids. *Microfluidics and nanofluidics*, 13(6), 977-985.
- Mohebbi, A. (2012). Prediction of specific heat and thermal conductivity of nanofluids by a combined equilibrium and non-equilibrium molecular dynamics simulation. *Journal of Molecular Liquids*, 175, 51-58.
- Munkhbayar, B., Tanshen, M. R., Jeoun, J., Chung, H., & Jeong, H. (2013). Surfactant-free dispersion of silver nanoparticles into MWCNT-aqueous nanofluids prepared by one-step technique and their thermal characteristics. *Ceramics International*, 39(6), 6415-6425.

- Murshed, S. S. (2011). Determination of effective specific heat of nanofluids. *Journal of Experimental Nanoscience*, 6(5), 539-546.
- Murshed, S. S. (2012). Simultaneous measurement of thermal conductivity, thermal diffusivity, and specific heat of nanofluids. *Heat Transfer Engineering*, 33(8), 722-731.
- Namburu, P., Kulkarni, D., Dandekar, A., & Das, D. (2007). Experimental investigation of viscosity and specific heat of silicon dioxide nanofluids. *Micro & Nano Letters, IET*, 2(3), 67-71.
- Namburu, P. K., Das, D. K., Tanguturi, K. M., & Vajjha, R. S. (2009). Numerical study of turbulent flow and heat transfer characteristics of nanofluids considering variable properties. *International Journal of Thermal Sciences*, 48(2), 290-302.
- Naphon, P., Assadamongkol, P., & Borirak, T. (2008). Experimental investigation of titanium nanofluids on the heat pipe thermal efficiency. *International Communications in Heat and Mass Transfer*, 35(10), 1316-1319.
- Naphon, P., Klangchart, S., & Wongwises, S. (2009). Numerical investigation on the heat transfer and flow in the mini-fin heat sink for CPU. *International Communications in Heat and Mass Transfer*, 36(8), 834-840.
- Nguyen, C., Desgranges, F., Roy, G., Galanis, N., Mare, T., Boucher, S., & Angue Mintsa, H. (2007). Temperature and particle-size dependent viscosity data for water-based nanofluids–hysteresis phenomenon. *International Journal of Heat and Fluid Flow*, 28(6), 1492-1506.
- Nguyen, C., Desgranges, F., Roy, G., Galanis, N., Mare, T., Boucher, S., & Mintsa, H. A. (2007). Temperature and particle-size dependent viscosity data for water-based nanofluids–hysteresis phenomenon. *International Journal of Heat and Fluid Flow*, 28(6), 1492-1506.
- Nine, M. J., Batmunkh, M., Kim, J.-H., Chung, H.-S., & Jeong, H.-M. (2012). Investigation of Al₂O₃-MWCNTs hybrid dispersion in water and their thermal characterization. *Journal of nanoscience and nanotechnology*, 12(6), 4553-4559.
- Novoselov, K. S., Geim, A. K., Morozov, S., Jiang, D., Zhang, Y., Dubonos, S., . . . Firsov, A. (2004). Electric field effect in atomically thin carbon films. *science*, 306(5696), 666-669.

- O'Hanley, H., Buongiorno, J., McKrell, T., & Hu, L.-w. (2012). Measurement and model validation of nanofluid specific heat capacity with differential scanning calorimetry. *Advances in Mechanical Engineering*, 4, 181079.
- Oh, D.-W., Jain, A., Eaton, J. K., Goodson, K. E., & Lee, J. S. (2008). Thermal conductivity measurement and sedimentation detection of aluminum oxide nanofluids by using the 3ω method. *International Journal of Heat and Fluid Flow*, 29(5), 1456-1461.
- Pak, B. C., & Cho, Y. I. (1998). Hydrodynamic and heat transfer study of dispersed fluids with submicron metallic oxide particles. *Experimental Heat Transfer an International Journal*, 11(2), 151-170.
- Pakdaman, M. F., Akhavan-Behabadi, M., & Razi, P. (2012). An experimental investigation on thermo-physical properties and overall performance of MWCNT/heat transfer oil nanofluid flow inside vertical helically coiled tubes. *Experimental Thermal and Fluid Science*, 40, 103-111.
- Pantzali, M., Kanaris, A., Antoniadis, K., Mouza, A., & Paras, S. (2009). Effect of nanofluids on the performance of a miniature plate heat exchanger with modulated surface. *International Journal of Heat and Fluid Flow*, 30(4), 691-699.
- Pantzali, M., Mouza, A., & Paras, S. (2009). Investigating the efficacy of nanofluids as coolants in plate heat exchangers (PHE). *Chemical Engineering Science*, 64(14), 3290-3300.
- Patel, H. E., Das, S. K., Sundararajan, T., Nair, A. S., George, B., & Pradeep, T. (2003). Thermal conductivities of naked and monolayer protected metal nanoparticle based nanofluids: Manifestation of anomalous enhancement and chemical effects. *Applied Physics Letters*, 83(14), 2931-2933.
- Paul, G., Chopkar, M., Manna, I., & Das, P. (2010). Techniques for measuring the thermal conductivity of nanofluids: a review. *Renewable and Sustainable Energy Reviews*, 14(7), 1913-1924.
- Petukhov, B. (1970). Heat transfer and friction in turbulent pipe flow with variable physical properties. *Advances in heat transfer*, 6(503), i565.
- Phuoc, T. X., & Massoudi, M. (2009). Experimental observations of the effects of shear rates and particle concentration on the viscosity of Fe₂O₃-deionized water nanofluids. *International Journal of Thermal Sciences*, 48(7), 1294-1301.

- Prasher, R., Song, D., Wang, J., & Phelan, P. (2006). Measurements of nanofluid viscosity and its implications for thermal applications. *Applied Physics Letters*, 89(13), 133108.
- Rea, U., McKrell, T., Hu, L.-w., & Buongiorno, J. (2009). Laminar convective heat transfer and viscous pressure loss of alumina–water and zirconia–water nanofluids. *International Journal of Heat and Mass Transfer*, 52(7), 2042-2048.
- Rostamani, M., Hosseinizadeh, S., Gorji, M., & Khodadadi, J. (2010). Numerical study of turbulent forced convection flow of nanofluids in a long horizontal duct considering variable properties. *International Communications in Heat and Mass Transfer*, 37(10), 1426-1431.
- Saeedinia, M., Akhavan-Behabadi, M., & Nasr, M. (2012). Experimental study on heat transfer and pressure drop of nanofluid flow in a horizontal coiled wire inserted tube under constant heat flux. *Experimental Thermal and Fluid Science*, 36, 158-168.
- Saleh, R., Putra, N., Prakoso, S. P., & Septiadi, W. N. (2013). Experimental investigation of thermal conductivity and heat pipe thermal performance of ZnO nanofluids. *International Journal of Thermal Sciences*, 63, 125-132.
- Samira, P., Saeed, Z., Motahare, S., & Mostafa, K. (2014). Pressure drop and thermal performance of CuO/ethylene glycol (60%)-water (40%) nanofluid in car radiator. *Korean Journal of Chemical Engineering*, 1-8. doi:10.1007/s11814-014-0244-7
- Sarkar, J., Ghosh, P., & Adil, A. (2015). A review on hybrid nanofluids: Recent research, development and applications. *Renewable and Sustainable Energy Reviews*, 43, 164-177.
- Shahi, M., Mahmoudi, A. H., & Talebi, F. (2011). A numerical investigation of conjugated-natural convection heat transfer enhancement of a nanofluid in an annular tube driven by inner heat generating solid cylinder. *International Communications in Heat and Mass Transfer*, 38(4), 533-542.
- Shahrul, I., Mahbubul, I., Khaleduzzaman, S., Saidur, R., & Sabri, M. (2014). A comparative review on the specific heat of nanofluids for energy perspective. *Renewable and Sustainable Energy Reviews*, 38, 88-98.
- Shen, B. (2008). *Minimum quantity lubrication grinding using nanofluids*: ProQuest.
- Shin, D., & Banerjee, D. (2011). Enhancement of specific heat capacity of high-temperature silica-nanofluids synthesized in alkali chloride salt eutectics for solar

thermal-energy storage applications. *International Journal of Heat and Mass Transfer*, 54(5), 1064-1070.

Shin, D., & Banerjee, D. (2014). Specific heat of nanofluids synthesized by dispersing alumina nanoparticles in alkali salt eutectic. *International Journal of Heat and Mass Transfer*, 74, 210-214.

Shirazi, S. F. S., Gharekhani, S., Yarmand, H., Badarudin, A., Metselaar, H. S. C., & Kazi, S. N. (2015). Nitrogen doped activated carbon/graphene with high nitrogen level: Green synthesis and thermo-electrical properties of its nanofluid. *Materials Letters*, 152, 192-195.

Sonawane, S., Patankar, K., Fogla, A., Puranik, B., Bhandarkar, U., & Kumar, S. S. (2011). An experimental investigation of thermo-physical properties and heat transfer performance of Al₂O₃-aviation turbine fuel nanofluids. *Applied Thermal Engineering*, 31(14), 2841-2849.

Sonawane, S. S., Khedkar, R. S., & Wasewar, K. L. (2013). Study on concentric tube heat exchanger heat transfer performance using Al₂O₃-water based nanofluids. *International Communications in Heat and Mass Transfer*, 49, 60-68.

Sudeep, P., Soumya, J., Ajayan, P. M., Narayanan, N. T., & Anantharaman, M. (2014). Nanofluids based on fluorinated graphene oxide for efficient thermal management. *RSC Advances*.

Sudeep, P., Taha-Tijerina, J., Ajayan, P., Narayanan, T., & Anantharaman, M. (2014). Nanofluids based on fluorinated graphene oxide for efficient thermal management. *RSC Advances*, 4(47), 24887-24892.

Sundar, L. S., Ramana, E. V., Singh, M., & De Sousa, A. (2012). Viscosity of low volume concentrations of magnetic Fe₃O₄ nanoparticles dispersed in ethylene glycol and water mixture. *Chemical Physics Letters*, 554, 236-242.

Sundar, L. S., Singh, M. K., & Sousa, A. (2014a). Enhanced heat transfer and friction factor of MWCNT-Fe₃O₄/water hybrid nanofluids. *International Communications in Heat and Mass Transfer*, 52, 73-83.

Sundar, L. S., Singh, M. K., & Sousa, A. C. (2014b). Enhanced heat transfer and friction factor of MWCNT-Fe₃O₄/water hybrid nanofluids. *International Communications in Heat and Mass Transfer*, 52, 73-83.

- Suresh, S., Chandrasekar, M., & Selvakumar, P. (2012). Experimental studies on heat transfer and friction factor characteristics of CuO/water nanofluid under laminar flow in a helically dimpled tube. *Heat and Mass Transfer*, 48(4), 683-694.
- Suresh, S., Venkitaraj, K., Hameed, M. S., & Sarangan, J. (2014). Turbulent Heat Transfer and Pressure Drop Characteristics of Dilute Water Based Al₂O₃-Cu Hybrid Nanofluids. *Journal of nanoscience and nanotechnology*, 14(3), 2563-2572.
- Suresh, S., Venkitaraj, K., & Selvakumar, P. (2011). *Synthesis, Characterisation of Al₂O₃-Cu Nano Composite Powder and Water Based Nanofluids*. Paper presented at the Advanced Materials Research.
- Suresh, S., Venkitaraj, K., Selvakumar, P., & Chandrasekar, M. (2011). Synthesis of Al₂O₃-Cu/water hybrid nanofluids using two step method and its thermo physical properties. *Colloids and Surfaces A: Physicochemical and Engineering Aspects*, 388(1), 41-48.
- Suresh, S., Venkitaraj, K., Selvakumar, P., & Chandrasekar, M. (2012). Effect of Al₂O₃-Cu/water hybrid nanofluid in heat transfer. *Experimental Thermal and Fluid Science*, 38, 54-60.
- Timofeeva, E. V., Gavrilov, A. N., McCloskey, J. M., Tolmachev, Y. V., Sprunt, S., Lopatina, L. M., & Selinger, J. V. (2007). Thermal conductivity and particle agglomeration in alumina nanofluids: experiment and theory. *Physical Review E*, 76(6), 061203.
- Timofeeva, E. V., Routbort, J. L., & Singh, D. (2009). Particle shape effects on thermophysical properties of alumina nanofluids. *Journal of Applied Physics*, 106(1), 014304.
- Turgut, A., Tavman, I., Chirtoc, M., Schuchmann, H., Sauter, C., & Tavman, S. (2009). Thermal conductivity and viscosity measurements of water-based TiO₂ nanofluids. *International Journal of Thermophysics*, 30(4), 1213-1226.
- Tyagi, H., Phelan, P., & Prasher, R. (2009). Predicted efficiency of a low-temperature nanofluid-based direct absorption solar collector. *Journal of solar energy engineering*, 131(4), 041004.
- Vajjha, R., Das, D., & Mahagaonkar, B. (2009). Density measurement of different nanofluids and their comparison with theory. *Petroleum Science and Technology*, 27(6), 612-624.

- Vajjha, R. S., & Das, D. K. (2009). Experimental determination of thermal conductivity of three nanofluids and development of new correlations. *International Journal of Heat and Mass Transfer*, 52(21), 4675-4682.
- Vajjha, R. S., & Das, D. K. (2012). A review and analysis on influence of temperature and concentration of nanofluids on thermophysical properties, heat transfer and pumping power. *International Journal of Heat and Mass Transfer*, 55(15), 4063-4078.
- Vanapalli, S., & ter Brake, H. (2013). Assessment of thermal conductivity, viscosity and specific heat of nanofluids in single phase laminar internal forced convection. *International Journal of Heat and Mass Transfer*, 64, 689-693.
- Vandsberger, L. (2009). *Synthesis and Covalent Surface Modification of Carbon Nanotubes for Preparation of Stabilized Nanofluid Suspensions*. McGill University.
- Wang, X.-j., & Zhu, D.-s. (2009). Investigation of pH and SDBS on enhancement of thermal conductivity in nanofluids. *Chemical Physics Letters*, 470(1), 107-111.
- Wang, X.-Q., & Mujumdar, A. S. (2008). A review on nanofluids-part II: experiments and applications. *Brazilian Journal of Chemical Engineering*, 25(4), 631-648.
- Wang, X., Xu, X., & S. Choi, S. U. (1999). Thermal conductivity of nanoparticle-fluid mixture. *Journal of thermophysics and heat transfer*, 13(4), 474-480.
- Xie, H., Gu, H., Fujii, M., & Zhang, X. (2006). Short hot wire technique for measuring thermal conductivity and thermal diffusivity of various materials. *Measurement Science and Technology*, 17(1), 208.
- Xie, H., Lee, H., Youn, W., & Choi, M. (2003). Nanofluids containing multiwalled carbon nanotubes and their enhanced thermal conductivities. *Journal of Applied Physics*, 94(8), 4967-4971.
- Xuan, Y., Li, Q., & Hu, W. (2003). Aggregation structure and thermal conductivity of nanofluids. *AIChE Journal*, 49(4), 1038-1043.
- Xuan, Y., & Roetzel, W. (2000). Conceptions for heat transfer correlation of nanofluids. *International Journal of Heat and Mass Transfer*, 43(19), 3701-3707.

- Yarmand, H., Gharekhani, S., Kazi, S. N., Sadeghinezhad, E., & Safaei, M. R. (2014). Numerical Investigation of Heat Transfer Enhancement in a Rectangular Heated Pipe for Turbulent Nanofluid. *The Scientific World Journal*, 2014.
- Yousefi, T., Shojaeizadeh, E., Veysi, F., & Zinadini, S. (2012). An experimental investigation on the effect of pH variation of MWCNT-H₂O nanofluid on the efficiency of a flat-plate solar collector. *Solar Energy*, 86(2), 771-779.
- Yu, L., Liu, D., & Botz, F. (2012). Laminar convective heat transfer of alumina-polyalphaolefin nanofluids containing spherical and non-spherical nanoparticles. *Experimental Thermal and Fluid Science*, 37, 72-83.
- Yu, W., France, D. M., Timofeeva, E. V., Singh, D., & Routbort, J. L. (2012). Comparative review of turbulent heat transfer of nanofluids. *International Journal of Heat and Mass Transfer*, 55(21-22), 5380-5396.
- Yu, W., Xie, H., & Bao, D. (2010). Enhanced thermal conductivities of nanofluids containing graphene oxide nanosheets. *Nanotechnology*, 21(5), 055705.
- Yu, W., Xie, H., Li, Y., & Chen, L. (2011). Experimental investigation on thermal conductivity and viscosity of aluminum nitride nanofluid. *Particuology*, 9(2), 187-191.
- Yu, W., Xie, H., Wang, X., & Wang, X. (2011). Significant thermal conductivity enhancement for nanofluids containing graphene nanosheets. *Physics Letters A*, 375(10), 1323-1328.
- Zhang, X., Gu, H., & Fujii, M. (2006). Experimental study on the effective thermal conductivity and thermal diffusivity of nanofluids. *International Journal of Thermophysics*, 27(2), 569-580.
- Zhang, X., Gu, H., & Fujii, M. (2007). Effective thermal conductivity and thermal diffusivity of nanofluids containing spherical and cylindrical nanoparticles. *Experimental Thermal and Fluid Science*, 31(6), 593-599.
- Zheng, R., Gao, J., Wang, J., Feng, S.-P., Ohtani, H., Wang, J., & Chen, G. (2011). Thermal percolation in stable graphite suspensions. *Nano letters*, 12(1), 188-192.
- Zhou, L.-P., Wang, B.-X., Peng, X.-F., Du, X.-Z., & Yang, Y.-P. (2010). On the specific heat capacity of CuO nanofluid. *Advances in Mechanical Engineering*, 2, 172085.

Zhou, S., & Ni, R. (2008). Measurement of the specific heat capacity of water-based Al₂O₃ nanofluid. *Applied Physics Letters*, 92(9), 093123.

Zhu, D., Li, X., Wang, N., Wang, X., Gao, J., & Li, H. (2009). Dispersion behavior and thermal conductivity characteristics of Al₂O₃-H₂O nanofluids. *Current Applied Physics*, 9(1), 131-139.

Zhu, H., Zhang, C., Tang, Y., Wang, J., Ren, B., & Yin, Y. (2007). Preparation and thermal conductivity of suspensions of graphite nanoparticles. *Carbon*, 45(1), 226-228.

Zubir, M. N. B. M. (2015). *Facile and highly scalable approach to enhance the stability of colloidal system for thermal application*. University of Malaya.

University of Malaya

List of publications and papers presented

Related to the thesis:

- 1- Yarmand, H., Gharehkhani, S., Shirazi, S. F. S., Amiri, A., Alehashem, M. S., Dahari, M., & Kazi, S. N. (2016). Experimental investigation of thermo-physical properties, convective heat transfer and pressure drop of functionalized graphene nanoplatelets aqueous nanofluid in a square heated pipe. *Energy Conversion and Management*, 114, 38-49.
- 2- Yarmand, H., Gharehkhani, S., Shirazi, S. F. S., Amiri, A., Montazer, E., Arzani & Kazi, S. N. (2016). Nanofluid based on activated hybrid of biomass carbon/graphene oxide: Synthesis, thermo-physical and electrical properties. *International Communications in Heat and Mass Transfer*, 72, 10-15.
- 3- Yarmand, H., Gharehkhani, S., Ahmadi, G., Shirazi, S. F. S., Baradaran, S., Montazer, & Dahari, M. (2015). Graphene nanoplatelets–silver hybrid nanofluids for enhanced heat transfer. *Energy Conversion and Management*, 100, 419-428.
- 4- Yarmand, H., S. Gharehkhani, S.F.S. Shirazi, M. Goodarzi, A. Amiri, W.S. Sarsam, M.S. Alehashem, M. Dahari, and S. Kazi, Study of synthesis, stability and thermo-physical properties of graphene nanoplatelet/platinum hybrid nanofluid. *International Communications in Heat and Mass Transfer*, 2016. 77: p. 15-21.

Unrelated to the thesis:

- 1- Yarmand, H., G. Ahmadi, S. Gharehkhani, S.N. Kazi, M.R. Safaei, M.S. Alehashem, and A.B. Mahat, Entropy Generation during Turbulent Flow of Zirconia-water and Other Nanofluids in a Square Cross Section Tube with a Constant Heat Flux. *Entropy*, 2014. **16**(11): p. 6116-6132.
- 2- Yarmand, H., S. Gharehkhani, S.N. Kazi, E. Sadeghinezhad, and M.R. Safaei, Numerical Investigation of Heat Transfer Enhancement in a Rectangular Heated Pipe for Turbulent Nanofluid. *The Scientific World Journal*, 2014. 2014.

- 3- Shirazi, S.F.S., S. Gharehkhani, H. Yarmand, A. Badarudin, H.S.C. Metselaar, and S.N. Kazi, Nitrogen doped activated carbon/graphene with high nitrogen level: Green synthesis and thermo-electrical properties of its nanofluid. *Materials Letters*, 2015. 152: p. 192-195.
- 4- Amiri, A., M. Shanbedi, H. Yarmand, H.K. Arzani, S. Gharehkhani, E. Montazer, R. Sadri, W. Sarsam, B.T. Chew, and S.N. Kazi, Laminar convective heat transfer of hexylamine-treated MWCNTs-based turbine oil nanofluid. *Energy Conversion and Management*, 2015. 105: p. 355-367.
- 5- Sarsam, W.S., A. Amiri, M.N.M. Zubir, H. Yarmand, S. Kazi, and A. Badarudin, Stability and thermophysical properties of water-based nanofluids containing triethanolamine-treated graphene nanoplatelets with different specific surface areas. *Colloids and Surfaces A: Physicochemical and Engineering Aspects*, 2016.
- 6- Gharehkhani, S., E. Sadeghinezhad, S.N. Kazi, H. Yarmand, A. Badarudin, M.R. Safaei, and M.N.M. Zubir, Basic effects of pulp refining on fiber properties—A review. *Carbohydrate Polymers*, 2015. 115: p. 785-803.
- 7- Navaei, A., H. Mohammed, K. Munisamy, H. Yarmand, and S. Gharehkhani, Heat transfer enhancement of turbulent nanofluid flow over various types of internally corrugated channels. *Powder Technology*, 2015. 286: p. 332-341.